NASA SP-8101

NASA
SPACE VEHICLE
DESIGN CRITERIA
(CHEMICAL PROPULSION)

LIQUID ROCKET ENGINE TURBOPUMP SHAFTS AND COUPLINGS

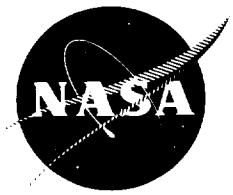

SEPTEMBER 1972

NATIONAL AERONAUTICS AND SPACE ADMINISTRATION

FOREWORD

NASA experience has indicated a need for uniform criteria for the design of space vehicles. Accordingly, criteria are being developed in the following areas of technology:

Environment
Structures
Guidance and Control
Chemical Propulsion

Individual components of this work will be issued as separate monographs as soon as they are completed. This document, part of the series on Chemical Propulsion, is one such monograph. A list of all monographs issued prior to this one can be found on the final pages of this document.

These monographs are to be regarded as guides to design and not as NASA requirements, except as may be specified in formal project specifications. It is expected, however, that these documents, revised as experience may indicate to be desirable, eventually will provide uniform design practices for NASA space vehicles.

This monograph, "Liquid Rocket Engine Turbopump Shafts and Couplings," was prepared under the direction of Howard W. Douglass, Chief, Design Criteria Office, Lewis Research Center; project management was by Harold Schmidt, assisted by Lionel Levinson. The monograph was written by L. K. Severud and C. C. Purdy, Aerojet Liquid Rocket Co., and was edited by Russell B. Keller, Jr. of Lewis. To assure technical accuracy of this document, scientists and engineers throughout the technical community participated in interviews, consultations, and critical review of the text. In particular, J. T. Akin of Pratt & Whitney Aircraft Division, United Aircraft Corporation; J. O. Pfouts of Rocketdyne Division, North American Rockwell Corporation; and D. W. Drier of the Lewis Research Center individually and collectively reviewed the monograph in detail.

Comments concerning the technical content of this monograph will be welcomed by the National Aeronautics and Space Administration, Lewis Research Center (Design Criteria Office), Cleveland, Ohio 44135.

September 1972

GUIDE TO THE USE OF THIS MONOGRAPH

The purpose of this monograph is to organize and present, for effective use in design, the significant experience and knowledge accumulated in development and operational programs to date. It reviews and assesses current design practices, and from them establishes firm guidance for achieving greater consistency in design, increased reliability in the end product, and greater efficiency in the design effort. The monograph is organized into two major sections that are preceded by a brief introduction and complemented by a set of references.

The State of the Art, section 2, reviews and discusses the total design problem, and identifies which design elements are involved in successful design. It describes succinctly the current technology pertaining to these elements. When detailed information is required, the best available references are cited. This section serves as a survey of the subject that provides background material and prepares a proper technological base for the *Design Criteria* and Recommended Practices.

The *Design Criteria*, shown in italics in section 3, state clearly and briefly what rule, guide, limitation, or standard must be imposed on each essential design element to assure successful design. The *Design Criteria* can serve effectively as a checklist of rules for the project manager to use in guiding a design or in assessing its adequacy.

The Recommended Practices, also in section 3, state how to satisfy each of the criteria. Whenever possible, the best procedure is described; when this cannot be done concisely, appropriate references are provided. The Recommended Practices, in conjunction with the *Design Criteria*, provide positive guidance to the practicing designer on how to achieve successful design.

Both sections have been organized into decimally numbered subsections so that the subjects within similarly numbered subsections correspond from section to section. The format for the Contents displays this continuity of subject in such a way that a particular aspect of design can be followed through both sections as a discrete subject.

The design criteria monograph is not intended to be a design handbook, a set of specifications, or a design manual. It is a summary and a systematic ordering of the large and loosely organized body of existing successful design techniques and practices. Its value and its merit should be judged on how effectively it makes that material available to and useful to the designer.

CONTENTS

LIST OF FIGURES

LIST OF TABLES

LIQUID ROCKET ENGINE TURBOPUMP SHAFTS AND COUPLINGS

1. INTRODUCTION

Turbopump shafts and couplings are critical elements of rocket engine turbopumps. The achievement of adequate strength and fatigue life for these basic pump components has not been a major problem in design because power torque loads relative to shaft size generally have been low. However, the achievement of acceptable shaft dynamic characteristics has required major design and development programs. Accordingly, this monograph considers all aspects of turbopump system shaft dynamics peculiar to and necessary to shaft and coupling design. Associated components (bearings, housing, etc.) that influence the shaft or coupling design also are treated to the extent necessary to define that influence. Other aspects of turbopump system design are covered in the design criteria monographs cited in references 1 through 5.

Inadequate designs for rocket engine turbopump shafts and couplings have resulted in development problems and in instances of catastrophic failure, as indicated by the following examples:

- Galling during assembly or removal of bearings from the XLR-87-AJ-3[1] pump shaft and the bearing-to-shaft retaining bolts from the XLR-87-AJ-9 pump.

- Rotor tip rubs caused by inadequate clearances in the M-1 fuel turbopump, the XLR-87-AJ-5 turbine, and the J-2 fuel pump.

- Sporadic bearing failures of the XLR-87-AJ-5 turbine shaft, primarily associated with inadequate margins for whirl critical speeds.

- Self-excited, unstable, subsynchronous rotor whirl of the Mark 25 turbopump, the "E"-blade Mark 9 axial-flow turbopump, and the RL-129 experimental liquid-hydrogen turbopump.

- Unstable, sharply fluctuating rotor response in certain speed ranges of the XLR-87-AJ-9 turbopump, associated with loose fits at the stator joints local to the bearings and large internal play of the roller bearing.

- Metal ignition and catastrophic failure during development of the F-1 LOX pump produced by fretting of the shaft-to-impeller splines.

---

[1] Terms, symbols, materials, and abbreviations used herein are defined or identified in the Glossary.

Of the many factors that influence the design of shafts and couplings, those considered vital are the imposed speeds; critical speeds; bearing and seal locations; coupling locations; size, shape discontinuities, and transitions; service environment; material fatigue strength and thermal properties; structural integrity; fits, deflections, and operating clearances; locking devices; and quality control of all components. Compromises are made in designing the shaft configuration and size to achieve acceptable relationships among rolling-contact bearing DN, seal rubbing velocities, shaft stiffness for critical-speed considerations, and, sometimes, shaft or coupling stress.

The analytical evaluation and prediction of shaft dynamics and critical-speed characteristics is one of the most important design tasks. Prediction accuracy is a function of the detail incorporated into the mathematical model and the capability of the computer program. Critical speeds must be appropriately considered and classified in importance if they are to be properly understood and treated in relationship to other design factors. Many types of forced and self-excited whirls occur in turbopumps, but forced synchronous whirls generally are the most important. The vibrational characteristics and critical-speed behavior of the shaft are covered extensively in this monograph; in addition, the techniques used to adjust critical speeds and response levels and to improve rotor balance are discussed.

Design confirmation tests usually are conducted to verify design adequacy and ensure reliability as well as to minimize operational problems. Guidelines are included in the monograph for nonrotating tests, rotating system tests, and static stiffness tests for components such as rolling-contact bearings, bearing support housings, and shaft coupling joints.

2. STATE OF THE ART

2.1 Shaft Design

The shaft design effort is directed principally to the determination of a shaft configuration that will adequately transmit rotational motion and power torque and also provide a suitable structure on which the various rotating parts such as impellers, bearing races, and turbine wheels can be assembled. Turbopump shafts are required to withstand torsional loads, overturning moments, imbalance whirl forces and vibration, bearing reactions, mechanical and thermal shocks, severe thermal and corrosive environments, steady-state operation conditions, and start accelerations and other transients.

The shaft configuration and the arrangement of the rotating parts usually are based on optimization and compromises of many features and requirements. These considerations include arrangement and type of turbine wheels, pump impellers and inducers, bearings, seals, gears, couplings, turbine manifolds, and pump housings; turbopump power and desired speed; turbopump system size and weight limitations; whirl critical speeds and shaft deflections; applied radial and axial loads; assembly and disassembly procedures and requirements; other turbopump system limitations; and, last but not least, cost effectiveness versus performance for a given design. Multishaft turbopumps using gearboxes to transmit power from turbine shafts to separate pump shafts have been used; both XLR-87-AJ-5 and XLR-91-AJ-5 turbopumps and the RL 10 and H-1 turbopumps are geared systems. However, because of power and speed limitations as well as added design complexity for geared designs, the trend is away from gearboxes and toward direct-driven power transmission.

Turbopump power and selected speed have been the most influential design factors, but shaft life, restart, and reuse requirements are becoming important. Designing a highly reliable, long-life, reusable turbopump shaft entails a continuing effort from preliminary design through the development phase and into the early flights. The effort begins with the configuring and sizing of the components on the basis of predicted loads and estimated environment, emphasis being placed on design practices and principles that maximize fatigue life. Material choices are made largely on the basis of low-cycle and high-cycle fatigue strengths, thermal expansion and contraction properties, fracture toughness, resistance to crack propagation, and environmental sensitivities. During fabrication, nondestructive testing (NDT) inspections are employed to assure product quality. Actual load and environmental data from the early research and development tests are mapped. These data, along with refined analytical and experimental stress and fatigue data, are fed back into an updated and more refined structural analysis. Based on the critical conditions found to be significant life-cycle determinants, controlled overstress tests are considered. The primary objective is to find the limits and failure modes by intentionally testing to failure. Then, study of the failure modes allows further design improvements.

2.1.1 Design Parameters

2.1.1.1 SHAFT SPEED

High shaft speeds allow overall turbopump size and weight to be kept relatively small; thus the design goal usually is to operate the shaft at the highest rotating speed that is feasible. However, definite limitations on shaft speed arise from pump suction and hydraulic design considerations, impeller and turbine wheel stresses, shaft-seal rubbing velocities, bearing DN, and shaft whirl critical speeds.

Many turbopump shafts operate at a constant or almost constant steady-state speed. However, some shafts, especially those for turbopumps with engines having throttling capability, are required to operate for substantial periods of time over a wide range of speed. When a design is undertaken, the question immediately arises as to whether the shaft should operate at speeds above or below the turbopump system first whirl critical speed.

The major advantages of subcritical shaft design are that no resonances or self-excited vibrations or instability whirls will occur from zero to full speed. Thus, concern for going through critical speeds and the need for special damping systems or more complex balancing procedures are eliminated.

Disadvantages of subcritical shaft design are primarily the requirements or limitations imposed on the other components of the turbopump. For example, to attain the maximum operating shaft speed, the weight of the rotating parts, the length of the shaft, and the amount of overhang have to be minimized. This minimization usually impacts turbine and impeller burst-speed capabilities. The large shaft diameter required for shaft stiffness usually results in high bearing DN or high seal rubbing velocity. The high bearing stiffness usually required results in dynamic coupling of rotor and machine casing or housing. Thus, housings also must be designed for high stiffness; and therefore, for accurate predictions, the dynamic model that includes the housing must be detailed and complex. Also, high bearing stiffness usually limits rolling-contact bearing choice to cylindrical roller bearings. Moreover, the requirement of subcritical shaft design may severely limit the maximum operating speed and thereby reduce turbopump hydraulic and aerodynamic performance.

Supercritical shaft design removes most disadvantages associated with subcritical design. In addition, if the first two criticals are controlled by using flex-mounted bearings, operation is practical up to speeds just below the third critical (the first mode to contain significant shaft bending). The associated bearing reactions usually are much lower than those in subcritical design, and thus bearing life and reliability are improved.

The major disadvantages of supercritical shaft design are that damage may occur during passage through the criticals and that self-excited or unstable subsynchronous whirls may occur at speeds above the first system critical. The causes of self-excited whirls are many,

and accurate means to predict magnitudes or conditions of occurrence do not exist. Thus, assurance that a design will have stable and tenable supercritical characteristics can be obtained only after the turbopump is built and tested. The needs for special damping mechanisms and for an accurate rotor balance effective over the entire operating range are additional disadvantages as compared with subcritical shaft design. Furthermore, supercritical shaft designs, because of their lower critical speeds, usually are limited in capability to throttle to low speeds safely.

A typical plot of shaft speed versus time from start for a liquid rocket engine turbopump is presented in figure 1. Considerable turbopump experience indicates that good engine system design can limit overshoot to 3 percent or less. However, some systems have produced

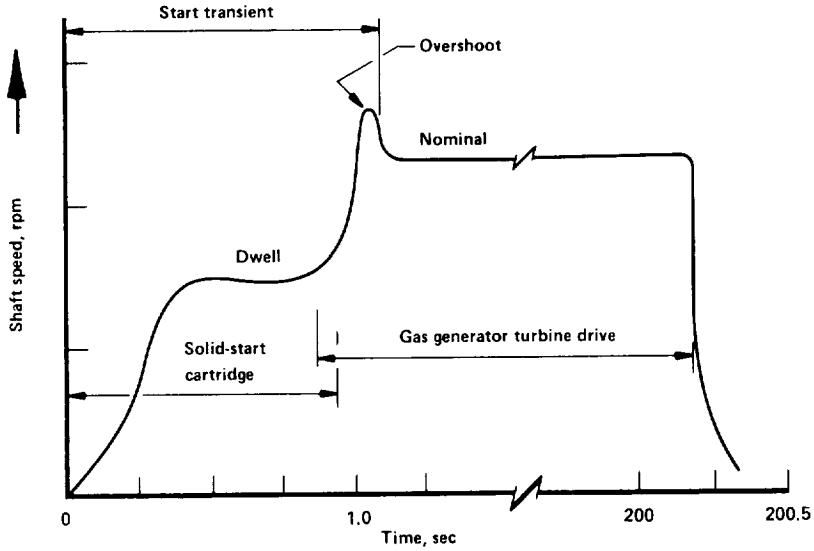

Figure I. – Typical plot of shaft speed vs time for constant-speed liquid rocket engine turbopump

overshoots of 5 to 10 percent of full speed, and some overshoots reached 25 percent. Because it takes only a very short time at a critical speed to induce detrimental rubbing between rotor and stator or fail a bearing, the shaft usually is designed to preclude operation at a critical speed at the start-transient dwell and overshoot speeds as well as at the maximum steady-state operating speed.

2.1.1.2 BEARING AND SEAL LOCATION

The locations of the bearings and seals relative to the major rotor components significantly influence the overall turbopump design complexity. Bearing locations have a significant effect on shaft critical speeds (refs. 6 through 9), shaft deflections, and stresses. If gears or

pinions are located on the shaft, a radial-support bearing usually is placed close to them so that shaft bending stresses are minimized. Thermal displacements and assembly tolerances usually require a bearing that will resist both thrust and radial loads, and this bearing is placed as close as possible to the thrust balance piston so that operating running clearances can be controlled. The environments and loads imposed on a bearing or seal and the effects on life capacities often are important factors in location. Bearings and seals sometimes have to be replaced during the life of the turbopump, and therefore accessibility and maintenance are considered in the choice of location.

Overhung turbine arrangements commonly are selected over cradled turbine designs in order to avoid locating the bearing or seal in the hot inlet region as well as to preclude aerodynamic compromise of the inlet. Centrifugal pumps usually have the bearing inboard of the impeller because bearing support struts in the pump inlet flow passage can compromise pump suction performance. Axial-flow pumps generally have the main-stage pump section straddled with radial-support bearings.

2.1.1.3 SHAFT SIZE

For most rocket engine turbopumps, shaft size at the bearing locations is governed by stiffness (critical-speed) criteria rather than by stress criteria. Usually, the shaft size is made as large as possible consistent with DN and seal-rubbing-velocity limitations. The current limit of DN for rolling-contact bearings in rocket engines is approximately 1.0 to 2.0 million. Table I lists demonstrated values for rolling-contact bearing DN and for seal rubbing velocity.

Table I – Demonstrated Values for Rolling-Contact Bearing DN and Seal Rubbing Velocity

Engine	Environment	Bearing DN, million	Seal rubbing velocity	
			ft/sec	m/sec
J-1	LH_2	1.6	275	83.8
M-1	LH_2	1.6	275	83.8
M-1	LOX	0.5	86	26.2
XLR-87-AJ-9	Oil	1.35	232	70.7
ARES engine	N_2O_4, A-50	1.6	275	83.8
XLR-87-AJ-3	Oil	1.19	204	62.1
XLR-87-AJ-5	Oil	1.08	185	56.4

Reference 1 should be consulted for more detailed data and limitations. For rolling-contact bearings, DN is a more restrictive factor than seal rubbing velocity. Fluid-film bearings apparently do not have any DN limitation; therefore, the face-seal rubbing velocity can become the limiting factor when fluid-film bearings are used. Face seals have been operated at rubbing velocities up to 500 ft/sec (152 m/sec)[1] in fluids such as LH_2, LOX, and RP-1.

Face-contact seals can be compared on the basis of PV, where P is the face load in psi (N/m^2) and V is the velocity in ft/sec (m/sec); typical values for PV are 40000 to 80000 psi-ft/sec (84 to 168 MN/(m-sec)). Time in contact also is a factor; high-speed face-contact seals can be of the liftoff type, closed at zero rpm and open at full speed. Detailed information on seals for turbopump shafts is presented in reference 5.

The shaft size, once defined, is checked for stress adequacy. For preliminary design, the allowable shaft shear stress at locations of rolling-contact bearings often is taken as two-thirds of the ultimate shear strength of the shaft material. The shaft mechanical joints (i.e., curvic couplings and bolted joints) also are evaluated for stiffness adequacy. Hollow, thin-wall shafts are checked for torsional buckling adequacy. Formulas for sizing nondrum-type shafts subjected to steady and alternating combined stresses are provided in several established references (refs. 10 and 11). In chapter 13 of reference 12, a design technique known as the Von Mises-Hencky-Goodman method is presented. This technique is more difficult to use than those of references 10 and 11, although it more closely predicts actual failure conditions.

Thin-wall, cylindrical, rotating-drum-type shafts such as those used in the M-1 fuel turbopump are diameter limited by centrifugal-stress considerations. Outer wall speeds up to 1100 ft/sec (335 m/sec) have been demonstrated successfully.

2.1.1.4 SHAFT DISCONTINUITIES AND TRANSITIONS

Shafts usually have numerous increases in cross section required to provide maximum overall shaft bending stiffness. In addition, shaft diameters at bearing locations are reduced to keep DN values acceptable, allow shoulders for bearing races and other shaft-riding elements, provide platforms for pressed or shrunk-on parts, and facilitate coupling design. The primary design consideration regarding these discontinuities and transitions is the resulting stress concentration and its effect on the shaft fatigue life.

Stress-concentration and fatigue-life-reduction factors have been determined for many common shapes (e.g., circular or elliptical fillets) in tension, bending, and torsion (refs. 13 through 16). Also, fatigue-reduction factors for transverse holes in the commonly used dimensional ratios have been published (refs. 17 and 18). Face-milled keyways and the more

[1] Parenthetical units are in the International System of Units (SI units). See Mechtly, E. A.: The International System of Units. Physical Constants and Conversion Factors, Revised. NASA SP-7012, 1969.

fatigue-damaging end-milled keyways have been studied in detail (ref. 19). The detail design of transition sections is discussed in reference 20. However, although the harmful effect of a sharp corner is well understood, designers frequently fail to realize that a similar adverse condition exists when a collar is pressed or shrunk into place on a shaft. Stresses increase sharply where the shaft protrudes from a tightly fit ring (refs. 21 and 22). This end effect, which is often overlooked in design, is important from the aspect of fretting corrosion and stress concentration. Although hyperbolic or elliptical fillets give rise to lower stress-concentration factors than do circular fillets, it has been the practice in rocket engine turbopump shaft design to use circular fillets because of minimum axial space requirement and the shape of mating parts (e.g., bearing race corner radii). The additional magnitude of stress concentration rarely has been a limiting design factor.

Surface conditions have a considerable effect on static tensile strength. From the fatigue aspect, a surface with outward projecting peaks and relatively flat broad valleys is preferred to one with sharp ravines and relatively flat broad plateaus even if both surfaces have equal roughness values (refs. 23 and 24). Both the minimum and maximum surface finishes must be controlled to obtain successful seal performance (ref. 25).

2.1.1.5 SERVICE ENVIRONMENT

The shaft is subject to thermal environments associated with engine prefiring conditions, transient heatup and chilldown, and steady-state temperature conditions imposed by the proximity of the turbine hot gas or pump fluid. Also, the bearing lubricant or coolant imposes thermal conditions on the shaft. When cryogenic propellants are pumped, the low-temperature end may reach -420°F (22 K), with attendant embrittlement of some of the common shaft materials. The heatup transient may span from a prechilled -420°F (22 K) to about 1400°F (1033 K). As the transient time usually is short, thermal shock gradients and associated stresses and strains in the metal may cause structural damage leading eventually to fatigue cracking. Service temperatures also can affect the shaft stiffness and critical speeds as well as the metal static strengths.

Restartable turbopumps may be affected by residual thermal conditions from previous firings. Measurements on Titan II stage 1 turbopumps 10 min. after shutdown indicated a soakback temperature of 560°F (566 K) at the bearing nearest the rotor; if Aerozine-50 is used as the bearing lubricant, the possibility of detonation exists at engine restart. High soakback temperature also can affect the temper of the metals in the bearing race and the rolling-element cage.

A high-pressure gaseous-hydrogen environment is known to embrittle many engineering alloys (refs. 26 and 27). The degree of embrittlement is a function of the metal temperature, environmental pressure, purity of the gas, and exposure time. Steels (ferritic, martensitic, and bainitic), nickel-base alloys, and titanium alloys become embrittled in pure-hydrogen environments at room temperature; the effects are more pronounced as the pressure increases. High-strength alloys are more susceptible than low-strength alloys. Austenitic

stainless steels such as types 310 and 316; certain aluminum alloys such as 6061-T6, 2219-T6, and 7075-T13; pure copper and beryllium copper; and the precipitation-hardened austenitic stainless steel A-286 are only slightly affected. Inconel 718, Inconel X, Waspaloy, and Rene 41 are severely embrittled in high-pressure gaseous-hydrogen environments. A large amount of experimental work currently is being done by industry and government laboratories to achieve better understanding of hydrogen-embrittlement effects.

Under certain environments, spontaneous failure of the metal may result from the combined effects of corrosion and stress. Such failures can occur under mildly corrosive conditions and nominal surface tensile stresses. Usually there is no advance indication (visual or microscopic) of the impending failure. Susceptibility to stress-corrosion cracking is variable in metals, even among some types of steels, the degree depending on temper.

For stress-corrosion cracking to occur, tensile stresses must exist at the surface of the structure; the higher the stress level, the greater the susceptibility to stress-corrosion cracking. These stresses may be a combination of internal and external stresses. Highly stressed shafts have been subject to stress corrosion (refs. 28 and 29). Many failures have been attributed to high residual stresses in the material. Multiple-material shafts developed for use where different sections of the shaft are exposed to different corrosive environments are reported in reference 30.

The oxidizing and corroding effects of the fluid being pumped can eliminate many materials from consideration for use in a pump. For example, N_2O_4 as a propellant greatly restricts material choices because N_2O_4 will combine with moisture to form nitric acid. However, the oxidizing action of N_2O_4 can be used to advantage for replenishing the oxide film removed during operation in hard vacuum.

Contact surfaces exposed to deep-space vacuum (10^{-8} torr [1.33×10^{-6} N/m^2] or lower) may be subject to cold welding or adhesion, depending on the metallurgical composition, exposure time, contact stress, and temperature. Decomposition and sublimation of materials at pressures in the range of 10^{-5} to 10^{-13} torr (1.33×10^{-3} to 1.33×10^{-11} N/m^2) restrict the use of cadmium, zinc, and magnesium in pure-element form (ref. 31). Aluminum coatings are used to replace cadmium in a hard-vacuum environment. Conventional lubricants cannot be used in a hard vacuum (ref. 32). Other major problems in hard-vacuum service may be microporosity of welds, entrapped gases, or solids that outgas (ref. 33).

2.1.2 Material Selection

In most design procedures, a turbopump shaft material is selected on the basis of strength, ductility, chemical compatibility, weldability, and machineability. In some instances, when the thermal expansion properties were ignored until the design became fixed, the effect of expansion was compensated for by the fit of the inner bearing race; this practice resulted in excessive strain on the bearing races. When the strength, ductility, and environmental compatibility of several materials satisfy the shaft design requirements, the primary

consideration is thermal effect, with fabrication properties as secondary criteria. Although thermal expansion data are available (refs. 34 and 35) for most shaft materials, it may be necessary to run special tests for critical applications. The development of alloys like Inconel 718, 17-4 PH, Rene 41, and Waspaloy has widened the selection of the high-strength materials for shafts that will match the typical bearing materials (M-50, 440C, and 52100).

As noted previously, in recent years the effect of a high-pressure gaseous-hydrogen environment on embrittlement of metals has been investigated. Many of the common shaft metals were found to suffer significant embrittlement; some new alloys were only slightly affected (sec. 2.1.1.5). In addition to these new alloys, the joining of different alloys has been successful in resisting embrittlement (refs. 34, 36, and 37). Other potential problem areas such as corrosion fatigue, stress corrosion, and hydrogen embrittlement during fabrication are discussed in reference 38. The designer must also consider the brittle transition that occurs in low-alloy steels at cryogenic temperatures. Cryogenic temperatures embrittle 9310, 4340, and 440C sufficiently that they rarely are used as shaft materials in this environment. Some of the materials that have been used successfully for shafts in rocket engine turbopumps are given in table II.

Table II – Materials Successfully Used for Rocket Engine Turbopump Shafts

Material	Service fluid						
	Hydrogen	Oxygen	Nitrogen tetroxide	Aerozine 50	Nitrogen	MIL-L-7808 lube oil	Fluorine
Inconel 718	X	X			X		
Inconel X	X	X					
K-monel	X						
Rene 41	X				X	X	
CRES 300	X						
AM 350			X	X			
9310						X	
4340		X					
440C							X

Note: X denotes that the given material performed satisfactorily with the given fluid; absence of X indicates no experience available or that the material cannot be used with the given fluid.

Case-hardening processes include nitriding and electrolyzing. Nitriding was used on the Titan XLR-87-AJ-5 and -91-AJ-5 gearbox shafts, and electrolyzing on the NERVA Mark 4 Mod 2. Nickel-base (AMS 4775) and Linde LW-5 alloys were used on a Rene 41 shaft in the liquid-hydrogen environment (ref. 36). The effect of chrome plating on shaft fatigue also has been documented (ref. 39).

Fretting is a potential source of ignition in oxidizer pumps. The usual remedy for fretting is to tighten the fit or clamp and use lubricants compatible with the oxidizer.

Galling was a problem when bearings were assembled on or removed from the 4610 shaft of Titan XLR-87-AJ-3. This problem was corrected for the -87-AJ-5 shafts by using AM 350 nitrided to a hardness value of Rockwell C58 as shaft material. Galling also was noted on a bearing-to-shaft retaining bolt in Titan XLR-87-AJ-9, where the AM 350 bolt and the Rene 41 shaft were approximately the same in hardness. A 7075-aluminum sleeve was added to the bolt to resolve the galling problem.

2.1.3 Structural Analysis

2.1.3.1 LOADS

The design of a shaft (and coupling) from a structural standpoint is based on the relationship between the loads that will be imposed on the shaft and the capacity of the shaft to withstand those loads. Allowable load, limit load, yield load, ultimate load, safety factor, and margin of safety are terms that are used to establish and define this relation between shaft loading and shaft loading capacity. These terms, as they are used in this monograph, are defined as follows:

Allowable load: the load that produces a stress equal to the material mechanical strength.

Limit load: the maximum load or combination of loads and environment expected to occur at least once during the life of the component.

Yield load: the load below which no detrimental deformation will occur; limit load multiplied by the yield safety factor.

Ultimate load: the maximum load that must be withstood without rupture; limit load multiplied by the ultimate safety factor.

Safety factor: an arbitrary multiplier greater than 1 applied in design to account for unexpected design conditions, e.g., slight variations in material properties, fabrication quality, and load distributions.

Margin of safety: fraction by which the allowable load exceeds the design load (yield or ultimate).

The magnitudes of most of the identified loads on a shaft are evaluated by computation during the design phase. Loads that do not lend themselves to this computational analysis (i.e., vibratory and malfunctioning loads) are given appropriate consideration by designing to minimize the magnitude of such loads.

The load predictions in some cases have been inaccurate. Radial loads due to rotor dynamics have sometimes been twice as large as the loads calculated in response analyses. Also, radial loads due to nonsymmetrical pressure distributions resulting from pump-housing discharge ports, in-flow obstructions, etc., do not lend themselves to accurate predictions of magnitude. Calculation of net pump or rotor axial thrust, which is the algebraic sum of large thrust component forces, has given values substantially different from the subsequently experimentally determined ones.

2.1.3.2 SAFETY FACTORS

Usually, the safety factors for static stresses are specified to the designer. Table III displays some examples of safety factors that have been used in turbopump shaft design.

Table III – Typical Safety Factors Used in Shaft Design

Rocket engine	Yield safety factor	Ultimate safety factor
XLR-87-AJ-3/5 and XLR-91-AJ-3/5	1.0	1.25
M-1	1.0	1.5
XLR-87/91-AJ-9	1.0	1.4
J-2 and F-1	1.1	1.5
ARES	1.2	1.6
RL 10	1.2	1.5

Generally, the fatigue safety factors are not specified. Values of 1.25 and 1.33 have been used.

Selecting safety factors in accordance with the desired reliability rather than more or less arbitrarily choosing them has become the desired engineering approach. The goal is to account for variations in material properties; effects of size; effects of machining and processing operations on properties; accuracy in predicting environments and loads; accuracy of stress analysis models; etc., by use of probabilistic mathematics (refs. 40

through 43). Rocket engine total reliability, however, is a function of the individual reliability of the many components, and a practical means of determining all the variances required to accomplish an accurate quantitative correlation of shaft or coupling safety factors to engine reliability is not yet possible (refs. 44 and 45). Nevertheless, the effort directed to establishing these variances, even as estimates, is valuable for identifying areas where more design data are required to establish which properties are governing factors in the design. At the present time, however, uniform design safety factors are selected largely on the basis of engineering judgment combined with prior experience in obtaining the desired level of reliability.

2.1.3.3 ANALYTICAL METHODS

The shaft structural analysis consists of determining the stress and strain states, deflections, shaft failure strengths, and margins of safety. Analytical determination of stress levels using standard beam and torsion formulas coupled with appropriate stress-concentration factors has been the most common method of stress analysis. However, complex shaft configurations have been analyzed by digital computer programs and by experimental techniques for stress analysis.

The failure-strength analysis has consisted primarily of using the high-cycle-fatigue failure theory for fluctuating combined stresses; this theory is known variously as the octahedral shear theory (ref. 46, pp 208-213), distortion energy theory (ref. 47), or Von Mises-Hencky theory (ref. 12, pp 183-189). When thermal shock stresses result in large inelastic strains, the low-cycle-fatigue failure theory (ref. 48) has also been employed. Welded shafts have been analyzed for strength by utilizing fracture-mechanics principles (ref. 49) to assess the impact of cracks and flaws that result from fabrication.

2.1.4 Assembly and Operation

2.1.4.1 DIMENSIONS AND FITS

Rocket engine turbopump design requires close control of pilots and radial fits between the shaft and bearings and other rotating components such as gears, impellers, and turbine wheels. Typical shaft and bearing tolerances for a few engines are shown in table IV.

Since the radial locations of the components are controlled by the radial bearings, it is common practice to define the corresponding shaft pilot diameter locations with respect to the shaft diameters on which the bearings register (datums). Room temperature (normally 68°F [293 K]) shaft dimensions are established to account for anticipated dimensional changes resulting from thermal expansion/contraction of the material, centrifugal growth of the mating parts, and response to applied loads. In the case of the XLR-87-AJ-9 gearbox, a

Table IV – Typical Shaft and Bearing Tolerances

Characteristic	XLR-87-AJ-5 40/55mm bore		M-1 110/120mm bore		RL 10 fuel pump front and rear	
	in.	μm	in.	μm	in.	μm
Bearing inside diameter	± 0.0001	± 2.5	± 0.00012	± 3.05	± 0.00010	± 2.54
Shaft outside diameter	± 0.0001	± 2.5	± 0.00015	± 3.81	± 0.00025	± 6.35
Total	± 0.0002	± 5.1	± 0.00027	± 6.86	± 0.00035	± 8.89

Rene 41 shaft and M-50 bearing were used. Because of the close matching of the thermal expansion properties, the change in fit was only 0.0002 in. (5.1 μm) for the 55mm bearing race during the 280°F (156 K) temperature rise. Conversely in the M-1, the use of 440C bearing material with Rene 41 (turbine end) and Inconel 718 (pump end) required increases in room temperature fit of 0.0012 in. and 0.002 in. (30.5μm and 51μm), respectively, to anticipate the effect of the -423°F (20 K) operating environment. Special procedures were necessary to shrink the bearings on and off the shaft without damaging components.

In general, shafts of equal diameter all have approximately the same change in diameter as a result of speed because most of the commonly used shaft materials have similar ratios of density to modulus of elasticity. The change in shaft diameter caused by centrifugal growth can produce significant reduction in bearing internal clearances when the DN value is greater than 1.0 million. Reference 50 contains a complete treatment on this subject. Conversely, pilots and fits that tend to open during high-speed operation (e.g., bore-mounted disks) may cause eccentric shifting of mass centers and result in added imbalance.

In some designs, in order to preclude excessive pilot or fit loosening due to the thermal environment or high-speed operation, extremely close component-to-shaft fit or pilot interference is required at room-temperature assembly; this is especially true for shafts with low-contact-angle ball bearings. Selective assembly of the components is then used to restrict the tolerance accumulation more than that indicated in table IV. For the SNAP 8 turbine shaft, each bearing was dimensionally coded to permit selective assembly for optimum shaft and housing fits (ref. 51).

When components are assembled and disassembled frequently, some damage to the surface finish of the parts may occur unless special procedures or surface treatment are used. The gearbox shafts on both XLR-87-AJ-9 and XLR-91-AJ-9 were nitrided to resist galling.

Because of LOX compatibility requirements, the XLR-87/91-AJ-3 gearbox shafts were not surface hardened. Use and damage limits were specified to control the degree of surface finish change caused by bearing removal.

2.1.4.2 COMPONENT RUNNING POSITIONS AND CLEARANCES

The running positions of the rotating parts relative to the stationary parts determine operating clearances. Operating clearances have presented problems during initial development testing of many rocket engine turbopumps; for example,

- In the J-2 engine development, blade rubbing was associated with vibration modes of the turbine rotor disks and subsynchronous shaft whirl. The disks were redesigned to raise the axial vibration critical speed, and the shaft was rebalanced at high speed.

- Axial thermal gradients across the turbine wheel of the M-1 fuel turbopump caused the wheel to dish upward and thereby allowed the turbine bucket to rub on the upstream nozzle.

- Accumulative creep distortion of a particular-design second-stage nozzle of the XLR-87-AJ-5 turbopump caused the operating clearances to be reduced during each firing. Thus, after a certain number of tests or after the nozzle developed residual creep distortions of a fixed magnitude, the nozzle required replacement. In one instance during research and development testing, the established creep-distortion limits of the nozzle unknowingly were exceeded; in a subsequent test, the rotor rubbed on this distorted nozzle and caused a catastrophic failure of the entire turbine.

Experience has shown that axial motions at rotor tip diameters can easily be four or five times as great as the radial values at the same locations. Both axial and radial operating clearances are carefully evaluated, because either clearance, if insufficient in magnitude, can lead to failure of a turbopump.

Computations of the thermal and mechanical distortions of both rotating and stationary parts have been useful in establishing required assembly clearances. However, experience indicates that, even with detailed and time-consuming computations, predictions of component running positions and resulting clearances are of questionable accuracy. Thus, initial tests of new designs often are made with machines having excessive clearances, and clearance-measuring devices are attached. After sufficient test data are acquired to establish limits of clearance changes during operation, the buildup clearances are reduced to tenable levels.

2.1.4.3 RETAINING BOLTS AND LOCKING DEVICES

Retaining bolts play a major role in successful operation of the curvic or parallel-sided face couplings (secs.2.3.2 and 2.3.3); they prevent loosening or overload during operation. To design a bolt properly, it is necessary to know the temperature gradients and loads during

assembly, start transient, operation, and postrun heatsoak. The following elements are involved in the design of retaining bolts and locking devices:

- Mechanical strength
- Preload
- Arrangement and fit
- Vibration effects
- Galling, seizing, and fretting
- Locking action
- Stackup and imbalance

In general, a material with high strength in combination with a high coefficient of thermal expansion has been used for retaining bolts. The high strength is required for a minimum-size bolt, and the high thermal expansion is desirable because the bolt normally is at a lower temperature than the surrounding rotor hubs. Inconel 718 has been a satisfactory bolt material except in a hydrogen atmosphere. The low modulus of elasticity for titanium results in a small bolt diameter, but titanium compatibility with the service environment must be verified. A long bolt usually gives the best overall ability to maintain tight axial joints but, in some cases, the shaft does not permit a long bolt. Also, the threads in the shaft become more difficult to machine as the length of the bolt increases. Vibration of long bolts by shaft rotational excitation can reduce the strength of the bolt by superposing a cyclic stress on the relatively high tensile preload steady stress.

The arrangement of retaining bolts is associated primarily with the coupling design and is covered in detail in section 2.3.2. When a parallel-sided face coupling is fastened with a single central bolt and the fits between the male and female portions of the coupling are loose, the power torque may impose a large lateral shear force on the bolt and one coupling tooth. Plastic deformation under such high loads usually allows more teeth to come into contact and share the total load, thus preventing fracture in ductile materials. However, adverse bolt bending with associated rotor imbalance, or fracture of a tooth or bolt if it has little ductility, is a potential problem. When bolt load is critical, elongation rather than torque is used to determine the bolt preload. The XRL-87-AJ-9 turbine assembly records show a variation in torque from 195 to 330 lbf-ft (264 to 448 N-m) for a 0.009-in. (0.23 mm) elongation under apparently constant conditions of lubrication and assembly.

If a stud bolt and nut is used instead of the head-type bolt, torque transmittal to the shank during tightening is eliminated. However, locking becomes more complicated because both the stud bolt and the nut must be locked.

Galling, seizing, and fretting of fasteners at times have presented problems. Generally such problems are avoided or solved by (1) use of an appropriate lubricant (refs. 52 and 53), (2) reduction of the vibration environment, (3) use of a positive locking device, or (4) use of materials with different surface hardnesses.

Positive locking devices for rotating parts are usually of the tab or crimped washer type (fig.2). (Although it is not shown in figure 2(b), the preferred method is to bend the tab in the direction of the centrifugal force whenever possible.) The crimp type is preferred because the crimp in the washer and the slot in the shaft are automatically aligned. Also, the crimp type requires fewer slots, usually 4 as compared with 12 or more for the tab type. The main disadvantage of the crimp type is the need for more elaborate tooling. The effect on rotor balance is a factor in the selection of the locking device.

2.1.4.4 ASSEMBLY AIDS

Assembly aids (e.g., slots, wrench flats, and bearing and gear removal tools), as well "fool-proofing" techniques, have an effect on shaft design. These factors normally are taken into account in the design stage by placing flats, slots, offset holes, or pins in locations of relatively low stress. Also, the flats and other assembly aids are placed symmetrically about a diametral line across the cross section of the shaft so that they do not result in rotor imbalance.

2.1.5 Quality Control

Nondestructive testing (NDT) of shafts usually is accomplished by one or more of four methods of inspection: magnetic particle, penetrant, X-ray, and ultrasonic.

In some instances the fluid used during the inspection (e.g., fluorescent penetrant) is incompatible with one or both propellants, and normal cleaning procedures are insufficient to remove all traces. Under these circumstances, especially when the propellant is liquid fluorine or liquid oxygen, the shaft drawing itself stipulates the exact procedure (usually baking at approximately 250°F [394 K]) by which the residual inspection-aid fluid can be removed. In many cases, because of large changes in cross section or special manufacturing operation, the inspection process itself is a development task. For example, special ultrasonic techniques were developed to detect defects close to the surface of the M-1 fuel turbopump shaft at the juncture of the weld between the Inconel 718 and Rene 41. This weld was also inspected by X-ray; 100,000 volts were required because of the high density and thickness of the materials.

Involute splines for lightly loaded applications normally are checked with go/no-go gages that include the effects of profile, index, lead, and tooth-thickness errors. For highly loaded splines, individual checks of tooth characteristics are made with the same equipment used for inspecting gear teeth. Couplings of the pilot and radial "dog" type require dimensional inspection with conventional inspection equipment. Curvic couplings, however, do not lend themselves to complete inspection even with special tools. Special gear checking equipment is used to inspect for index error and runout. Tooth contact is tested visually against a master mating-coupling half, marking compound being used to establish the adequacy of the profile. The test is subject to errors in interpretation unless it is conducted by specially trained technicians.

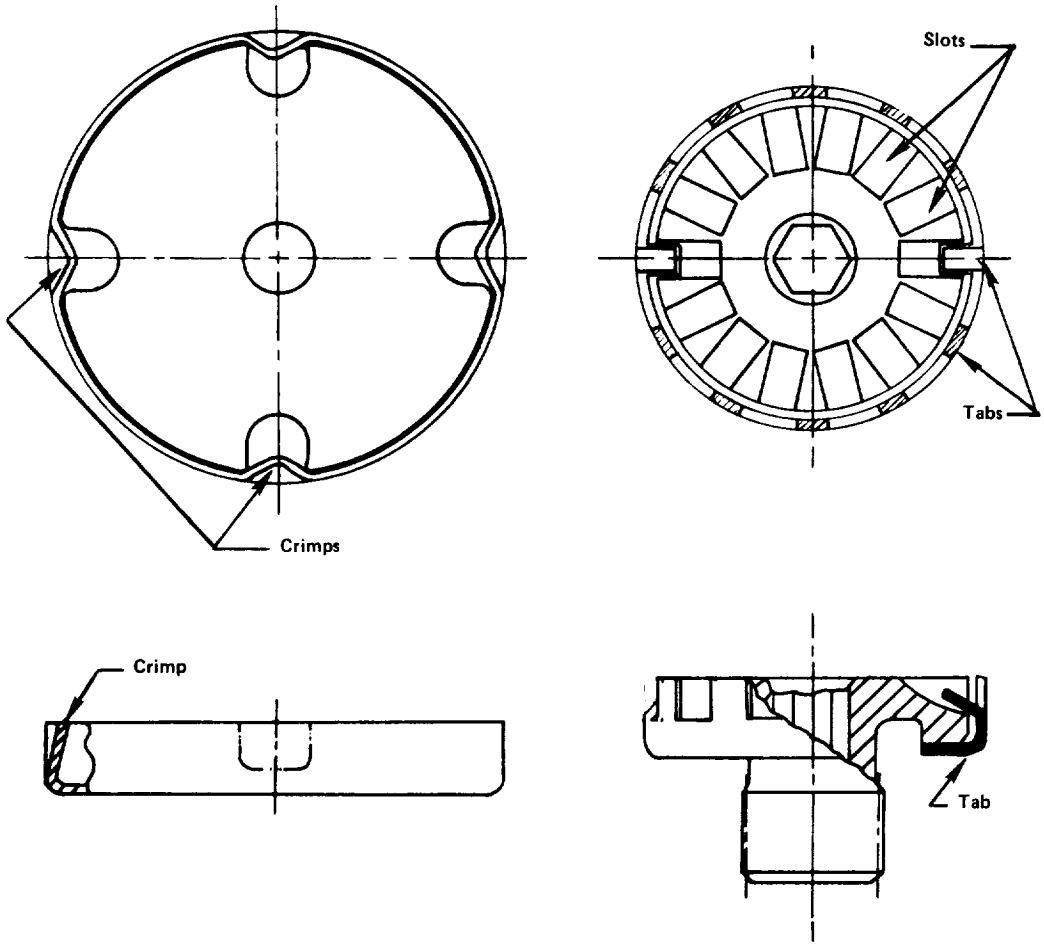

Figure 2. – Locking devices for rotating parts

2.2 Shaft Dynamics

A vast amount of material has been published on the subject of shaft dynamics. The more complete treatments, which cover important aspects not usually covered in standard textbooks, are given in references 54 through 70. The treatment herein is restricted to those aspects of shaft dynamics that must be taken into account in the design of the shaft and coupling.

2.2.1 Dynamic Behavior

2.2.1.1 WHIRL MOTIONS

Shaft whirling usually is described in terms of shaft motion about an external longitudinal axis; whether this motion is forced or self-excited is noted also. Motions of the shaft during whirling normally are described by the type of whirl path or orbit and by the direction and speed of the whirl relative to the shaft rotation. Some of the basic classifications of shaft motion are illustrated in figure 3. In the examples shown, when shaft speed Ω equals the magnitude of whirl velocity ω, the motion is called synchronous. Shaft motions can become highly complex as illustrated in figure 3(f) and as discussed in references 58, 71, and 72.

2.2.1.2 FORCED WHIRLS AND CRITICAL SPEEDS

Types of forced whirls and their causes identified by Yamamoto from his work with rolling-contact bearings (refs. 58 through 61) are presented in table V. Other causes of forced whirls are associated with trapped fluids (ref. 73), bearing clearances (refs. 72, 74, and 75), bearing-noise vibrations (ref. 76), gear-meshing excitations, and rotating-stall excitations at a frequency approximately half the shaft speed (ref. 77). Shaft torque and thrust misalignment between coupled shafts can induce lateral and torsional vibrations.

A critical speed is defined as a shaft rotative speed at which a rotor-stator system natural frequency coincides with a possible forcing frequency. If all the possible system critical speeds of a given machine are considered as speeds at which operation is untenable, then the operating speed zones are severely limited. For example, figure 4, a plot similar to those of Yamamoto (refs. 58 through 61), shows numerous critical speeds for a shaft supported in rolling-contact bearings. Here the natural frequencies of various shaft modes of vibration are plotted as a function of shaft speed. "Rays" emanating from the zero point of the curve show corresponding forcing functions (e.g., impeller vane-to-housing frequency and bearing-ball translation frequency). Theoretically, the intersection of each ray with a natural frequency is a critical speed; however, experience has shown that many of these critical speeds have negligible practical importance.

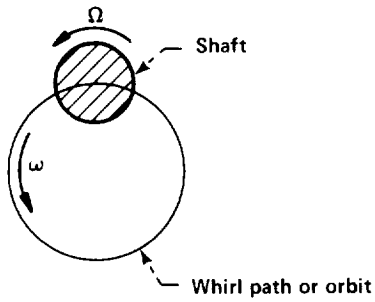

(a) Forward circular whirl

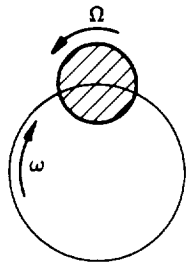

(b) Reverse or backward circular whirl

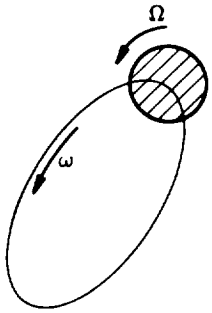

(c) Forward elliptical whirl

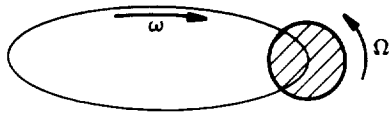

(d) Reverse elliptical whirl

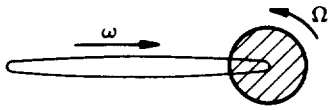

(e) Lateral vibration

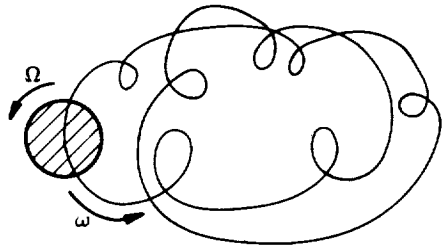

(f) Complex whirl

Figure 3. – Basic classifications of shaft motion

Table V – Types and Causes of Forced Whirling Identified by Yamamoto (refs. 58 through 61)

Type	Cause
Forward circular precession, $\omega = \Omega$	Rotor imbalance
Backward circular precession, $\omega = \Omega$	Unequal bearing stiffness in different radial directions
Noncircular precessions, $\omega = \pm \Omega$	Unequal bearing stiffnesses in different radial directions, or Transient changes in Ω, or Externally applied rectilinear vibrations
Shaft whipping caused by guard ring or shroud rub	When the shroud rubs, more stiffness is added to the shaft; and thus the critical speed is driven up ahead of the operating speed
Nonsynchronous motions, $\omega = (0.4 \text{ to } 0.5)\ \Omega$	One oversized or undersized ball or roller in bearing; thus motion is excited at cage rotational speed
Nonsynchronous motions, $\omega = 2\Omega, 3\Omega, 4\Omega, \ldots\ldots$	Bearing defects, such as oval inner or outer races
"Sum and difference" critical speeds, $\omega_i \pm \omega_j = \Omega$	Nonlinear, nonsymmetrical spring characteristics
Subharmonic precession, $\omega = \frac{\Omega}{2}, \frac{\Omega}{3}, \ldots\ldots\ldots$	Nonlinear, nonsymmetrical shaft stiffness
Unexpected jumps in response	Nonlinearity in shaft system stiffness or forcing functions

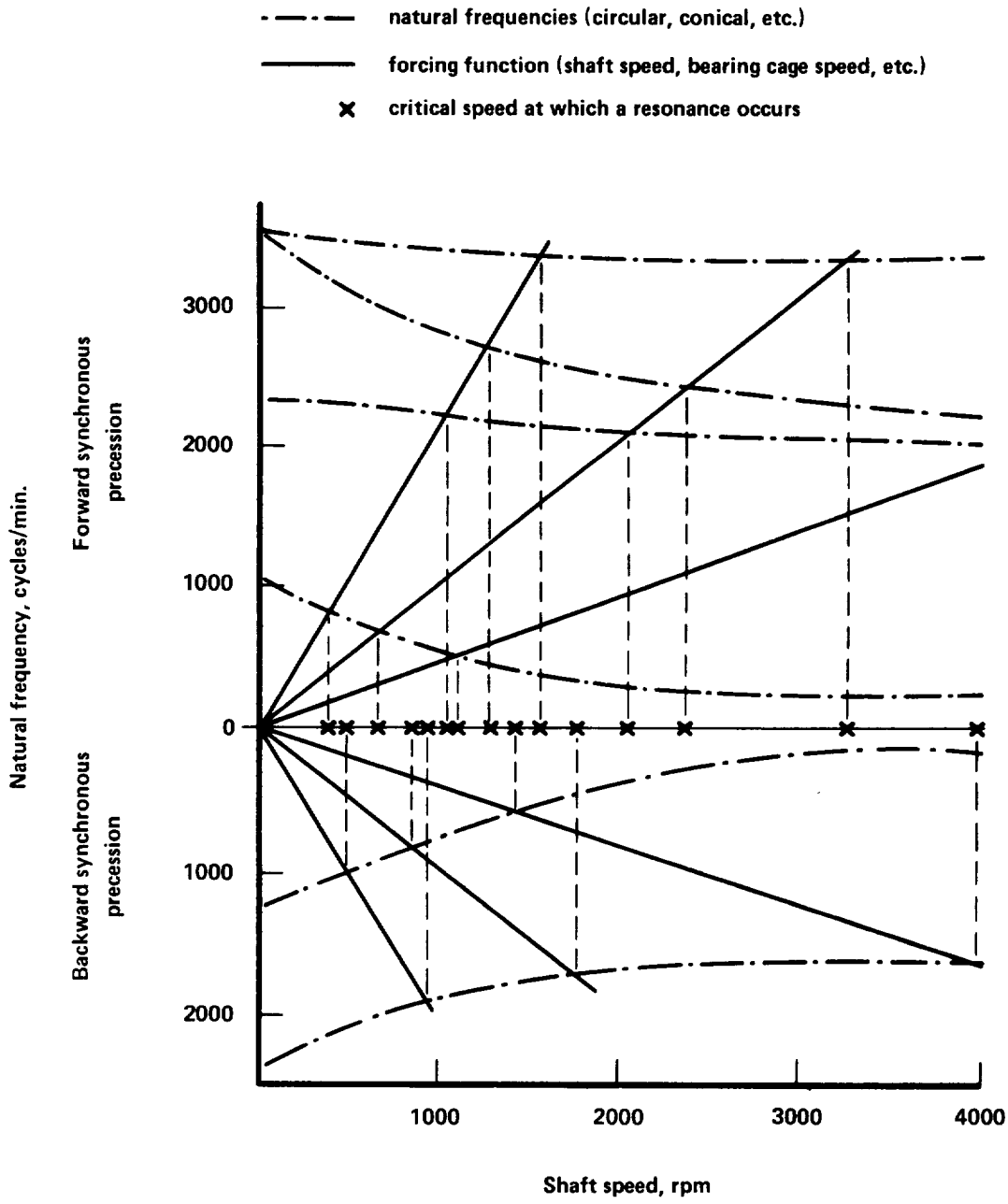

Figure 4. – Typical plot of shaft speed vs natural frequency (showing many secondary critical speeds for a shaft supported in rolling-contact bearings)

Usually, critical speeds associated with synchronous forward forced motions or precessions that are excited easily by rotor imbalance are considered as the most important. These synchronous-forward-precession critical speeds, whose values are governed primarily by the rotor mass and the combined or individual stiffnesses of the rotor, bearings, or bearing supports, are herein referred to as "major" critical speeds. "Secondary" critical speeds or resonances refer to all other critical speeds not classified as major. Thus, secondary critical speeds include the nonsynchronous criticals identified by Yamamoto, rotor/bearing/casing system criticals that are controlled primarily by the casing dynamics, and backward-whirl criticals. It is common practice to ignore the secondary critical speeds and consider only major critical speeds when designing a new turbopump, even though it is recognized that the nonsynchronous whirls described by Yamamoto can occur and can be troublesome. Accordingly, experimental evaluation after the machine is built usually is appropriate.

Parts (a), (b), and (c) of figure 5 show shaft motion of the Titan III (87-9) turbine shaft as measured by distance detectors mounted at right angles to each other and perpendicular to the shaft axis. These plots display some secondary resonances when increasing amounts of imbalance weight are added to the rotor. The secondary criticals, which were coupled system modes, were governed primarily by the casing dynamic characteristics. Note that the shaft orbit amplitudes were magnified dynamically by factors of only 2 or 3. The secondary criticals did not result in significant resonant buildup; with a well-balanced rotor, these secondary resonances were difficult to detect experimentally.

The casing local to the turbine bearings had a complex, irregular, asymmetric configuration. Tests showed both a generally soft radial direction and a stiff radial direction with intermediate local stiffness perturbations. These stiffness variations were responsible for a lateral vibration that was indicated by one distance detector peaking at the same time that a second detector decreased.

Other phenomena found experimentally are as follows:

(1) Unstable, sharply fluctuating response (fig. 5(d)) occurred when loose fits existed between the bearing outer race and the bearing sleeve and housing. During this unstable motion, the turbine gave off a "growling" noise.

(2) Tests with tight fits and very small bearing internal play showed very smooth response (fig. 5(e)).

(3) Tests with tight fits and nominal bearing internal play (0.001 in. [25μm] TIR) sometimes showed secondary unstable very-low-amplitude vibration throughout almost the entire zero- to full-speed range when rotors were well balanced. Adding imbalance stabilized the motion.

(4) The location of some of the secondary criticals shifted as much as 10 percent as a result of loose fits.

Sometimes it is difficult during the design phase to establish whether a particular rotor/bearing/casing critical should be considered as a major or secondary critical speed.

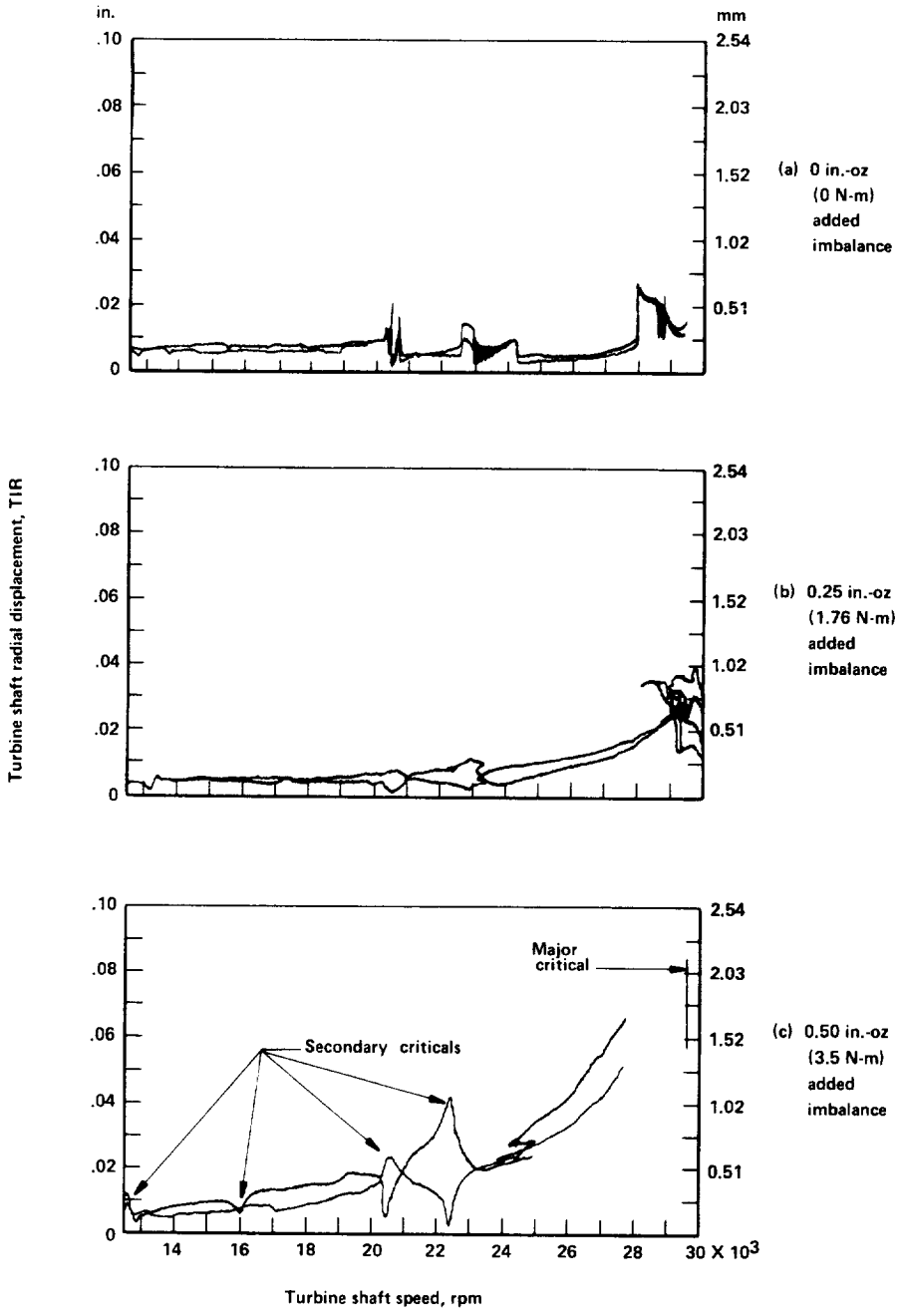

Figure 5. – Spin test data for Titan III XLR-87-AJ-9 turbine

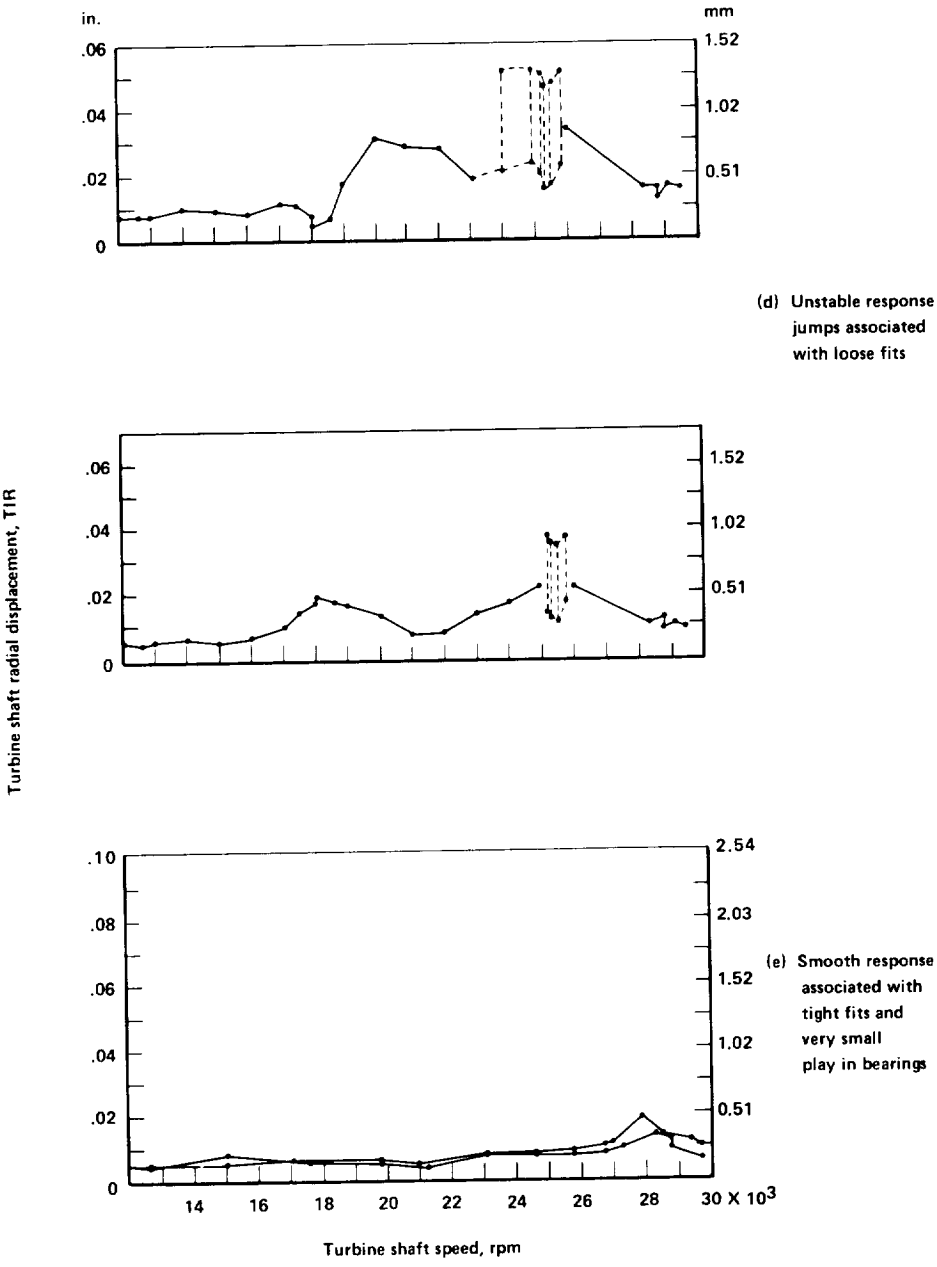

Figure 5. – Concluded

However, computed mode shapes for such system criticals frequently have been sufficient basis for judgment. For example, when the casing mass is much greater than the rotor mass and inspection of a mode shape shows most of the vibrational amplitudes to be in the casing, a good possibility exists that the associated critical speed rotor amplitude buildup will be limited to tenable levels, because casings usually can dissipate considerable vibrational energy. However, if the vibrational amplitudes are controlled only by bearing or bearing support displacements while the rotor and casing are acting essentially as rigid bodies, then untenable vibration amplitude buildup is probable if the shaft operates a sufficient time at the critical speed.

Inspection of only the mode shapes is not always adequate. The amount of energy dissipated each cycle is approximately equal to the product of the logarithm of the damping decrement and the vibrational kinetic energy of the structure. Some modes show little amplitude in the casing, and inspection alone would indicate large rotor amplitudes at the associated critical speed. When the system distribution of kinetic energy is evaluated, a large percentage of the vibrational energy may be found in the casing. This distribution is possible because of the relatively large mass of the casing, even though casing amplitudes are relatively small when compared with those of the rotor. Experience has shown that passing through or running at the system critical speeds that show most of the motion in the casing is practical as long as fatigue failures of the casing components do not develop. However, if the casing does not contain a large part of the vibrational energy, high bearing loads and attendant damage may occur. Durability of the casing is demonstrated by analysis and test.

Sometimes the mode shapes at the second and higher shaft-bending critical speeds are considerably different from those predicted by theory. It has been found experimentally that both second and third criticals have modes that consist of the usually predicted shapes super imposed with the first-mode shape (fig. 28.9 of ref. 78).

If a rotor, its bearings, and the casing have essentially symmetric mass and stiffness properties about the shaft axis, the most probable orbital motion is circular. For asymmetrical properties, the usual orbital motion is elliptical and, at the criticals, approaches lateral vibration. The Titan II (87-5) shaft, which utilized angular-contact bearings and was a built-up shaft with many joints, was supported in a casing that was highly asymmetric in both stiffness and mass. Shake tests of the rotor supported in "rigid" bearing mounts yielded fundamental bending frequencies ranging from 315 to 365 cps, the value depending on excitation amplitude. When the rotor was assembled in the casing, the lateral-vibration natural frequencies dropped a small amount in magnitude and assumed some directional dependency. When the shaft was spin tested in the assembled casing, dual resonant peaks were found at approximately 290 and 340 rps. Normally, a spinning-shaft natural frequency (critical speed) is expected to be somewhat higher than the lateral-vibration natural frequency because the disk gyroscopic moment stiffens the shaft. However, the dual resonance peaks corresponded to lateral-vibration shaft motions in planes at right angles to each other. As the motions were lateral rather than circular, the disk gyroscopic stiffening moments associated with forward circular orbits vanished.

Response predictions usually are accomplished during the design analysis phase to obtain such data as bearing reactions, whirl orbits, shaft shear and bending moments, and sensitivity to locations of imbalance. These data then are compared with bearing capacities, rotor tip clearances, joint and bolt preload and stiffness capabilities, and the planes of balancing, respectively.

Gear teeth, misaligned crowned splines, and flexible couplings have been known to couple shaft lateral and torsional motions. Rotor blades that had a natural frequency close to a shaft critical suffered fatigue cracking failure. Thus, comparison of the critical speed to other known resonant speeds is useful.

When fluid-film bearings are used, in most instances the undamped-critical-speed calculations wherein bearing stiffness is considered but damping is neglected are insufficient. Often, undamped critical speeds do not correspond to the speed of maximum rotor imbalance response (ref. 79). Thus, response computations usually are used to evaluate the effect of bearing damping on locations of critical speeds; vibration amplitudes at critical speeds; and response of the rotor, throughout the operating speed range, resulting from the amount and distribution of imbalance.

2.2.1.3 SELF-EXCITED WHIRLS AND INSTABILITIES

Self-excited whirls of shafts supported in rolling-contact bearings have been linked with aerodynamic excitation forces, internal rotor friction attributable to causes such as shrink fits and builtup rotors, and dry friction. Shafts using fluid-film bearings can develop hydrodynamic-excited whirls.

Self-excited whirls and instabilities of shafts operating supercritical still do not lend themselves to accurate computational evaluation. Only for the simplest machines can the whirl threshold speed be accurately predicted, and whirl amplitudes are not predictable for any machine. The present practice for supercritical designs is to minimize those design factors that promote instabilities (e.g., shrink fits, builtup shafts, and rotor flexibility), build the machine, and experimentally confirm its stability or develop it into a stable operating machine.

2.2.1.3.1 Aerodynamic-Induced Instability

The E-blade Mark 9 axial-flow turbopump exhibited strong nonsynchronous whirl motion under certain operating conditions. The exact cause, or the mechanism that initiated this behavior, was not established conclusively. However, the instability appears to have been a hydrodynamic effect created by a circumferential variation in the pump pressure distribution. One E-blade Mark 9 pump failed catastrophically; self-excited whirl was strong among the possible causes identified by failure analysis reported in reference 80. Figure 6 (from ref. 80) illustrates the typical rotor motions arising from aerodynamic-induced instability.

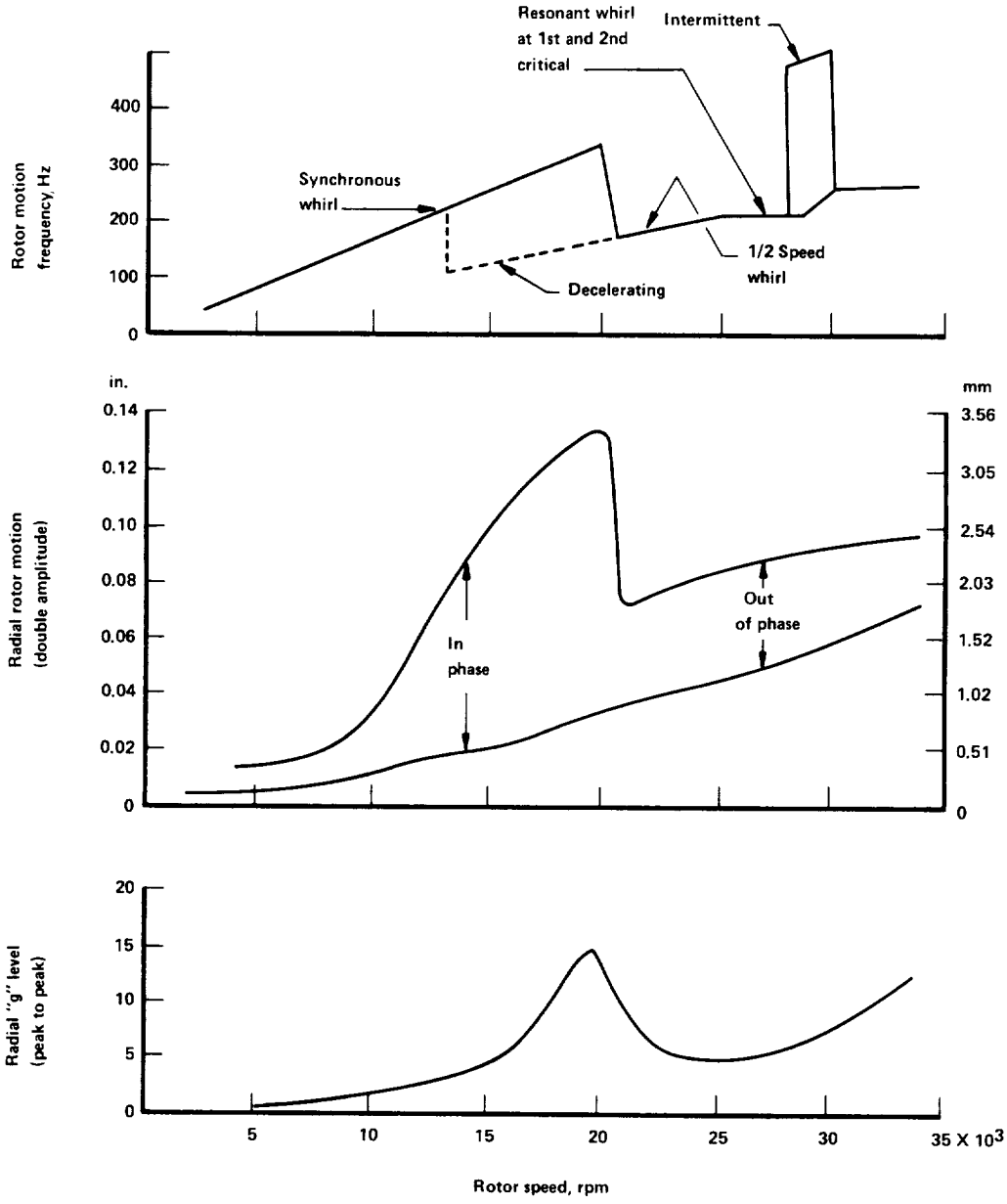

Figure 6. – Typical rotor motions due to aerodynamic–induced instabilities (ref. 80)

The Mark 25 axial-flow pump exhibited subsynchronous whirl (ref. 81). However, no known hardware damage occurred during the many system tests conducted, even though the resulting vibration levels were undesirable. An experimental liquid-hydrogen turbopump experienced nonsynchronous whirl caused by either hydraulic instability or loose fits (ref. 82).

Severe aerodynamic-excited whirl of several jet-engine axial compressors and turbines resulted from two causes (ref. 83): (1) the circumferential variation of static pressure acting on the cylindrical surface of the rotor, particularly within the labyrinth seals; and (2) the eccentricity of the rotor causing circumferential variation of the blade-tip clearance and a corresponding variation in local efficiency and imbalance torque. Several different designs exhibited whirling. All rotors that whirled had relatively large rotor flexibility, which was demonstrated by the low critical speed of the rotor and support system. In almost every instance, stability was achieved by increasing the stiffness of the rotor or that of the rotor support or both. The whirl speed was approximately 40 to 50 percent of the rotation speed. Reference 83 states that damper bearings providing friction relative to fixed axes effectively help protect against shaft whip and whirl. Self-excited whirl caused by pressure changes associated with varying clearances around the labyrinth seals also is mentioned in reference 84.

Fluid-film thrust bearings sometimes are used in conjunction with rolling-contact radial-load bearings. If the fluid has sufficient viscosity, these thrust bearings may develop damping forces in the direction normal to the shaft axis and thus tend to inhibit self-excited whirl. A reduction of thrust, however, could reduce the damping enough to permit whirl; such a possibility was mentioned in association with the removal of the gravity field from a vertically mounted rotor (ref. 85). Film thrust bearings used in liquid hydrogen are not expected to produce much damping.

2.2.1.3.2 Instability Caused by Internal Friction

Whereas external frictional forces usually aid in damping the oscillations, the internal frictional forces can, under certain circumstances, cause unstable whirl buildup if the shaft is operating above its first critical speed. Sources of internal friction found to be significant are builtup shafts and joints or disks shrunk or firmly bolted onto the shaft. Hysteresis forces in the shaft material have been identified as a possible source of internal-friction-induced instability, but no instabilities attributable to this cause have been reported. Most of the available information on effects of internal friction on the stability of high-speed rotors is summarized in reference 86.

2.2.1.3.3 Whirl Induced by Dry Friction

The phenomenon of a violent shaft backward whirl or whip caused by friction in a dry-clearance bearing (i.e., the clearance between outer race and housing is not lubricated) or by the shaft striking a rough or unlubricated guide is described on page 292 of reference 84.

A recent study (ref. 87) shows how the occurrence of slip between the shaft and the bearing can contribute to the violence of the whirl and can cause it to develop into near-resonant motion over a large range of speeds. This whirl motion and instability buildup can occur also when the shaft is operating below the system first critical speed. This kind of problem is relieved by tightening the bearing fit, or by pinning the bearing to prevent rotation, or, in extreme cases, by making the inner bearing race integral with the shaft.

2.2.1.3.4 Whirl Induced by Fluid-Film Bearing

Subsynchronous whirls sometimes are referred to as oil whip, resonant whip, half-frequency whirl, or just nonsynchronous whirl. Such whirls caused by the characteristics of fluid-film bearings are again becoming of concern in the design of rocket engine turbopump shafts. Most recent turbopump shaft designs utilized rolling-contact bearings. However, the needs for increased performance, higher speed, and longer life have resulted in the serious consideration of fluid-film hydrostatic bearings. Rolling-contact bearings have DN and life limitations related directly to shaft size and speed, whereas fluid-film bearings apparently do not. Thus a shaft with rolling-contact bearings is more restricted in diameter than a shaft with fluid-film bearings, the result being a shaft with less stiffness and lower shaft bending critical speeds.

Within the last few years, the state of the art has been enlarged greatly in regard to the mathematical modeling of the fluid-film bearings and accuracy of the analysis of the influence of these bearings upon shaft stability and response to imbalance force (refs. 63 through 65, 68, and 79). The improved dynamic analyses give good predictions of actual operating characteristics.

2.2.1.4 TORSIONAL CRITICAL SPEEDS

The torsional vibrational modes in rocket engine turbopump shafts have not limited or controlled design. Often, torsional critical speeds are not even calculated; but, when they are, the calculated values usually are compared with the possible forcing frequencies of (1) gear teeth meshing (when gears are used), (2) low orders of rotational speed (i.e., speeds equal to rotor speed or low multiples thereof) caused by shaft imbalance or misalignments of couplings, and (3) impeller-vane and stator-vane passing frequencies.

In addition, these calculated torsional natural frequencies are compared with other system natural frequencies (e.g., shaft whirl or lateral vibration, turbine blades, and impeller vanes) to ascertain whether any possible coupling or energy transfer is likely.

2.2.1.5 THIN-WALL HOLLOW-SHAFT VIBRATIONS

Thin-wall, cylindrical, drum-type shafts, which are characteristic of axial-flow pumps, have experienced critical-speed problems and fatigue cracking associated with nodal-circle and

nodal-diameter vibrations of the type shown in figure 7. The usual design modification is to change the environment acoustics to reduce the magnitude of excitation, change the driving frequencies, or change the shaft vibration natural frequencies.

2.2.2 Analysis of Shaft Dynamic Behavior

2.2.2.1 MODELING FOR THEORETICAL ANALYSES

Even though simple models have been adequate in some cases, experience has shown that the classical models for predicting shaft whirl critical speeds and response usually yield very crude estimates. This has been attributable primarily to the exclusion of, or improper account for, the effects of influential items: rotor mass and stiffness distributions, mechanical joints, shaft-riding elements, abrupt changes in shaft cross section, casing and machine mount effects, bearing spring and damping forces, shear deformation, gyroscopic and rotary inertia moments, rotor imbalance forces, and virtual mass and damping associated with operating in dense fluids. Details of current techniques for modeling and analyzing these critical items are presented in the sections that follow.

The technology of modeling for torsional critical speeds is adequately set forth in references 88 through 90. Reference 88 covers modeling procedures and summarizes many formulas and charts for modeling common shaft components to obtain equivalent mass and stiffness distributions. Consideration is given to the hollow circular shaft with an eccentric bore; the solid shaft with a linear taper (a gradual change in cross section); the abrupt-step shaft; the shaft with a keyway; the splined shaft; the shaft with a flat side; a branched system running at different speeds; torsional stiffness of spur and bevel gears, spiral gears, helical gears, couplings, and clutches; and other significant conditions. No further discussion of torsional critical speeds will be presented herein.

2.2.2.1.1 Mass and Stiffness Distributions

Significantly improved models for shaft-dynamics analyses have been developed over the past decade (refs. 6, 54, 79, and 91 through 93). Figure 8 illustrates two of the typical improved shaft dynamic models. In figure 8(a) (ref.6) K^L represents the lateral spring constants of the casing mounts and bearings, and K^T symbolizes the torsional spring constant at the shaft/rotor splines; C^L and C^T represent corresponding damping coefficients for use with the indicated spring constants. In figure 8(b) (ref. 92), the bearing lateral spring constant K is subscripted p or t to identify the bearings at the pump or turbine end, respectively.

Tradeoffs between model and analysis complexities have resulted in the Myklestad lumped-mass model or an extension thereof being the one most commonly used. In its simplest form, this model consists of the rotor masses lumped at stations along the rotor and connected by massless elastic beams and linear support springs (refs. 94 through 96). The usual refinements to this model include the addition of shear deformation to the beam and

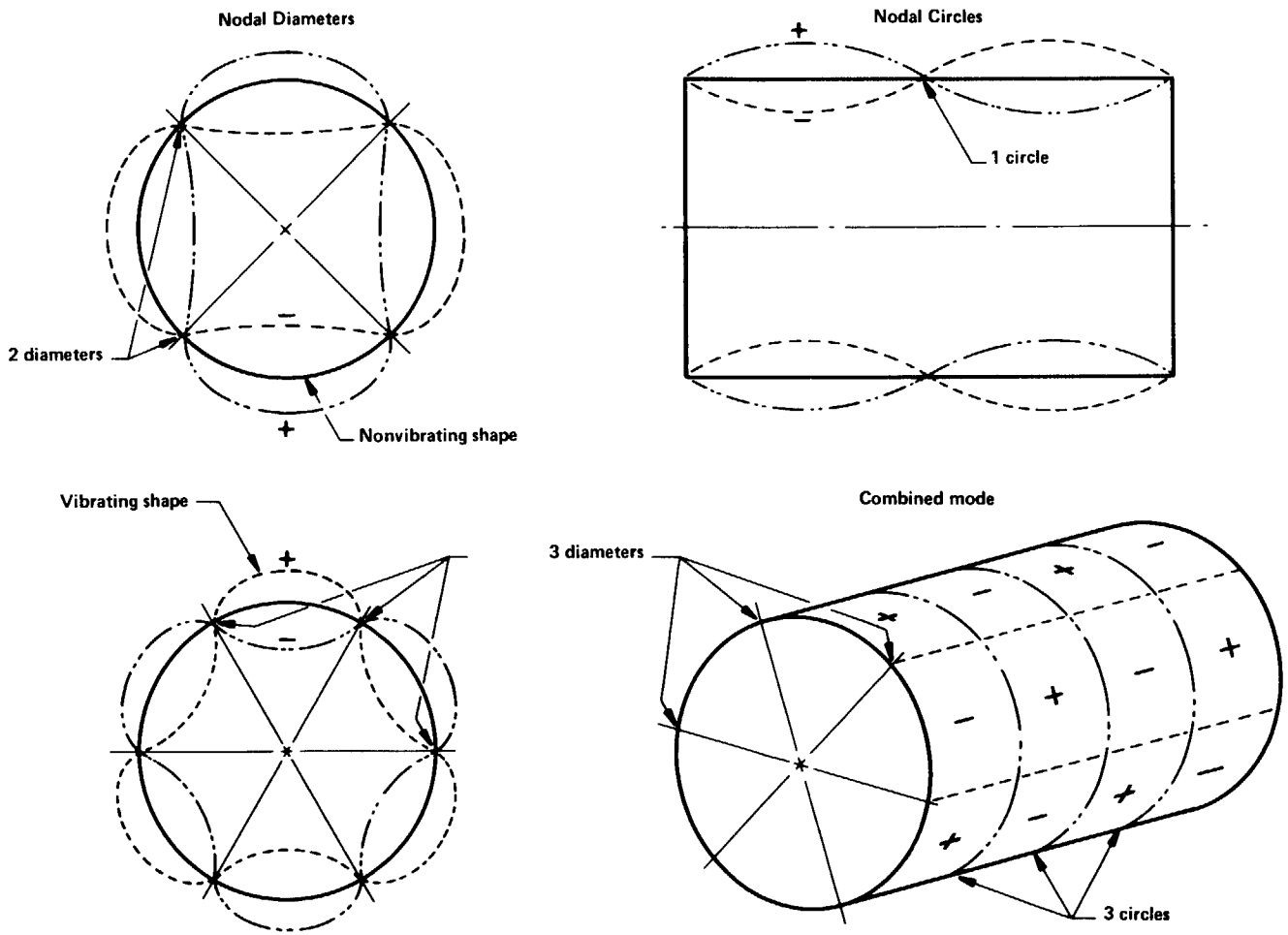

Figure 7. – Nodal-circle and nodal-diameter vibrations in a thin-wall hollow shaft

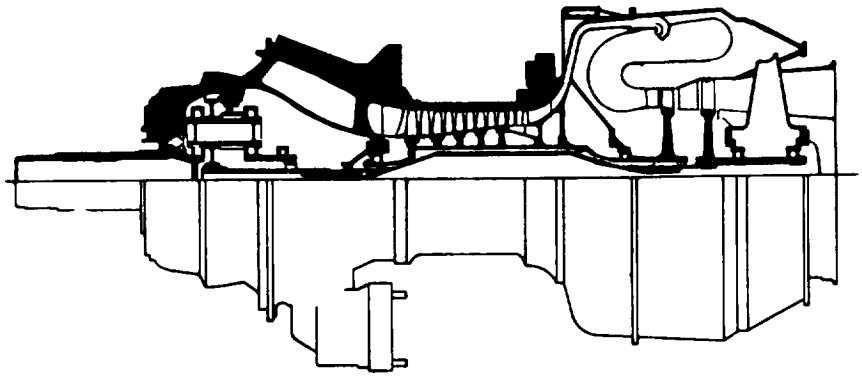

(T53 turboprop engine)

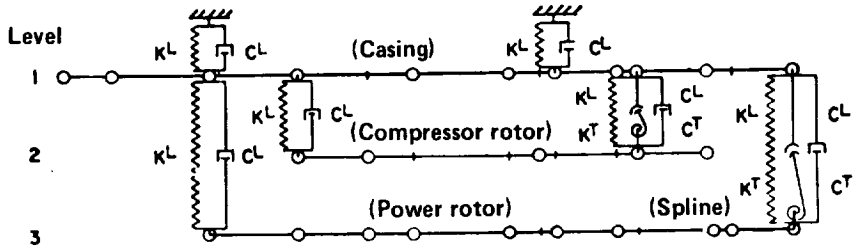

(T53 equivalent dynamic system used in connection with the vibration analysis)

(a) T53 turboprop engine (ref. 6)

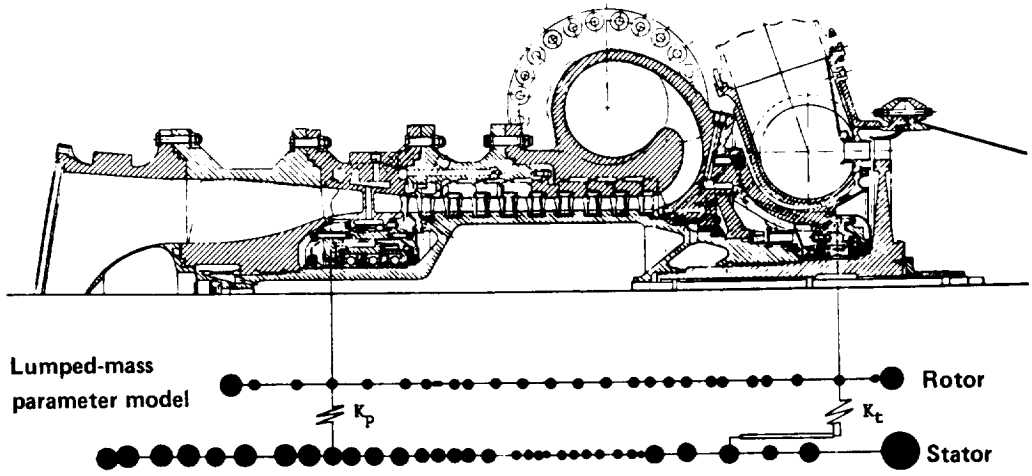

(b) M-1 fuel turbopump (ref. 92)

Figure 8. – Typical models for shaft dynamics analysis

gyroscopic moments (ref. 97). Further refinements have included the use of uniform continuous-mass beams instead of massless beams (refs. 54, 79, and 88), unsymmetrical bearing stiffness and damping models for fluid-film bearings (refs. 54, 79, and 91), nonlinear bearing stiffness for rolling-contact bearings (ref. 92), gyroscopic representation for nonsynchronous whirl (ref. 98), and coupled rotor/casing multiple-beam models (refs. 6, 92, 93, and 97).

2.2.2.1.2 Mechanical Joints, Shaft-Riding Elements, and Abrupt Changes in Shaft or Casing Cross Sections

The stiffness of a builtup rotor usually is far less than that of a one-piece rotor even when the joints are preloaded at assembly. If the forces applied to the joint during operation exceed the preload, the joint can open up and cause a loss in overall stiffness. Figure 9

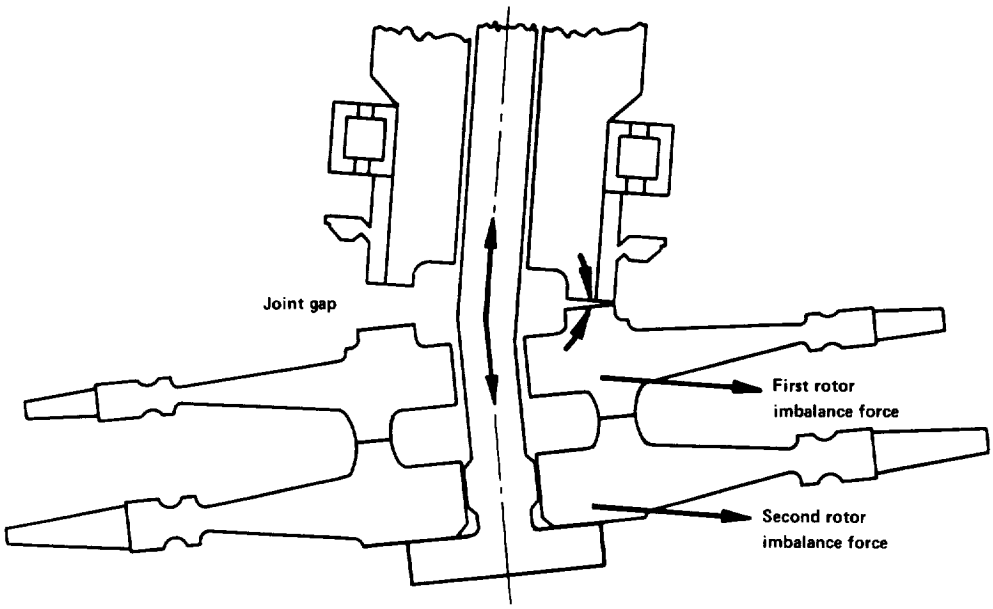

Figure 9. – Curvic coupling joint loosening under load

depicts the condition wherein the centrifugal forces of the turbine wheels imposed sufficient moment to overcome the joint preload and cause a great increase in joint flexibility. Even properly preloaded joints do not ensure that a builtup rotor will develop stiffnesses approaching that of one-piece construction. Curvic couplings with full preload are inherently a local flexibility in comparison with welded joints of similar size. However, if the coupling is placed in a position of low shaft bending moment, the local softness may not result in a significant reduction in rotor stiffness and natural frequencies. Couplings used as shown in figure 10 have exhibited additional flexibilities.

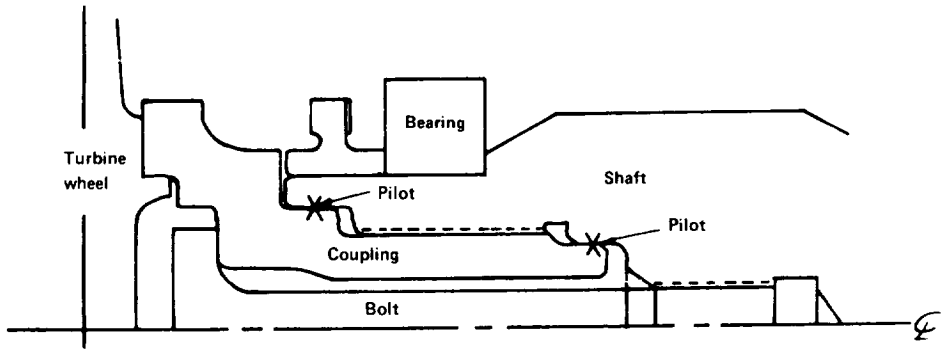

Figure 10. – Coupling between shaft and turbine that results in additional flexibilities

Shaft-mounted components (e.g., shrunk-on impellers, shaft sleeves, and bearing races) usually result in stiffening of the shaft; however, the degree of stiffening may be influenced by axial preloading. Long stackups of shaft-riding elements sometimes do not obtain good axial preloading when each piece is put on the shaft with interference fits. Gaps as shown in figure 11 cause a reduction in shaft stiffness. Any abrupt changes in shaft cross sections, such as the transition in a hollow shaft from a small to a large diameter, produce local flexibilities as indicated in figure 12.

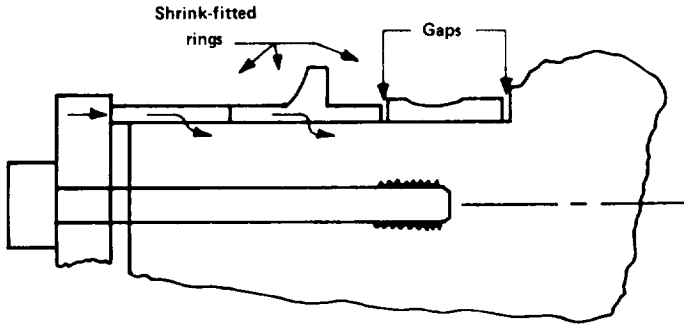

Figure 11. – Gaps on shaft-mounted components that affect overall shaft stiffness

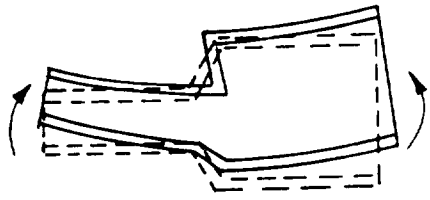

Figure 12. – Local flexibility of hollow shaft at transition from large to small diameter

2.2.2.1.3 Casing and Machine Mount Effects

Bearing-support flexibility can exert significant influence on critical speeds (refs. 6, 7, 54, 55, 93, and 99 through 102). The following are the four major considerations regarding casing and machine mount effects:

(1) Gross trends in casing mass and mount stiffness
(2) Dynamic coupling with the rotor
(3) Casing stiffness local to the bearings and near locations where loads are concentrated (e.g., struts)
(4) Symmetry of the casing mass and stiffness about the shaft axis

Analysis of the simple 2-degree-of-freedom system (ref. 99) provides some insight into the first major consideration. Figure 13 shows the general solution. Here M_1, K_1, M_2, K_2

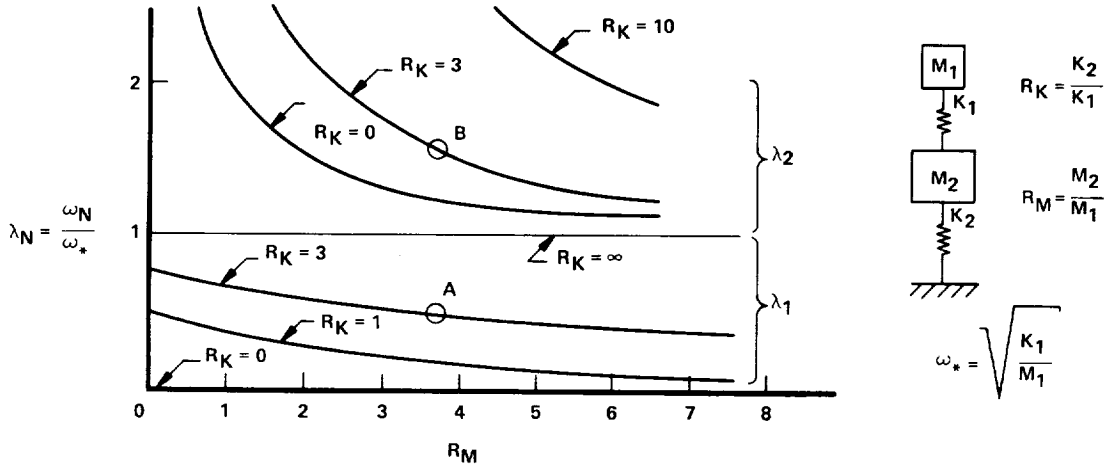

Figure 13. – General solution for simple 2-degree-of-freedom system

represent the rotor mass, rotor and bearing stiffness spring constant, casing mass, and casing mount stiffness spring constant, respectively; ω represents the whirl frequency, subscript i (i = 1 or 2) denoting the first or second system natural frequency and * denoting the simple rotor/bearing natural frequency. The symbols R_K and R_M are ratios of the casing-to-rotor spring constants and casing-to-rotor masses; λ_i is the ratio of shaft system natural frequency to the simple 1-degree-of-freedom rotor/bearing natural frequency.

If the casing mass M_2 is much larger than the rotor mass M_1 (i.e., R_M is relatively large) and the casing mount stiffness spring constant K_2 is relatively small, a system natural frequency less than ω_* will exist. This frequency, corresponding to point A, will be substantially lower than the rotor/bearing natural frequency $\sqrt{K_1/M_1}$ indicated by $\lambda_1 = 1.0$, analogous to K_2 and

therefore R_K tending toward infinity. A second system natural frequency such as point B will exist above the simple rotor/bearing natural frequency.

This analogy suggests that if proper mass and stiffness proportions are used in the design of the machine housing and mounting, two results will follow:

> First: There will be low natural frequencies whose modes consist of the entire machine vibrating in a rigid-body fashion on the mounting springs with very little relative motion between the rotor and its casing. The shaft speeds that excite these vibrations will be equal to the low natural frequencies. Damping could easily be supplied to limit the amplitudes of these vibrations.
>
> Second: The first significant shaft whirl critical speed will be equal to or above that of the rotor/bearing model.

Experience with rocket engine turbopumps has shown the first expected condition to be an accurate prediction. Usually, the low rigid-body modes occur at approximately 5 to 10 percent of the nominal shaft speed. Thus, no loss in accuracy occurs in predicting high-speed shaft response as a result of omitting the mounting stiffness in the analytical model. However, the second consequence indicated often is not valid because of the effects of dynamic coupling of the casing with the rotor and because of the effects of casing stiffness local to the bearings.

Dynamic coupling of the casing with the rotor has been found to be very influential in machines using rolling-contact bearings in conjunction with flightweight casings (refs. 6, 103, and 104). Use of a variable-property beam to model the casing in a manner similar to that for modeling the rotor has given good results.

A flexible tie between the rotor and casing (e.g., a low-stiffness hydrodynamic oil journal bearing or a flexible housing supporting the bearing) can, if it has an appropriate amount of flexibility, effectively decouple the casing from the rotor dynamics. In this case, a model considering the casing as ground yields good predictions.

Casing flexibility local to the bearing is undesirable when the shaft is designed to operate below the first system critical speed. This local flexibility, which is typical of an overhung turbine with rolling-contact bearings, usually occurs in the housing between the bearing outer race and the larger diameter pump casing. An M-1 turbopump bearing-support housing that exhibited flexibility was evaluated both analytically and experimentally for static spring rate (ref. 92). The analytical evaluation utilized two methods: an approximate-beam solution, and a finite-element solution (ref. 105); the experimental evaluation consisted of testing scaled aluminum models. The major findings were as follows:

(1) Shear deformation and warping of the end circular cross section into an oval pattern were the major flexibility sources.

(2) The stiffness computed by the approximate-beam method was 2½ times greater than the actual value.

(3) The stiffness values computed by the finite-element method were within 4 percent of the model test data.

The degree of symmetry of the casing mass and stiffness about the shaft axis influences the critical speeds. When symmetry exists, the shaft usually executes forward synchronous circular whirls as a result of imbalance. The critical speeds then are predicted on the assumption that disk gyroscopic stiffening is operative. When asymmetry in casing mass and stiffness exists, the shaft starts to execute elliptical whirl as it approaches a critical speed, and the whirl will become a lateral vibration. Where a symmetrical casing normally would have a single critical, the asymmetry causes two criticals to occur. Further, the criticals can occur at much lower speeds because the lateral motion causes the disk gyroscopic stiffening effects to vanish and disk rotary inertia softening to occur (ref. 106).

2.2.2.1.4 Bearing Spring and Damping Forces

Cylindrical roller and angular-contact ball bearings are the only types of rolling-contact bearings that have been used extensively for radial support in rocket engine turbopumps. Since internal damping of a rolling-contact bearing is negligibly small, stiffness is the important bearing characteristic that influences shaft dynamics. Approximate values of spring rate can be computed using the Palmgren formulas (refs. 107 and 108). Methods for more accurately determining spring rates are available in references 108 through 112. Reference 1 presents additional material on bearing load characteristics.

Usually, the shaft whirl is assumed to be circular. When unidirectional radial bearing reactions are small compared with the expected rotating radial bearing reactions associated with whirling, the spring-rate value K has been taken as the secant rather than the tangent value, i.e., $K = R/\delta$ instead of $K = dR/d\delta$, where R is the radial load and δ is radial displacement (refs. 72 and 92).

The bearing spring rate usually is nonlinear. The cylindrical roller bearing, which is a load-stiffening system, is well represented by an exponential function relating radial load R to radial displacement δ, e.g., $R = A\delta^B$ where A and B are constants, and $K = R/\delta = A\delta^{B-1}$. The spring-rate behavior of the angular-contact bearing can vary from almost linear to highly nonlinear, depending on the preload, applied load, and rotational speed. Stiffness characteristic ($K = dR/d\delta$) curves that have been published (ref. 56) were developed with equations that account for preload, applied load, and change in contact angle but exclude the effects of ball centrifugal and gyroscopic loads that are important at high rotational speeds (ref. 113). However, mathematical formulations described in reference 112 include all the effects associated with high rotational speed. A computer program based on these formulations was applied (ref. 114) to 40mm, 15° angular-contact bearings; the spring-rate characteristics shown in figure 14 resulted.

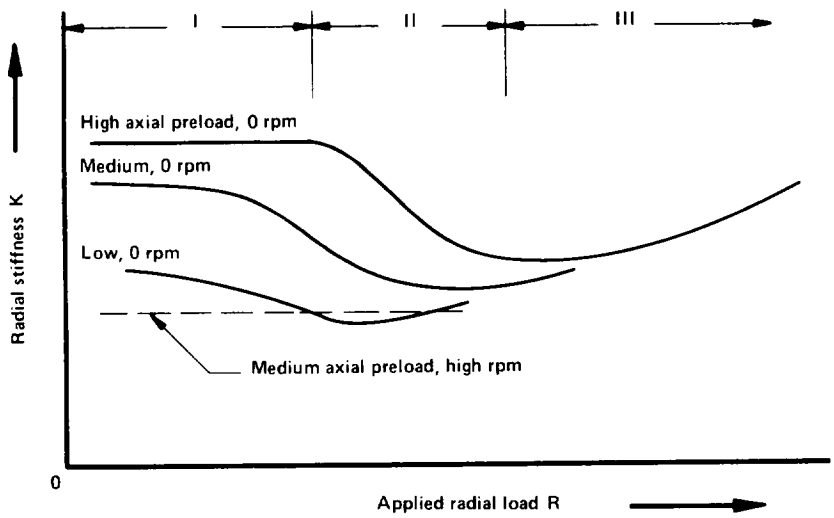

Figure 14. – Typical stiffness characteristics calculated for angular-contact bearings (ref. 114)

Neglecting speed effects, the charateristics are identical to those given in reference 56. There are three basic regions: the first (I) shows almost constant stiffness, the second (II) shows a decrease to a minimum stiffness, and the third (III) shows increasing stiffness. Region I is typified by sufficient axial preload to hold the stiffness high and constant. In region II, the magnitude of radial load approaches the axial preload and fewer balls are in contact, the result being a decrease in stiffness. In region III, the axial preload is no longer effective and, as the radial load increases, the stiffness starts to increase because the ball contact areas are increasing rapidly. Most importantly, when the speed effects were included in the analysis, it was found that the stiffness dropped approximately 50 percent in the regions of low applied radial load. Thus, it appears that the speed effects negated the expected beneficial effects of axial preload on radial stiffness. This effect is shown in other published works (refs. 80 and 115).

Cylindrical roller bearings develop radial resistance to radial motion only. However, angular-contact ball bearings can develop both radial and axial reactions. The radial reaction for a radial displacement is, by far, the primary resistance. However, in cases where the bearing stiffness controls the shaft dynamics at operating conditions, all resistances may have to be included to achieve good predictions.

Some analysts have attempted to account for the moment resistance in angular-contact bearings by using a radial spring located at an "effective bearing center" instead of at its actual location on the shaft, as shown in figure 15.

The effective-bearing-center location has in the past been taken incorrectly as point CP. One investigator (ref. 116) considered this condition and concluded that the location lies approximately halfway between points CP and BL. Experience has shown that, with shafts

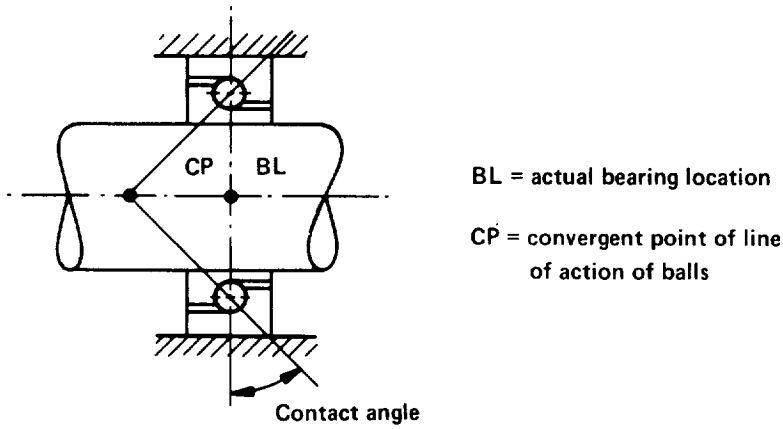

Figure 15. – Model for locating effective bearing center for angular-contact bearings

supported by angular-contact bearings, often only the radial resistance represented by a nonlinear spring located at the actual bearing center is necessary to obtain good predictions of shaft dynamics.

The representation of all-fluid-film journal bearings by linearized equations has produced good design information (refs. 54, 57, 79, 117, and 118). Eight coefficients representing both spring and damping forces are used. These coefficients are calculated from lubrication theory and the properties of the particular bearing. Moreover, coefficients have been published for many of the types of fluid-film bearings (refs. 57, 119, and 120).

2.2.2.1.5 Rotor-Imbalance Forcing Functions

A shaft usually exhibits synchronous whirl during operation because of the centrifugal forces associated with rotor imbalance. The amplitude of this whirl is related to the rotor-imbalance forcing functions. Actual rotor imbalance in rocket turbopump shafts rarely is equal to the balancing limits specified by the engineering drawings. This difference results from the shaft usually being balanced initially by subcomponents and then as an assembled rotor on a balancing machine (ref. 121), disassembled, and then reassembled in the turbopump. Misalignments allowed by factors such as pilot tolerances, runouts, parallelism, and perpendicularities can alter the very fine balance attained with the balancing machine (refs. 122 and 123).

Fits shift during operation as a result of effects such as thermal expansion differences between adjacent parts and mechanical deformations attributable to centrifugal forces. Sometimes these fit shifts allow eccentric shifting of adjacent rotor parts and thereby produce rotor imbalance. Furthermore, when roller bearings are used to support the shaft, the internal play in these bearings can allow the shaft to excite cylindrical or conical whirl modes of motion; this is especially true if the magnitudes of unidirectional radial loads from sources other than whirling are small relative to the potential whirl forces. This whirling associated with bearing internal play (fig. 16) can develop centrifugal loads that reach an

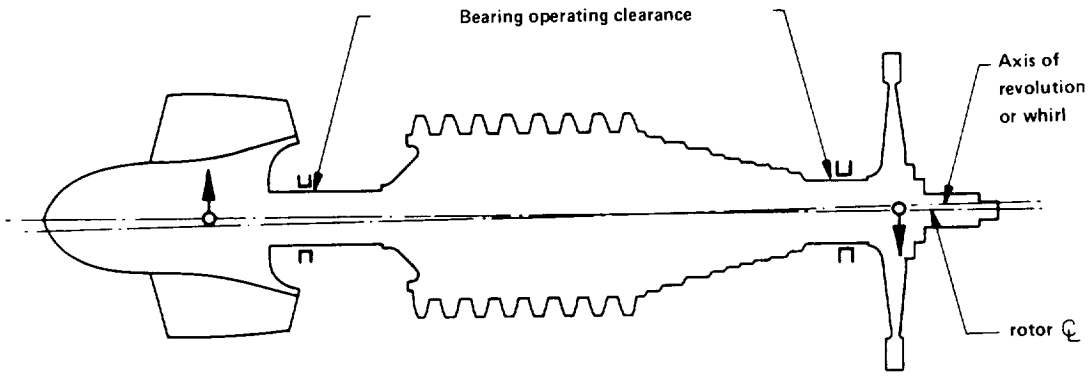

Figure 16. – Conical whirl associated with bearing internal play

order of magnitude greater than those resulting from the specified balance limits (refs. 92, 124, and 125). The effects of clearance between the outer race and the casing for an axially preloaded ball bearing are best determined experimentally; analytical treatments of possible effects are discussed in references 72 and 74 through 76.

The following examples indicate the possible magnitudes of imbalance and its influence on shaft response:

> In the XLR-87-5 engine, the high-speed shaft weighed approximately 25 lb (11.3 kg); it was balanced to a specified value of 0.01-in.-oz (0.071 N-mm) static and 0.05-in.^{2}-oz (9.0 N-mm^2) dynamic imbalance. Blueprint tolerances allowed 0.001-in. (25μm) looseness between the pilot diameters at the two joints holding the two overhung turbine rotors and shaft together. Disassembly after balancing was necessary. Based on the pilot tolerances, reassembly static imbalance could be on the order of 0.4 in.-oz (2.8 N-mm), which is 40 times the specified requirement. Checks made on the balance machine verified that loosening of the turbine rotor bolts and radial shifting of the rotors could induce the above stated limits (ref. 123). Eventually the entire shaft was redesigned to eliminate this problem and others that had developed.
>
> In another case (ref. 122), a gas-turbine rotor was to be balanced to an error of 0.02 in.-oz (0.141 N-mm). However, in production, runouts could not be held to better than 0.001 TIR, which was equivalent to 0.10 in.-oz (0.71 N-mm). Also, the rolling-contact inner race runout tolerance of 0.002 TIR added another 0.02 in.-oz (0.141 N-mm). Thus, imbalance six times greater than the balance error was possible. The problem was solved by redesigning the bearing system, replacing rolling-contact bearings with fluid-film bearings.
>
> As a final example, figure 17 shows the source and magnitude of residual imbalances in the M-1 fuel turbopump rotor (ref. 92).

Component	Weight		Specified balance limit	
	lb	kg	in.-oz	N-mm
Rotor and blades	380.0	172.4	0.141	0.02
1st-stage inducer	82.0	37.2	.141	.02
2nd-stage inducer	9.3	4.2	.141	.02
Thrust balance disk	19.3	8.8	.072	.01
Turbine rotor	215.0	97.5	.353	.05
Balance plane I:	.35 in.-oz (2.47 N-mm) spec.; .25 in.-oz (1.76 N-mm) actual			
Balance plane II:	.75 in.-oz (5.29 N-mm) spec.; .48 in.-oz (3.39 N-mm) actual			

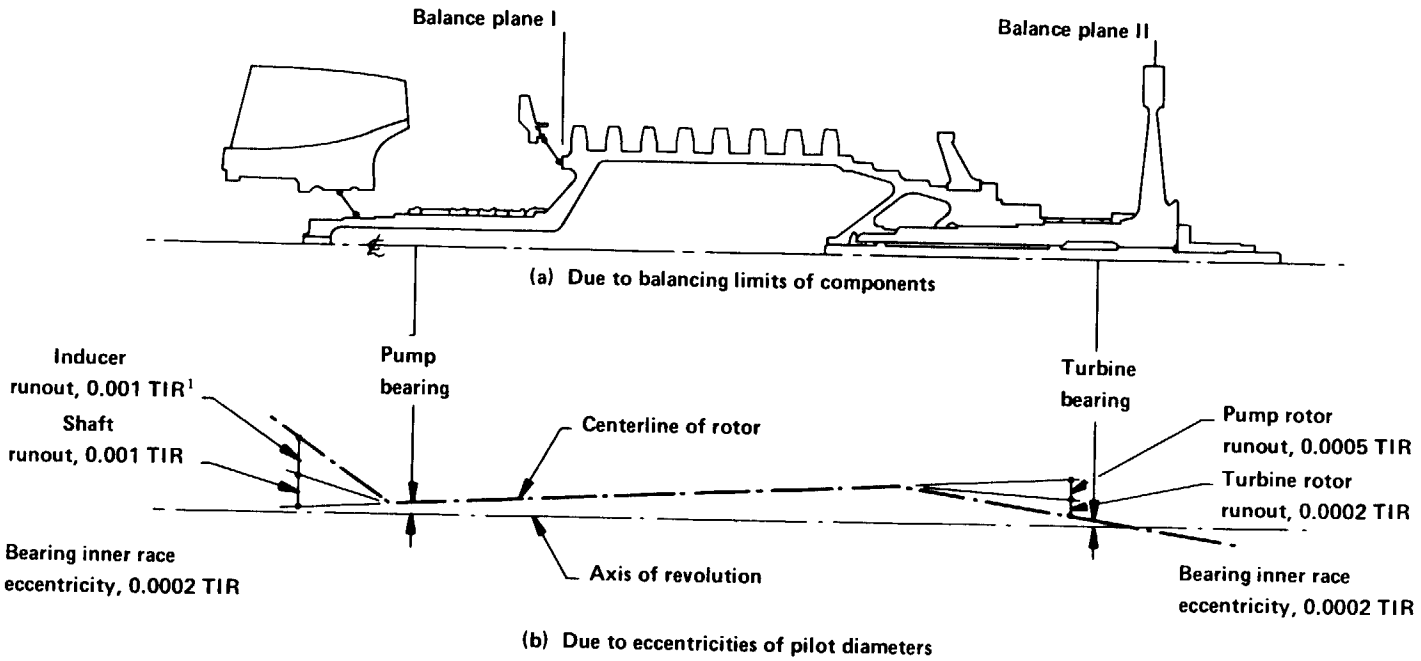

[1] TIR units are in inches (.001 in. = 25.4 μm).

Figure 17. – Residual imbalances, M-1 fuel turbopump rotor (ref. 92)

2.2.2.1.6 Virtual Mass and Damping

Virtual mass and damping associated with operation in dense fluids can have significant effects on the shaft dynamics. Unfortunately, a good quantitative analysis to evaluate these effects does not exist at the present time.

A study of the effect of gear restraint on the whirl of a pinion shaft (ref. 126) found that (1) whirl amplitude was reduced by frictional damping; (2) the resonant frequency was reduced, presumably by the inertia effects of the gear; (3) subharmonic as well as superharmonic resonances appeared in some of the tests because the vibration system was nonlinear; and (4) a self-sustained whirl frequency occurred.

2.2.2.2 MATHEMATICAL METHODS AND COMPUTER SOLUTIONS

Most of the digital computer programs suitable for calculating the natural frequencies, mode shapes, and imbalance response are based on or are extensions of the techniques given in references 96, 127, and 128. Good discussions of these methods are available in references 97 and 129.

References 88, 89, and 90 describe the appropriate methods for calculating torsional critical speeds. In addition, reference 88 provides a computer program in FORTRAN.

2.2.2.2.1 Analysis of Rotors Supported by Fluid-Film Bearings

Reference 65 includes program descriptions, a user's manual, and FORTRAN listings; it is available to qualified users from the U.S. Defense Documentation Center, Alexandria, VA.

Two programs are outlined in the reference:

(1) Imbalance response of a rotor in fluid-film bearings

(2) Stability of a rotor in fluid-film bearings

Program (1) is very general; it calculates the rotor whirl amplitude and the force transmitted to the base as the result of a given rotor imbalance. The rotor is flexible and can have any arbitrary geometry. Also, there can be splined couplings in the rotor, and several bearings. The bearing pedestals can be assigned both flexibility and damping. Because the bearing film forces are not the same in all directions, the whirl motion of the rotor is treated as two-dimensional in such a way that it becomes an orbit around the equilibrium position. The orbit is elliptical, and its dimension as well as orientation vary along the length of the rotor. The computer program calculates the whirl orbits for a number of points along the rotor and also gives the components of the force transmitted to the foundations.

Program (2) applies to an arbitrary rotor geometry. There can be several bearings, and the stiffness as well as damping of the bearing pedestals can be included. The program calculates the speed at the onset of instability (the threshold speed) and the corresponding whirl frequency.

In both programs, the dynamic properties of a fluid-film bearing are expressed in terms of eight coefficients: four spring coefficients, and four damping coefficients. The values for these coefficients depend on the bearing type, the bearing dimensions, the viscosity of the lubricant, the bearing load, and the rotor speed. The rotor mass and elastic properties are represented by lumped masses connected by elastic beam elements typical of the Myklestad model. A special treatment of the gyroscopic moment is used to account for the elliptical orbit motion.

2.2.2.2.2 Analysis of Rotors Supported by Rolling-Contact Bearings

A preferred program for this analysis is presented in reference 92. This program is available from COSMIC, University of Georgia, Athens, GA.

Basically, this program is an analysis of the forced undamped vibrations of two elastically coupled, lumped-parameter beams. The whirl analysis of a rotor/bearing/casing system is facilitated by the assumptions that the rotor, casing, and bearing stiffness characteristics are axially symmetric and that the shaft executes circular orbits. Bearing nonlinearities, casing as well as rotor distributed mass and elasticity, rotor imbalance forcing functions, gyroscopic and rotary inertia moments, and shear and flexural deformations are included in the system-dynamics analysis.

The analysis is based on a lumped-parameter model using a modified Myklestad-Thomson transfer-matrix technique. Bearings are characterized as springs that can have constant spring rates or load-dependent values defined by $K = A \cdot L^B$ or by a table of L vs K points, where A and B are constants, L is the load transmitted through the spring, and K is the spring rate. The bearings have nonlinear load displacement characteristics, and therefore the solution is achieved by iteration. Rotor imbalances allowed by factors such as pilot tolerances and runouts as well as bearing clearances (which allow conical or cylindrical whirl) determine the forcing-function magnitudes. The computer programs first obtain a solution wherein the bearings are treated as linear springs of given spring rates. Then, based on the computed bearing reactions, new spring rates are predicted, and another solution of the modified system is made. The iteration is continued until the changes to bearing spring rates and bearing reactions become negligibly small.

If the machine operating speed is near a critical speed, the magnified bearing reaction is of interest for comparison with the bearing capacity. The nonlinear treatment of the bearings by this method shows that the predicted bearing reactions based on a linear representation of the bearings can be lower than the actual values.

2.2.2.2.3 Analysis of Shaft Systems with Unsymmetric Supports

Reference 88 includes a program description, a user's manual, and FORTRAN listings. It is available to qualified users from the U.S. Defense Documentation Center.

The lateral undamped natural frequencies and mode shapes of shaft systems with unsymmetric supports can be obtained with this program. The rotor is modeled with both continuous and lumped mass elements. The elasticity elements utilize beam theory; flexural deformations are included, but shear deformation is excluded. Moreover, this program does not include any treatment of the casing. Many designs purposely utilize a flexible housing between the rolling-contact bearing and the main machine casing in order to obtain low values for the first two critical speeds. In these cases, the casing is effectively decoupled from the rotor, and a dynamic model of the rotor supported on springs that are tied to ground is sufficient for good predictions.

2.2.2.3 PREDICTION ACCURACY

Locations of operating whirl critical speeds that are governed mainly by the rotor mass and the combined or individual stiffness of the rotor, bearing, or bearing support mount usually can be predicted within ± 5 percent. When the casing dynamics couple with the rotor sufficiently to require a system rotor/bearing/casing model for analysis, the prediction accuracy of critical-speed locations is approximately ± 10 percent provided that the conditions listed in section 3.2.2.1 are met. When these conditions are not satisfied, errors in predictions of criticals can easily be ± 20 percent and sometimes as great as ± 50 percent.

The prediction of response levels in general has been even more inaccurate. It is not uncommon for measured data to differ by a factor of 2 or 3 from the predicted data. These large discrepancies arise because values of imbalance are hard to predict accurately, and most turbopump operating speeds usually come within 15 to 20 percent of a major critical speed or closer to a secondary critical. A small error in predicting the locations of these criticals can result in significant error in predicting the response level (fig. 18).

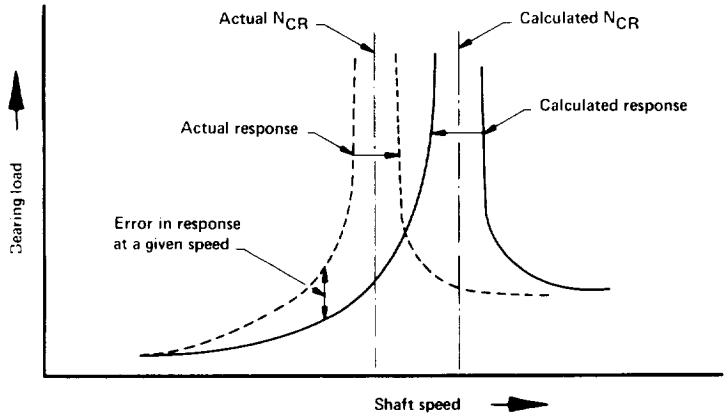

Figure 18. – Error in prediction of response resulting from a small error in prediction of critical speed N_{CR}

Table VII shows a typical comparison of calculated and experimental natural frequencies and the associated kinetic energy distribution. Additional information on prediction accuracy is available in the literature (e.g., refs. 6, 8, 54, 78, and 79).

2.2.3 Adjustment of Critical Speeds and Response Levels

The following major factors influence critical speeds:

(1) Shaft mass and stiffness magnitude and distribution

(2) Bearing and seal location, stiffness, and damping

(3) Bearing mount stiffness

(4) Casing mass and stiffness magnitude and distribution

The first factor, although obvious to most shaft designers, has often been overlooked. Stiffness of a shaft that has shaft-mounted components such as shrunk-on impellers, shaft sleeves, and bearing races can be changed markedly by changing the fits and the axial preloading. Furthermore, curvic couplings and other mechanical joints not maintained in compression will allow considerable flexibility.

Critical speeds can be influenced significantly by the flexibilities of the bearings, the bearing mounts, and the machine casing (refs. 7 and 93). Advantage has been taken of the support effects to effectively adjust or tune the critical speeds to the desired values (refs. 130 through 132). Flexible bearing mounts, as indicated in figure 19, have been used to produce low first and second criticals, which are rigid-body translation and rotation modes, as well as to yield a large available speed range for operation between the second and third criticals, the third critical being basically the first shaft bending mode.

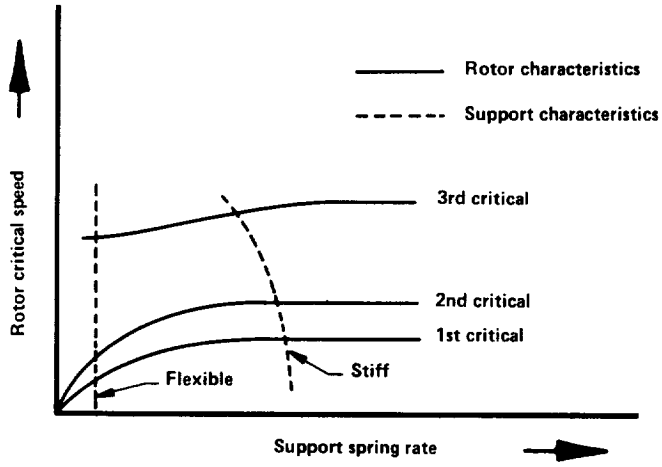

Figure 19. – Effect of support spring rate on rotor critical speed

TABLE VI – Summary of Calculated and Experimental Natural Frequencies for the XLR-87-AJ-9 Turbine Shaft

(a) Calculated natural frequencies, Hz

Rotor/bearing model[1]		Rotor/bearing/casing models			
		Dynamic stiffness method		Refined double-beam model[2]	
Lateral vibration	Forward Circular Whirl	Lateral vibration	Forward circular whirl	Lateral vibration	Forward circular whirl
—	—	—	—	198/220	200/220
—	—	265	265	327/372	328/374
—	—	400	440	403/480	456/530
517	630	590	650	635/671	> 650

[1] Model not valid for lower frequencies

[2] First value corresponds to min. stiffness casing model, and second corresponds to max. stiffness casing model.

(b) Experimental data

Spin tests. – Speeds of vibration buildup, rps				Shake tests. – Natural frequencies, Hz	
Tight fits and small bearing clearances		Loose fits and large bearing clearances			
Elliptical whirls	Circular whirls	Elliptical whirls	Circular whirls	Casing without rotor	Rotor/bearing (rigid mounting)
200-215/260-270	not meas.	200-215/235-250	not meas.	195-200	not meas.
330-343/372-390	" "	300/350	" "	230-250/300	" "
407 /440-450	470-485	not meas.	427-440	480	" "
>500	>500	>550	>550	not meas.	540

(c) Kinetic energy distribution for various natural frequencies, calculated on the basis of the associated rotor/casing system mode shapes

Natural frequency, Hz	Kinetic energy distribution, %	
	Rotor	Casing
198/220	7	93
327/372	13	87
403/480	4	96
456/530	74	26
635/671	95	5

Seals and wear rings can act as fluid-film bearings and produce stiffness and damping, and thus affect critical speed locations as well as rotor stability (ref. 133).

A significant reduction in response levels has been accomplished by using improved balance techniques. The use of squeeze-film dampers for adding or increasing damping to reduce response is gaining considerable interest among designers of shafts for aircraft engines. Both hydraulically mounted rolling-contact bearings (refs. 134 and 135) and squeeze-film dampers between two nonrotating parts in parallel with a flexible bearing support (refs. 130, 131, and 136) have been used. Although damper bearings of the Coulomb-friction type have been used successfully in jet engines (ref. 83), squeeze-film dampers have not yet been used successfully in rocket engine turbomachinery. Providing nonlinear stiffness properties to the bearing support also has been used to limit resonant-amplitude buildups (ref. 132). Nonlinearity without any added damping has the advantage over the damped, flex-mounted technique (ref. 130) in that lower force is transmitted at supercritical speeds. However, care must be taken to preclude "superwhirling" (refs. 72 and 75) and delayed resonances.

2.2.4 Balancing

References 54, 84, 121, and 137 through 142 represent a good survey of the major literature on balancing. There are two main classes of rotor balancing: the rigid rotor, and the flexible rotor. The object of rigid-rotor balancing is to ensure that the center of mass of the rotor lies in the centerline of the bearings and that no couple is transmitted to the bearings. At low balance speeds, the imbalance is independent of speed. Conversely, a flexible rotor balanced in one mode is not necessarily balanced in another mode. Rotors that have only two correction planes available generally operate below the first bending critical speed. Imbalance usually is measured by radial runout.

Balancing of the complete assembly has been sufficient for low speeds, but separate balancing of components has been the practice for higher speeds. The advantage of component balancing is that it allows for the interchangeability of parts and reduces internal shaft moments. Eccentricity tolerances result in imbalance at assembly. Modal balancing is a step-by-step method for balancing at successive critical speeds with corrections made so that the balance at the previous modes is unaffected. Modal balancing is preferred for shafts operating steady-state at critical speeds, but it is very costly.

Balancing capability has not been a limiting factor for turbopump rotors operating below the first bending critical speed. In some cases, a known imbalance has been added to create a bearing radial load and prevent ball or roller skidding.

The procedure for rotor assembly balancing has varied. Either the rotating assembly is balanced by removing material in specified planes or it is balanced by relocating previously balanced components rotationally with respect to each other. The latter method is used when the components are joined by curvic couplings, and it is merely a matter of remating the curvics in a different radial position. Even with a carefully balanced shaft, however,

imbalance has occurred when a curvic coupling joint that was tight at assembly became loose during operation because vibrations relieved the frictional binding. Imbalance also has occurred when the coupling was misaligned as a result of foreign material lodged between the teeth.

2.3 Coupling Design

The types of couplings most commonly used for liquid rocket engine turbopumps are the involute spline, curvic coupling, and parallel-sided face coupling; fitted-bolt, friction-bolted-flange, and ball-spline couplings are very rarely used. The involute spline, curvic coupling, and parallel-sided face coupling are discussed in detail in the three sections that follow. The design requirements of the fitted-bolt and friction-bolted flange are comparatively simple and are not discussed herein.

2.3.1 Splines

Splines have been used more than any other coupling because of large load-carrying capacity, low cost, and reliability. Splines require a change in shaft diameter. Most turbopump splines have an involute profile similar to gear teeth in that they can be cut and measured with the same machines used for gear teeth. However, splines differ from gears in that they have no rolling action and 25 percent or more of the teeth contact at once. Splines seldom pit or break at the root, although they do fail by shear, fretting, corrosion, and fatigue. Fixed splines permit no relative or rocking motion between internal and external teeth. The fit between mating parts can be either tight or loose. Flexible splines are vulnerable to wear because they permit some rocking motion, and under torque the teeth slip axially to accommodate axial expansion or runout. Fully crowned splines have been successful with as much as a 3° misalignment. Various splines (e.g., aligned, misaligned, and precision) have been used with various types of fits such as major diameter, side, interference, loose side, and combination with stepped pilot diameters at each end. Minor-diameter fits are not used because of the relatively small contact surface area on which to provide good positioning and because large root stresses are induced in the weaker member of the coupling. Fretting in the splines of inducers or impellers of oxidizer or monopropellant pumps is a potential source of ignition. This fretting can be controlled by using a tight axial clamp-up in the assembly and by setting tight fits on the radial positioning surfaces. After test, minor contact marks usually are acceptable for the splines of oxidizer and monopropellant pumping elements, but clearly defined fretting normally is not allowed.

Most fixed splines have been of the 30°-involute stubbed-tooth configuration. When the splines are used as a flexible coupling, the tooth form usually is special, tending toward (1) a lower contact angle (14.5°) to minimize runout effects on balance and (2) a longer addendum to provide larger contact areas.

The current trend is to design splines so that an increased percentage of the teeth make contact. Special tolerances and inspection techniques are required when over 25 percent of the teeth make contact. For fixed splines with a width one-third the pitch diameter, the

teeth have the same shear strength as the shaft (assuming that all teeth are loaded uniformly). There is always some error in tooth spacing; therefore, the face width usually is designed to be two-thirds or more of the pitch diameter.

It is general practice to have aluminum- or titanium-alloy impellers splined to steel or nickel-alloy mating parts. It also is general practice to adjust the spline dimensions and tolerances to suit the thermal expansion of the materials used, but standard dimensions and tolerances are used whenever the penalty is not too great.

The boundary line of spline practice for case-hardened ferrous materials is a shear stress of about 65,000 psi (448 MN/m^2) for a solid shaft and 95,000 psi (655 MN/m^2) for a hollow shaft with a bore 75 percent of the outside diameter. Common practice for rocket engine turbopumps is to use 50 percent of the teeth in contact for computing compressive stress and tooth shear stress. Some main shaft splines are sized initially by bearing contact stress; the limits range from 4500 psi to 20,000 psi (31.0 MN/m^2 to 138 MN/m^2), the value depending on the type of spline.

Ball splines have been used in test equipment (e.g., Phoebus turbopump) where axial freedom is required and where some misalignment is present. However, these conditions normally do not occur in flight-type hardware; in addition, ball splines are not as rugged as involute splines. As a result, ball splines have not been used in flight hardware.

2.3.2 Curvic Couplings

The curvic coupling provides a high load-carrying capacity in a minimum of axial space. In one case a torque of nearly 800,000 in.-lb. (90 kN-m) was transmitted by a curvic coupling with an 8.43-in. (21.32 cm) mean effective diameter and 0.62-in. (15.75 mm) effective face. Precision centering is provided without additional pilots. Tooth contact angles range from 20° to 30° with 30° most commonly used (fig. 20). As the contact angle increases, the coupling separating force increases, thus increasing the load on the retaining bolt.

Of particular importance for joint stiffness and stability is the relationship between the size of the coupling and the size of the connecting parts (fig. 21). A ratio of D/C = 2 is normal. For Titan III-M and SNAP-8,a ratio of D/C =4 was used, but this value is unusual. The inside diameter of the curvic coupling usually is 75 percent of the outside diameter.

Much valuable information on the design of curvic couplings is contained in reference 143; it should be noted that the maximum working stress levels recommended therein are on the conservative side.

The bolting arrangement for a curvic coupling is an important design consideration. In some cases, the bolting arrangement not only determines the design arrangement but also classifies the coupling as one of the types shown in figure 22.

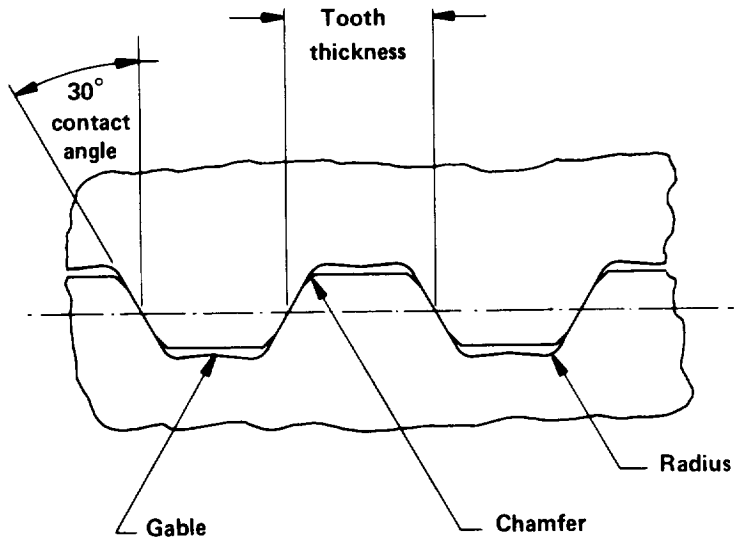

Figure 20.- View of typical curvic coupling teeth

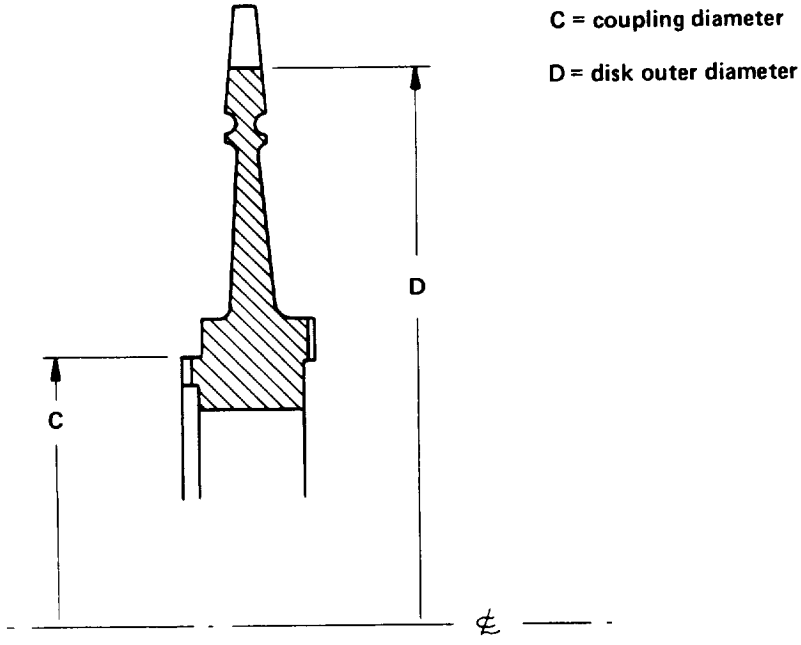

Figure 21. – Relative sizes of curvic coupling and disk

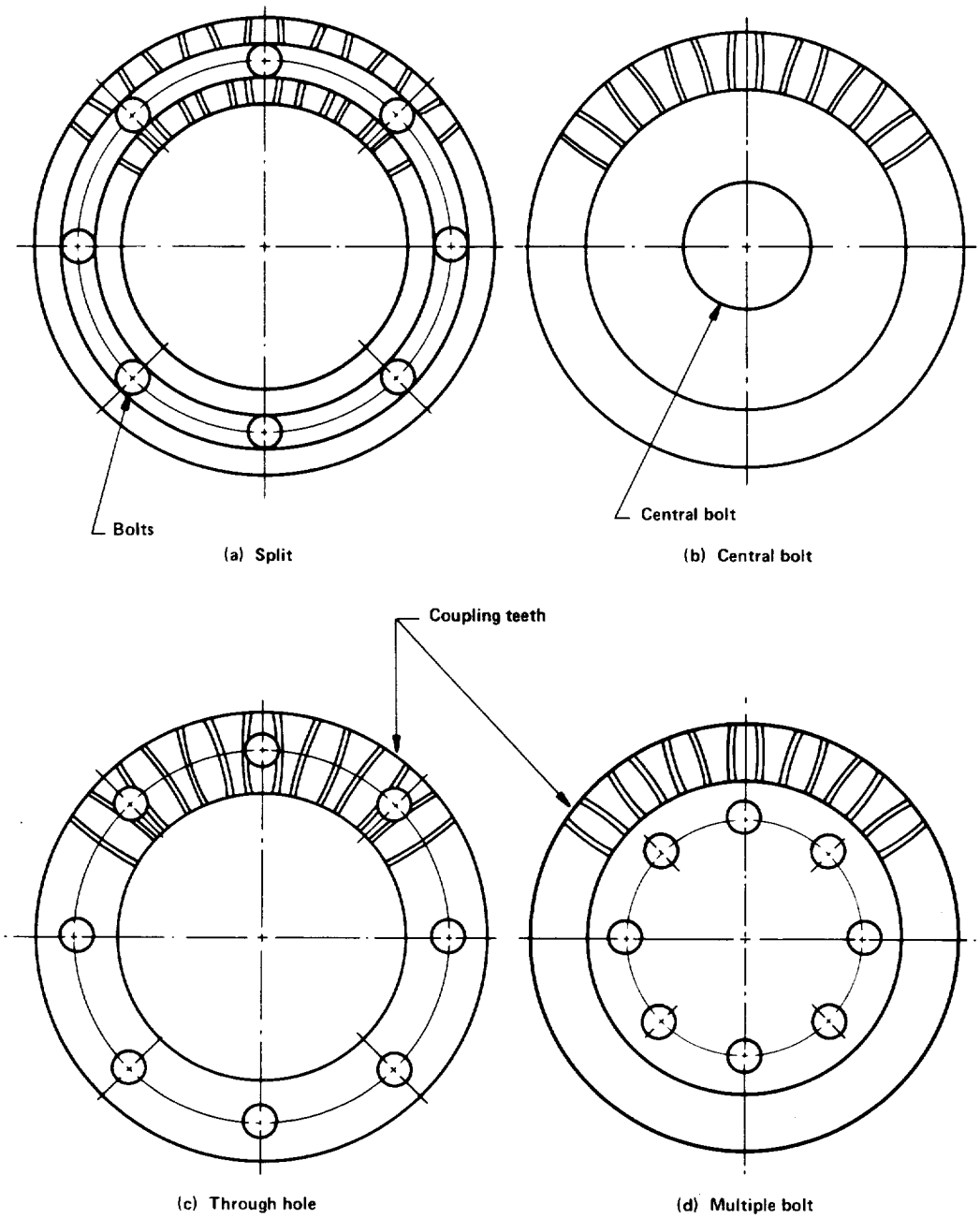

Figure 22. – Bolting arrangements for curvic couplings

Figure 22(a) shows a coupling of the "split" type in which elements of the coupling teeth lie on both sides of an annulus that is provided for bolt-hole relief. This kind of coupling is often used in conjunction with rotors and disks where sufficient space is available for multiple bolts. The coupling indicated in figure 22(b) generally is used with smaller shafts or disks. The single central bolt requires a stiff end piece or bolt head, and the disk also may require additional stiffness to withstand the bending couple induced by the distance from the disk center to the coupling teeth.

The couplings illustrated in figures 22(c) and 22(d) are variations of that shown in 22(a). In the through-hole type, the holes must be relieved to eliminate stress raisers and local machining deformations. The multiple-bolt type utilizes a bolt pattern inside the tooth diameters. Bolting arrangements wherein the clamping forces tend to center the coupling teeth are preferred over designs wherein the bolt pattern is outside the coupling teeth. This latter configuration requires a closely controlled bolt torquing sequence to ensure uniform contact of the coupling teeth.

Bolting arrangements for curvic couplings vary within the industry. For highly loaded couplings, extremely diligent attention is given to details of stress raisers (e.g.,fillets) or to tolerances that control contact surfaces. In some instances, curvic couplings have been mated deliberately with a force great enough to cause yielding and a subsequent increase in tooth contact surface.

2.3.3 Parallel-Sided Face Couplings

A typical parallel-sided face coupling is shown in figure 23.

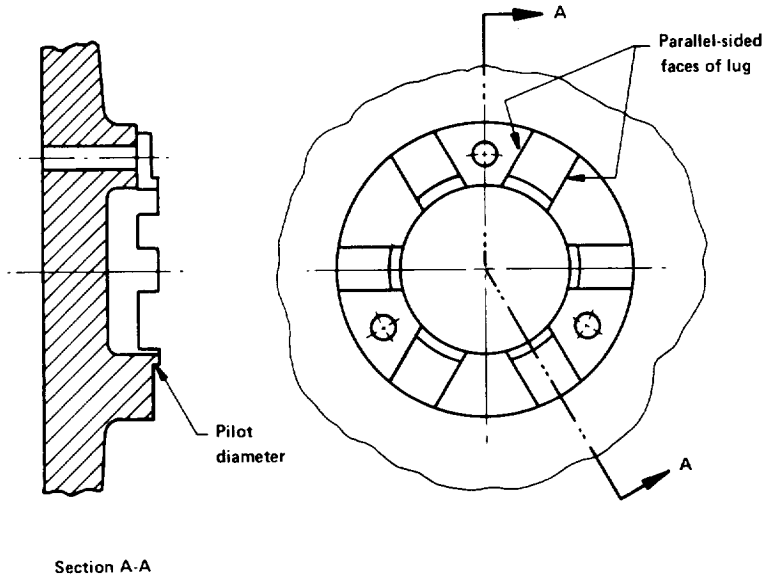

Figure 23. – Parallel-sided face coupling

Under initial loading, these couplings contact at less than the total number of faces because of the spacing tolerance. Plastic deformation usually is necessary to develop significant load sharing. The radial piloting of the adjacent parts is accomplished by a dimetral fit.

Parallel-sided face couplings were used in the early Titan III XRL-87-AJ-9 pumps at the rotor-to-shaft and rotor-to-rotor joints but were replaced by curvic couplings in a later design. The design deficiency associated with the parallel-sided coupling in this application was the inability of the pilot fit to keep the joined parts aligned and in proper radial fit relative to each other. The integral load transmission and precision centering features of the curvic couplings removed this deficiency.

2.4 Design Confirmation Tests

Shaft and coupling designs are subjected to component tests to evaluate dynamic characteristics, stiffness, and strength. These tests usually are performed early in the design phase because the test results often provide data necessary to obtain an adequate final design. Initially, simple component test setups are used, but final design confirmation usually is not complete until a full-scale test program on a prototype turbopump rotating system is accomplished.

2.4.1 Nonrotating Tests

Nonrotating (i.e., shake) tests are a good means for checking the accuracy of the analytical model used for the rotor and bearings. Comparisons of shake test and analytical data for three different systems are given below:

System	Natural frequency, Hz	
	Test	Analytical
XLR-87-AJ-5 turbine shaft	340	330
NERVA turbopump (3-stage turbine)	1st: 295 2nd: 520	1st: 305 2nd: 522
XLR-87-AJ-9 high-speed shaft	540	517

The good correlation of the two sets of results is qualified because the test setups and procedures used with the first two systems were such that the test conditions fairly well matched those assumed for the analytical model. For example, the bearings were mounted in "rigid bases," bearing clearances were eliminated, and excitation levels were kept low so that there was little likelihood of the opening-up of preloaded joints and reduction of shaft stiffness that might take place under higher excitation levels.

Shake tests have shown that the mounting fixture as well as the riding elements and joint stiffness of the shaft significantly influence the resonant locations. Asymmetry in mount-fixture stiffness (i.e., one of the principal stiffness axes is not in line with the shaker vibration plane [fig. 24]), has caused dual resonances where normally the symmetrical stiffness support will give only one resonance.

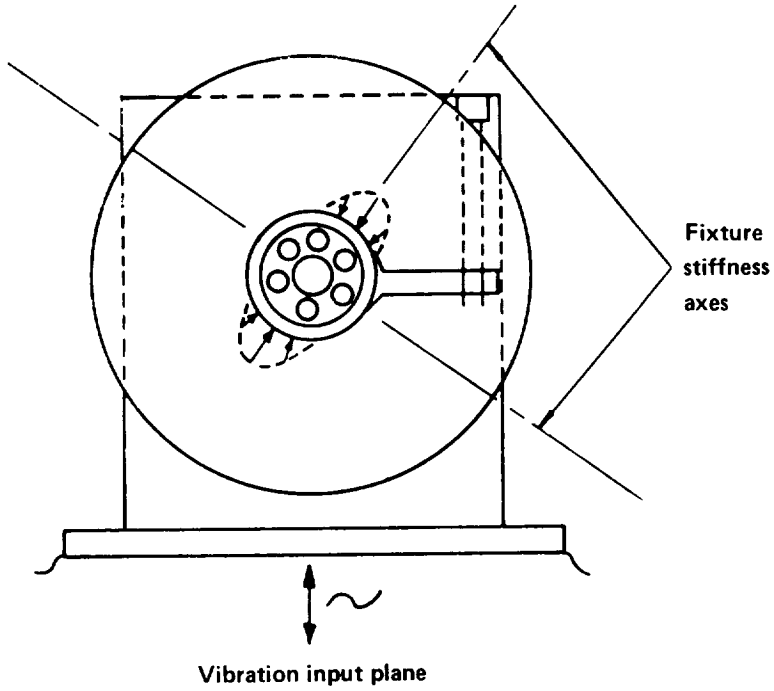

Figure 24. – Misalignment of mount-fixture stiffness axes and plane of vibration

The undesirable effect associated with a built-up shaft (i.e., the loosening up of the axial joints between the shaft parts as vibration amplitude increases) is shown in figure 25 in terms of the reduction in shaft natural frequency. (The dual natural frequencies in the figure appeared as a result of a misalignment as depicted in figure 24). Also, note the abrupt change in slope at the bearing location in the mode shape of the lower frequency in figure 26. This softening effect was found to occur at much lower vibration amplitudes than was expected from prior analysis of the joint preloads and the applied opening loads.

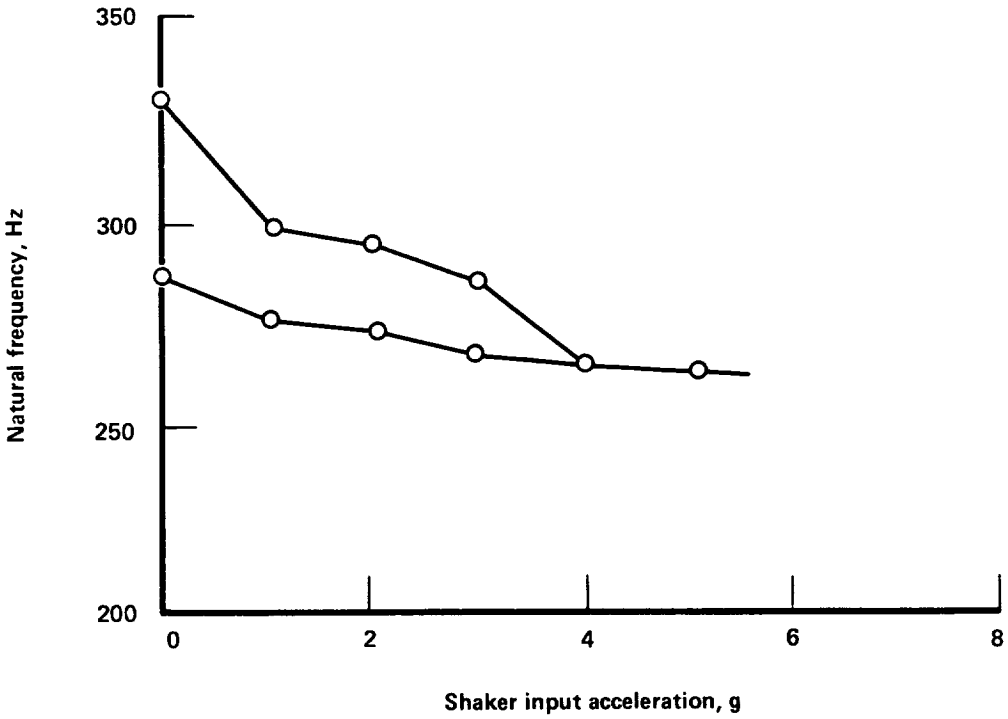

Figure 25. – Effect of shaker-test vibration amplitude on natural frequency of a built-up shaft

Angular-contact bearings usually are preloaded such that their stiffness characteristics are quite linear in the low load range (see sec. 2.2.4.3). Thus, the bearing effective stiffness usually remains fairly constant throughout low-excitation shake tests. However, roller bearings usually have internal clearance (δ_c, fig. 27) and therefore exhibit stiffness that is sensitive to both load and clearance. When shafts supported by roller bearings are shake tested, the effect of bearing internal clearance on stiffness can cause errors in the determination of natural frequencies.

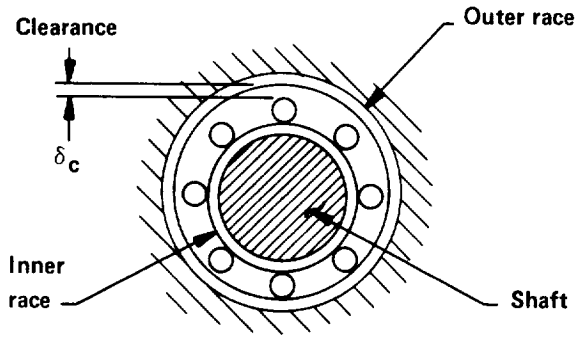

Figure 27. – Roller-bearing internal clearance

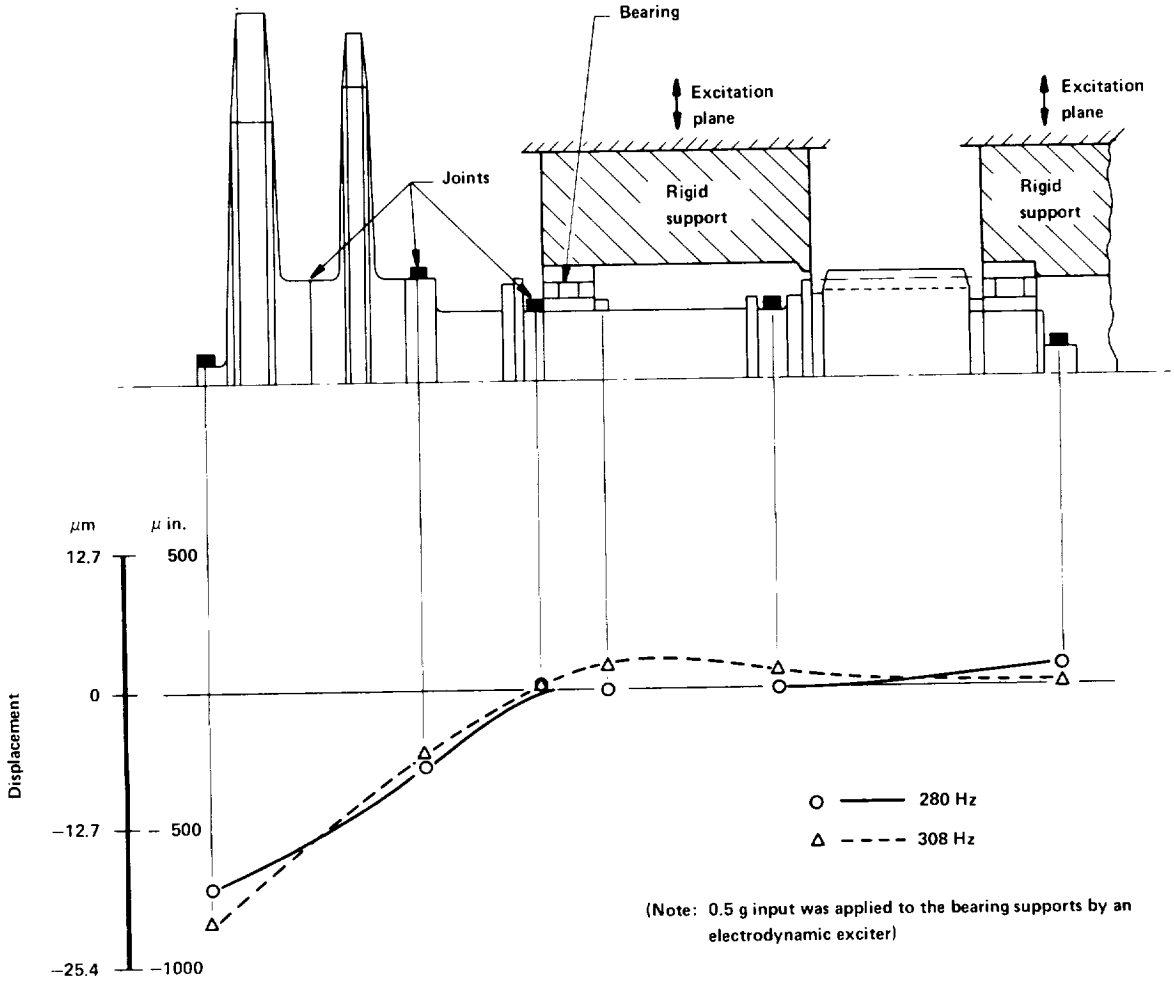

Figure 26. – Shaft lateral deflection modes affected by loosening of axial joints

When shaft motion is circular, the shaft is always in contact at the bearing stationary support. However, when the shaft motion is transverse, as in lateral vibration, the clearances affect the spring rate and reduce the natural frequency (ref. 105). An approximate analysis of the effect of bearing clearances on the spring rate is given in reference 47, p. 167.

2.4.2 Rotating System Tests

Rotating system tests, with instrumentation for measuring the system dynamic characteristics, are used to evaluate vibration levels, map critical speeds, measure bearing loads, and confirm mechanical integrity of the shaft, bearings, and couplings. Almost all the turbopump development tests have some instrumentation for monitoring the machine dynamic characteristics. Spin tests, wherein rotation is achieved by means other than a hot-gas turbine drive, also are used.

2.4.2.1 INSTRUMENTATION

The kind of instrumentation and its sensitivity and range usually are selected on the basis of previous experience. A magnetic tape record of the instantaneous data may be used to allow permanent or temporary storage of the information; this feature is particularly important for the short-duration runs typical of rocket engines.

During testing, tracking filters, oscilloscopes, and x-y plotters monitor the shaft motion. Accelerometers, velocity pickups, and distance detectors are the primary instruments used to define rotating shaft motion and position. Accelerometers are small and respond to high frequencies. Velocity probes, used up to 1000 Hz, inherently filter out high frequencies. Accelerometers and velocity pickups are mounted close to the shaft supports. Distance detectors usually are mounted in the housing or on special fixtures. Thermocouples are used to measure temperature, and strain gages measure load and stress. Torque is measured by devices discussed in references 139 and 144; telemetry is discussed in reference 145.

The following characteristics of the high-speed rotating portions of turbomachinery have been determined by monitoring the reaction of the stationary supporting structures (ref. 146):

(1) Static and dynamic load exerted on the bearing
(2) Amount of slip between rolling elements and bearing race
(3) Critical speed of rotating assembly
(4) Motion of center of high-speed shaft

These phenomena were measured and recorded by resistance strain gages mounted either on the bearing or on the support structure.

During development testing of the XLR-87-AJ-9 high-speed shaft, both room-temperature spin tests and hot firings were instrumented with capacitor-probe distance detectors, and data describing the rotor whirl orbits as a function of time and speed were obtained. In addition, accelerometers located at appropriate points on the casing made possible the determination of how the casing influenced the rotor dynamics.

2.4.2.2 INTERPRETATION OF DATA

Viewing the vibration wave form on an oscilloscope is helpful in analyzing the vibrations of rotating systems. Sometimes it is difficult to understand the wave form, however, because the wave usually is not a pure single-frequency sinusoid but consists of several frequencies resulting from several different mechanisms. With the use of tape recorders for permanent records, "off-line" analysis of the tapes has proven economical and frequently necessary. The raw data can be evaluated quickly for areas of further interest and then filtered for more detailed study.

It has been found useful to trace the path of the shaft center from vibrograms acquired by means of two distance detectors lying in the same plane but 90° apart. The resulting Lissajous patterns can yield valuable information about the mechanism of excitation. The ways of interpreting various patterns are explained in references 72, 132, and 146 through 149. General procedures for analyzing the vibration data of rotating systems are described in references 150 and 151.

The "growling" noises mentioned previously are indicative of abnormal behavior often associated with "tangled yarn" precessional-motion patterns (ref. 148). This growling or humming noise phenomenon also has been identified with skidding of the bearing rolling elements (ref. 152).

2.4.3 Special Tests

The preload on the retaining bolt for a curvic coupling usually is determined during assembly by measuring elongation of the bolt or compression of the rotor; a calibration test of load against elongation is needed for accurate control of bolt preload.

Early insight into design structural margins and potential causes of failures may be provided by (1) running at rotor speeds and gas temperatures above normal tolerance limits, (2) unbalancing rotors beyond design imbalance limits, and (3) introducing large-amplitude, low-frequency vibrations (ref. 153). These abusive tests also are useful in reducing the number of development tests required to establish reliability. Special tests, consisting of static load application and measurement of relative motion, often are carried out to evaluate stiffness of built-up rotors as well as spring rates of bearing and housing. Impeller-attachment preload on pumps with large impeller pressure-area forces is confirmed or determined by means of special tests. Axial compressive tests to determine stiffnesses of curvic coupling joints frequently are conducted (sec. 2.3.2).

3. DESIGN CRITERIA and Recommended Practices

3.1 Shaft Design

3.1.1 Design Parameters

3.1.1.1 SHAFT SPEED

3.1.1.1.1 Optimization

The shaft operating speed or speed range shall be based on pump, turbine, bearing, seal, and shaft design parameters that result in satisfaction of requirements imposed by the engine and turbopump system studies.

Tradeoff studies of the various limiting design parameters should be made to determine the optimum set of compromises associated with speed. References 1 through 5 should be consulted to aid in establishing the design-parameter considerations and limitations.

A major goal of the tradeoff studies should be the highest practical shaft operating speed, because maximum speed usually results in the smallest overall size and lowest weight for the turbopump. Limitations on maximum shaft speed that should never be overlooked are centrifugally induced stresses in the impeller and turbine disks; bearing DN; seal rubbing velocity; and shaft dynamics and whirl critical speeds. Shafts should be designed purposely for either subcritical or supercritical operation. The choice should be based on an assessment of the advantages and disadvantages of each in conjunction with the intended use and the ease of satisfying the associated design requirements.

3.1.1.1.2 Transient Dwells and Overshoots

The shaft and coupling shall withstand start-transient speed dwells and overshoots.

Analysis of stress/strength relations and fatigue life for the proposed limits of operating shaft speed should account for effects of start-transient dwell or overshoot conditions. A speed higher than the nominal maximum operating speed should be used for evaluation of strength and high-cycle fatigue life. This speed should be the maximum 3-sigma steady-state operating speed determined from past experience or from calculations if applicable. If 3-sigma limits cannot be established during the design phase, it is recommended that mechanical design speed exceed nominal maximum operating speed by a factor of 1.1 to 1.2.

Transient dwell and overshoot speeds should be compared with the shaft whirl critical speeds. Use shaft-dynamics analysis techniques given in section 3.2 to determine the degree of danger in operating at, near, or traversing through a critical speed. Excessive speed overshoots that impose severe penalties (high loads, excessive stress, or need for heavier structure) on related components and on the turbopump should be prevented by modifying the system design as necessary.

3.1.1.1.3 Steady-State Operations

The shaft and coupling shall not suffer damage or induce damage in associated components while operating at steady-state speeds.

The shaft should be designed to have the required strength to withstand reliably the critical design loads (sec. 3.1.3) and environmental conditions (sec. 3.1.1.5). The shaft speed or range of speeds should be considered as a source of forcing frequencies. Natural frequencies of all associated components such as shaft-mounted components (impellers, turbine wheels, etc.), bearing support housings, pump casings, turbine manifolds, and turbopump mount structures should be compared with the shaft rotational speed and multiples of 2 and 3 thereof. Damage by resonance should be avoided by design modifications to detune any dangerous resonant conditions. Procedures for this type of design modification should be obtained from references 1 through 4. However, the shaft designer should be aware that changes in the associated components may affect the shaft dynamic characteristics (sec. 3.2).

3.1.1.2 BEARING AND SEAL LOCATIONS

The locations for bearings and seals shall be based on a compromise of their effects on

- *Shaft critical-speed characteristics*
- *The environment, loads, and DN value imposed on the bearing or seal*
- *Shaft deflections and stresses*
- *Design complexity*
- *Thermal displacements and assembly tolerances*
- *Accessibility and maintenance*

Parametric studies of critical speeds versus bearing and seal location should be utilized to determine optimum locations; an example of such a study for a simple overhung turbine can be found in reference 9. Radial-load bearings should be located as close to the heavy rotating elements as possible without compromising the bearing as a result of thermal

soakback or heat transfer during operation. Gears should be located close to supporting bearings so that shaft deflection and bending moment are minimized. However, as a fail-safe measure, splines should be kept a safe distance from main bearing areas, so that in case of bearing failure the load-carrying capacity of the splines will not be decreased seriously by the heat generated. Thrust balance pistons should be located close to the thrust bearing in order to minimize thermal and mechanical distortion effects on the piston gap clearances and the bearing axial play. When bearings or associated support mechanisms are designed to provide damping, the bearings should be placed at locations where rotor displacement is largest for the modes associated with the critical speeds to be passed through and with the first critical speed above the maximum operating speed. The bearing and seal locations should be evaluated for (1) influence on turbine scroll aerodynamic and mechanical design complexity, (2) possible complications in pump inlet housing hydraulic and mechanical design, (3) thermal displacements and assembly tolerances, and (4) accessibility and maintainability.

3.1.1.3 SHAFT SIZE

The shaft diameter shall satisfy the requirements for strength, shaft stiffness for whirl critical speed, bearing DN for rolling-contact bearings, and seal rubbing velocities.

The shaft diameter at bearing locations should be made as large as practical so that the rotor is as stiff as possible. Use the guidelines set forth in references 1 and 5 to establish specific DN values and rubbing velocity limitations. When the shaft size is compromised by bearing speed limitations, a larger shaft diameter may be used, if the material can be appropriately hardened, by machining the shaft to act as a bearing inner race. If shaft-riding-seal speed compromises shaft size, other components (e.g., labyrinths) should be considered as replacements for the seals. In some turbopumps, liftoff seals can be substituted for face seals to permit the use of a larger diameter shaft. Shaft torsional shear stress rarely is a controlling factor in establishing shaft diameter.

Thin-wall shafts should also be checked for shear-buckling critical stress levels (ref. 154). When the wall thickness of hollow shafts at bearing locations is determined, consideration should be given to the effect of the wall flexibility on the fatigue life of the rolling-contact bearing. For designs using the shaft as the inner race of a rolling-contact bearing, the hollow-shaft wall thickness should be at least twice the thickness of a normal race thickness and the material must be appropriately hardened. For a hollow shaft with separate inner race, the shaft wall thickness should be made equal to the race thickness (ref. 155).

3.1.1.4 SHAFT DISCONTINUITIES AND TRANSITIONS

Shaft discontinuities and transitions shall not contribute to fatigue failure.

For highly stressed shafts and couplings, the radii of grooves and keyways should be evaluated for stress concentration and associated reduction in fatigue life. The

stress-increasing effects of press-fitted or shrunk-on collars or sleeves and the effect of surface finish on fatigue or seal operation also should be evaluated, preferably by principles given in references 13 through 16.

The ideal transition should be designed by following the guidelines in the tables in reference 20 or by using a fillet radius that is three times the diameter of the smaller section. In practice, machining and other considerations may dictate the use of a smaller radius; therefore, stress-concentration factors in accordance with the curves shown in references 13 and 156 must be applied. Of the three grind-relief configurations shown in figure 28, configuration (a) is preferred to either (b) or (c); if dimension d is 0.010 in. (0.254 mm) or less, configuration (b) may be used.

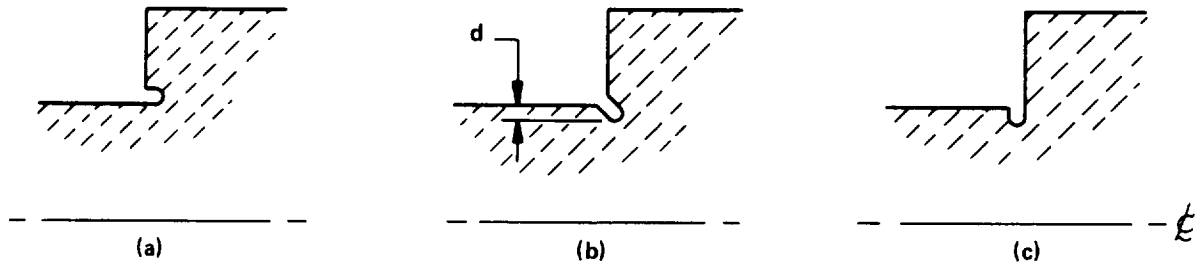

Figure 28. – Grind relief configurations

Use experimental techniques such as photoelasticity when the shape of the discontinuity or transition or the loading condition does not conform to a type for which stress-concentration or fatigue-strength-reduction factors exist.

Generous radii should always be provided at the corners of grooves and keyways. Cold-rolling will increase the fatigue strength at these corners. A method is available (ref. 21) for evaluating the stress-raising effects of pressed or shrunk-on collars. Keyways and wrench slots should be symmetrically spaced to prevent adverse imbalance. A surface finish of 16μ in. (0.41μm) rms is acceptable for control of the quality and condition of the surface to reduce fatigue failure. For shaft face-seal surfaces, a finish of 10 to 20 μ in. (0.25 to 0.51μm) rms should be used in combination with control of the direction of the finish lines. The designer also should be aware of the effect of machine lead on leakage. If transverse holes or grooves are required for instrumentation, the effect of these discontinuities should be considered in the stress analysis.

3.1.1.5 SERVICE ENVIRONMENT

The shaft and coupling shall withstand any harmful environment encountered during fabrication, processing, storage, and operation.

Initially, all possible environments and chemicals that may be encountered during fabrication, processing, storage, and operation should be reviewed to identify any conditions harmful to the shaft. Then steps should be taken to eliminate exposure to the harmful environments and to use chemicals that have minimum deleterious effect. When deleterious environments cannot be eliminated, shaft material and configuration should be selected for inherent resistance to degradation in the harmful environment, or external methods of protection should be used, as discussed below. Do not use titanium in oxygen turbopumps, as any rubbing could cause the metal to ignite.

3.1.1.5.1 Thermal Environment

The shaft and coupling shall withstand the effects of transient and steady-state heating and cooling.

Shaft and coupling components should be designed for the critical operating conditions created by the combination of mechanical loads and temperatures that will exist during engine transient and steady-state operation. Prediction of metal temperatures should be based on comprehensive heat-transfer analyses and experimental evaluation during development testing. Temperature-sensitive paints, braze patches, and thermocouples should be considered for temperature measurements. Thermocouples, although more difficult to employ (they usually require slip rings for transmitting the measured data from the rotating shaft to the stationary recording facility), are very desirable in that they provide time-correlatable data that the other methods do not. Experimental data obtained from test programs for similar hardware should be used to corroborate the analysis whenever such data are available. A temperature increment of 50°F (28K) or 5 percent of the maximum metal temperature, whichever is lower, should be applied to the result of such analysis as a safety factor to arrive at maximum temperatures or thermal gradients. No other factors of safety should be applied to thermal loading.

The material strength and resulting component strength should be assessed with due account given for reductions in yield, ultimate tensile, and creep-rupture strength at elevated temperatures and for the reduction of material ductility and increased tendency to embrittle at low and especially at cryogenic temperatures.

Thermal shock gradients and associated stresses and strains should be evaluated for potential inducement of fatigue cracking. When restart of the turbopump is necessary after only a short nonoperating time period, adverse temperatures throughout the shaft caused by heat soakback from the turbine should be minimized or eliminated.

3.1.1.5.2 High-Pressure Gaseous-Hydrogen Environment

When necessary, the shaft and coupling shall withstand the harmful effects of a high-pressure gaseous-hydrogen environment.

The shaft or coupling material should be evaluated for susceptibility to hydrogen embrittlement by performing specimen tests in the appropriate environment (ref. 157). Smooth and notched tensile tests, smooth strain-controlled low-cycle fatigue, and sustained-load and low-cycle fatigue tests with precracked fracture-mechanics specimens – all should be accomplished if a material is expected to show any significant degree of hydrogen embrittlement (ref. 27).

Avoid the use of ferritic and martensitic steels. If possible, avoid using nickel-base and cobalt-base superalloys such as Inconel 718, Inconel X, Waspaloy, and Rene 41. If any of these alloys is used, its selection should be justified by experimental data from tests mentioned above. Materials that have demonstrated good resistance to embrittlement by high-pressure gaseous hydrogen and are therefore recommended for use are the austenitic stainless steels such as the 300 series, ARMCO 21-6-9, ARMCO 22-13-5, and A-286. Aluminum alloys such as 6061-T6 and 7075-T73 also have demonstrated resistance to this environment and should be considered if otherwise suitable for use.

3.1.1.5.3 Corrosive Environments

The shaft and coupling properties shall not be degraded below acceptable limits by a corrosive environment.

Materials known to be susceptible to stress-corrosion cracking, for example, should not be used in a configuration and environment conducive to stress corrosion. The factors that play major roles in stress-corrosion cracking are the material and its fabrication, exposure to a corrosive environment, stress levels from both residual and applied sources, temperature, and time. If any candidate alloy for a shaft or coupling may be susceptible to stress-corrosion cracking, tests (ref. 158) should be conducted to demonstrate that the alloy has adequate resistance to stress-corrosion cracking under the conditions of its application.

The longer the duration of exposure to a corrosive environment, the greater the likelihood of stress-corrosion cracking. Susceptibility to stress corrosion should be allowed only when the expected useful life of the shaft or coupling is significantly shorter than the time required for corrosive effects to reduce reliability below established values.

The following three principal avenues for reducing or avoiding damage from stress-corrosion cracking should be examined for applicability in a given design:

(1) Eliminate the dangerous tensile stresses.

(2) Remove the corrosive environment or render it less harmful by using protective barriers (coatings, platings, material processing, etc.).

(3) Replace the metal in the particular application with another material that does not fail in the specific environment.

Steel alloys that should be avoided because of very low resistance to stress-corrosion cracking (ref. 159) are the following:

Alloy	Temper
17-4 PH	All tempers
17-7 PH	All except CH 900
PH15-7 Mo	All except CH 900
AM 355	<SCT900 FH
H-11	All tempers
Vascojet 1000	All tempers
Low-alloy	>180 ksi (1.24 GN/m^2) yield strength

3.1.1.5.4 Hard Vacuum

The shaft and coupling properties shall not be degraded below acceptable limits by cold-welding or adhesion, evaporation, decomposition, or sublimation in prolonged hard vacuum.

Use aluminum coatings in place of cadmium, zinc, or magnesium in a prolonged hard vacuum. Special lubricants (refs. 52 and 53) that do not evaporate, sublime, or decompose must be used.

3.1.2 Material Selection

3.1.2.1 MECHANICAL PROPERTIES

The minimum mechanical properties of the shaft and coupling material shall not be less than those required to satisfy the critical operating loading and environmental conditions.

The main mechanical properties to consider in choosing the material are the tensile yield and ultimate strengths, creep strength, ductility as measured by reduction in area and fracture toughness (ref. 160), fatigue strength, thermal expansion or contraction

coefficients, and modulus of elasticity. The material strengths and other physical properties should be evaluated for the entire range of operating and nonoperating environments. Property values should be selected from authoritative sources such as MIL-HDBK-5A (ref. 161), Department of Defense reports, or documented test values when appropriate. Property values should be based on statistical evaluation of the test data, and the values used for design should be those for which the probability is 95 percent that 99 percent of the samples exceed the design values (e.g., "A" values in ref. 161).

A material that has good low-cycle fatigue (LCF) strength does not necessarily have good high-cycle fatigue (HCF) strength (ref. 48). For good HCF life, a material with high tensile strength is best, whereas for LCF a material with lower tensile strength but high ductility is best (fig. 5). Furthermore, for long life in high-temperature use, good creep-rupture strength also is necessary (refs. 162 and 163).

3.1.2.2 THERMAL PROPERTIES

Differential thermal expansion or contraction of the shaft and bearing-race materials shall not result in race fracture or loose fits.

The thermal-expansion properties of the shaft and the bearing materials at operating temperature should be matched as closely as possible. The effect of differential expansion on bearing clearance and bearing race-to-shaft fit should be calculated for conditions of assembly, nonoperating chilldown, and transient and steady-state operation as appropriate. For critical applications, the available material thermal-expansion data may not be accurate enough; in such cases, conduct special thermal-expansion tests.

3.1.2.3 STRESS CORROSION AND HYDROGEN EMBRITTLEMENT

The shaft and coupling material shall not suffer deleterious effects of stress-corrosion cracking or hydrogen embrittlement.

The material selected should be compatible with the propellant and environment. When there is potential exposure to high-pressure gaseous hydrogen, avoid the use of materials that become brittle in that environment. Refer to section 3.1.1.5 for a more complete discussion of stress corrosion and hydrogen embrittlement.

3.1.2.4 LOW-TEMPERATURE EMBRITTLEMENT

The shaft and coupling materials shall not be susceptible to brittle fracture due to low-temperature embrittlement.

The material should have at least 5-percent reduction-in-area ductility, more than 15 lb-ft (20.3 N-m) of Charpy V-notch impact energy, and adequate fracture toughness (ref. 160) at the operating temperature. In establishing the minimum fracture-toughness requirements, consideration should be given to the size of fabrication flaws and cracks that may go undetected during NDT inspection, the operating stress levels, and the desired life (ref. 49).

Low-alloy steels such as 9310, 4340, 440C, and AM-350 should not be used at cryogenic temperatures.

3.1.2.5 SURFACE CONDITION

The shaft and coupling shall not suffer surface wear, fretting, or galling of sufficient magnitude to cause shaft, coupling, or associated parts to fail.

The shaft or coupling material should be selected with due account for the possible need to heat treat, case harden, or coat the surfaces. These surface treatments and the materials for mating parts should be evaluated for the effects on the material tensile and fatigue strength as well as effects on wear, fretting, or galling. Typical past solutions are described in section 2.1.2 and in reference 164.

3.1.3 Structural Analysis

3.1.3.1 LOADS

The structural analysis of the shaft and coupling shall evaluate the critical combinations of radial, axial, and torsional loads, both steady and alternating, encompassing all anticipated conditions in the operating and test range.

"Worst-case" design operating conditions should be used in evaluating each load, and the loads should be combined vectorially to yield the "worst-case" combined loads.

Probable accuracy of computed loads should be assessed and, if applicable, calculated values modified to obtain conservative worst-condition predictions. For example, small percentage variations in large pressure forces on the impeller front and back faces always result in considerable variations in magnitudes of net thrust.

The following kinds of loads should be evaluated as indicated:

Radial

Rotor dynamics. – Rotating imbalance and self-excited whirl forces. An analysis of shaft response to imbalance forces should be accomplished as outlined in section 3.2.2.1.4. For fail-safe considerations, include in rotor dynamic loads the loads induced

by rotor imbalance caused by failure of one blade and assume that these loads will act over the entire engine operating period required for the mission.

Rotor pressure loading. – Unequal pressure around impeller shrouds, discharge outlets, etc. The pressure profiles should be integrated for load magnitudes.

Vehicle accelerations. – Longitudinal and lateral flight motion; engine gimbal snubbing; gyroscopic action of rotor, vehicle rotation, or engine gimbaling. Engine and vehicle specifications should be reviewed for acceleration, gimbaling, and maneuver requirements.

Gear and bearing reactions due to shaft power torque.

Constraint of thermal expansions or contractions. – Conduct a heat-transfer analysis to obtain the thermal profiles of the assembly. Then calculate thermally-induced loads and their interaction with assembly loads.

Axial

Rotor axial vibrations. – The natural frequency of the rotor/bearing system treated as a rigid rotor mass on a simple spring should not coincide with the shaft operating speed (or multiples of 2 or 3 thereof) unless a response analysis or test demonstrates that no adverse effect occurs. For preliminary design, axial vibration loads may be considered to have amplitudes about 5 percent of the bearing thrust loads. If testing shows that these vibrations are significant, then experimental evaluation is recommended.

Rotor pressure loading. – Unbalance thrust across impellers, turbine wheels, balance pistons, and thrust bearings should be integrated for load magnitudes.

Vehicle accelerations. – Same sources listed above for radial.

Gear reactions to shaft power torque. – Helical gears, misaligned splines.

Assembly axial preload. – Built-up shafts, turbine and impeller retaining bolts.

Self-constrained or bearing-constrained shaft thermal expansions or contractions. – Evaluate as above for radial.

Torsional

Shaft power torque.

Torsional vibration inertia forces. – For preliminary design, torsional vibration loads may be considered to have amplitudes of about 5 percent of the nominal power torque load. If operation shows these vibrations to be more significant, then experimental evaluation is recommended.

3.1.3.2 SAFETY FACTORS

The shaft and coupling design safety factors shall be adequate to achieve the specified reliability.

Safety factors applied to limit loads should be equal to or larger than 1.1, 1.3, and 1.25 for yield, ultimate, and fatigue strengths, respectively. The preferred values are 1.1, 1.4, and 1.33. If sufficient statistical data are available for a particular application to justify the use of probabilistic-reliability methods (refs. 40 through 45), then the statistically determined values for safety factor should be used.

3.1.3.3 ANALYTICAL METHODS

Structural analysis shall verify that the shaft and coupling have adequate strength throughout service life to preclude structural failure due to deformation or collapse, fracture, or wear.

The shaft should be analyzed for all critical loading conditions defined in 3.1.3.1, due account being given to stress concentrations, environmental considerations, material strength properties, required safety factors, and clearances between the stationary and rotating parts. Adverse deformation or collapse failure margins should be calculated, consideration being given to potential elastic, plastic, or creep deflections or buckling. Specific details of such analyses can be found in almost any book treating machine design or strength of materials.

Fracture-failure margins should be evaluated for both time-dependent and time-independent failure mechanisms. Time-independent mechanisms include the well-understood simple ductile overload and the much-less-understood, complicated, and less-predictable brittle rupture. Factors that may contribute to brittle rupture are low material ductility and low fracture toughness, fabrication flaws, weld defects, design notches and stress raisers, degree of stress triaxiality, high strain rates, low temperature, hostile environments (chemical or physical), and improper material heat treatment. The most promising engineering approach for assessing sensitivity to brittle fracture is the use of the principles of linear elastic fracture mechanics (refs. 165 and 166).

Time-dependent fracture mechanisms encompass both static and cyclic loads. The possibility of delayed fracture under static loads due to creep rupture, stress-corrosion cracking, or hydrogen embrittlement should be assessed. The shaft design should be analyzed for fracture potential due to fatigue induced by cyclic or combined static and cyclic loads; the analysis should include thermal stress that may induce low-cycle fatigue or large residual mean tensile stresses that reduce the alternating stress capability.

In the evaluation of high-cycle fatigue, the critical effective stress levels should be determined by use of the distortion-energy (i.e., Von Mises-Hencky theory) definition of effective stress for multiaxial stress states (refs. 11 and 12). The shaft-material fatigue endurance strength should be established by using existing guidelines (refs. 12, pp. 166-176 and 46, pp. 221-229) and by reducing the smooth-bar material-specimen fatigue strength to allow for the modifying effects of surface finish, size, temperature, notch sensitivity, residual stresses, material directional effects, corrosion, plating, and reliability. For combined alternating and steady stress levels, use experimentally determined stress-range diagrams or modified Goodman diagrams (refs. 167 and 168). To assess the combination of multilevel magnitudes of cyclic stress, the Miner theory of linear cumulative damage (ref. 169) may be used to predict fracture with a usage factor of 0.70 (refs. 169 through 172). However, the accuracy of any cumulative-damage theory suffers under certain conditions, and the designer should be acquainted with the limitations as presented in the cited references.

All shaft components should be stress analyzed with sufficient depth to identify peak stress levels associated with all the applicable load sources previously identified. For long life and multiple reuse applications, special emphasis should be given to the evaluation of thermal and geometrical discontinuity stresses, as they are common causes of fatigue. Critical buckling stress levels of hollow thin-wall shafts also must be evaluated, and a margin to preclude buckling must be provided.

The critical effective stress and strain levels that govern cyclic fatigue life must be kept below the endurance limit of the material for the required number of duty cycles times an appropriate safety factor. Stress concentrations should be minimized by using maximum radii in fillets, optimizing transition sections, locating mechanical and weld joints in low-nominal-stress areas, and undercutting and placing relief holes to smooth out the distribution of stress. Analytical determination of the stress levels by comprehensive digital-computer structural-analysis programs and experimental-stress-analysis techniques, where applicable, may be necessary to determine locations and magnitudes of critical effective stress levels. The methods for predicting low-cycle fatigue life are continually being modified and improved; the present recommended methods are those described in references 173 through 176.

(Wear failures of the adhesive type such as galling or scoring are caused primarily by a lack of separating film; many times these failures can be precluded simply by use of a lubricant. Abrasive wear failure due to shaft rubs should be minimized by providing clearances adequate to preclude rubbing. Fretting-corrosion wear, which is caused by the relative oscillatory motion of two surfaces under normal force such as in press fits, can be overcome by using tight fits, inducing residual surface compressive stresses, and reducing the vibration level).

3.1.4 Assembly and Operation

3.1.4.1 DIMENSIONS AND FITS

3.1.4.1.1 Datums

Datums shall result in minimum tolerance stackup.

The thrust-bearing shaft shoulder should be used as the longitudinal datum, except for hydrodynamic thrust bearings where a gage point in the thrust piston should be used. The roller-bearing shaft surface should be used as the diametrical datum. Unnecessary tolerance stackup should be avoided by locating important features from one datum only.

3.1.4.1.2 Dimensional Inspection

Dimensional inspection of critical parts shall account for thermal expansions at the time of measurement.

Measurements should be made only when the measuring tool and the critical part are at a standard temperature of 68° ± 1°F (293.2 ± 0.6K). Otherwise, the measurement must be corrected for the differential expansion.

3.1.4.1.3 Bearing Clearances

Clearances for rolling-contact bearings shall be based on the extreme tolerance conditions.

Despite the apparent improbability of simultaneous assembly of components in the extreme tolerance conditions, the extreme tolerance limits of the shaft, bearing, and housing should be used for stackup where rolling-contact-bearing internal clearance is concerned. For splines and other parts, the root-mean-square method of combining tolerances may be used.

3.1.4.1.4 Tolerance Limits

Tolerance limits shall be consistent with use and damage limits.

For components that are assembled and disassembled a number of times, use and damage limits should be established so that the original tolerance limits may be exceeded by a certain specified amount. This action may necessitate closer tolerances for the initial assembly.

3.1.4.1.5 Piloting

Piloting dimensions and fits shall be tight enough at all operating conditions to prevent relative motion and potential fretting or shifting of shaft parts that results in adverse rotor imbalance.

The selection of pilot dimensions and fits should be based on the class of fit desired and should take into account the effects of operation, process of manufacture, method of assembly, assembly-imposed stresses, dimensional changes due to operating thermal and stress environments, and material strengths.

The thermal expansions of the mating materials should be matched so that under all conditions, from assembly through operation, the interface pressure does not exceed design limits or allow the parts to become loose. During chilldown, thin parts could contract faster than a thick mating part, thereby increasing stress. The effect of centrifugal force should also be included in the calculations for press-fit at operating conditions. For press fits, the stress should be calculated and evaluated.

Double piloting (fig. 29) may be used when differential expansion of mating parts is severe.

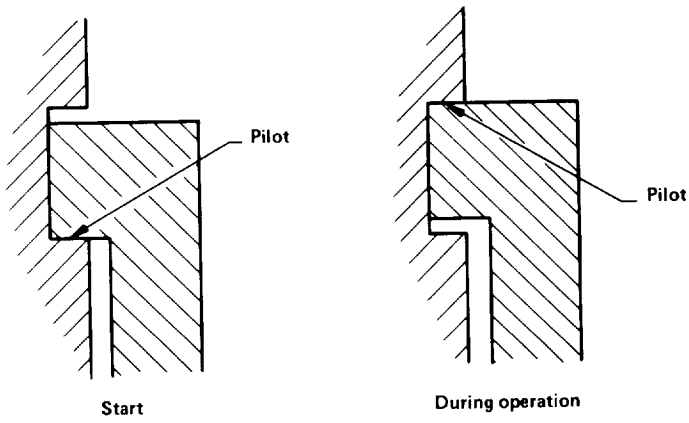

Figure 29. – Double piloting

However, although double piloting provides a tight fit at both extremes, it may result in looseness between extremes. Thus, double piloting is best limited to situations wherein the change in thermal environment takes place when the shaft is not operating (e.g., pre-engine-start chilldown of cryogenic fuel turbopump).

Tight-fitted parts should never be pressed together at assembly; they should be shrunk on.

3.1.4.2 COMPONENT RUNNING POSITIONS AND CLEARANCES

Component and assembly stackup dimensions and tolerances shall ensure adequate operating clearances between the rotating and stationary parts.

Both transient and steady-state running positions of the rotating parts relative to the stationary parts should be computed during the turbopump design phase. Critical clearances should be measured or reliably deduced during the initial testing of new machines. Engineering assembly drawings and specifications must clearly state minimum acceptable values for assembly buildup critical clearances. In some cases, where close running clearances are necessary for performance requirements, materials and construction that can withstand rubbing (e.g., honeycomb) should be used.

In determining axial operating clearances, calculations should account for

(1) Axial thrust loads and resulting rigid-body shaft position shifts

(2) Shaft extension or compression caused by axial thrust loads

(3) Axial distortions of both rotating and stationary parts induced by axisymmetric and non-axisymmetric temperature changes, thermal gradients, and creep

(4) Deflections and distortions in rotating and stationary parts induced by pressure and mechanically applied loads

(5) Shaft whirl slopes and resulting axial displacements at such locations as rotor tips

(6) Axial vibration amplitudes of such subcomponents as turbine wheels and impellers

(7) Minimum design clearances at assembly buildup (determined by tolerance stackup analysis or measured or both)

(8) A moderate amount of clearance allowed for contingencies

In determining radial operating clearances, calculations should account for

(1) Radial displacements of the rotating parts, especially turbine wheels and impellers, resulting from centrifugal, thermal, creep, pressure, and maneuver loads

(2) Shaft bending deflections resulting from unidirectional forces

(3) Shaft whirl orbit amplitudes

(4) Deformations of the stationary parts by pressure, external force (e.g., inlet and discharge line loads), temperature change, and thermal gradients

(5) Minimum design clearances at assembly buildup (determined by tolerance stackup analysis or measured or both)

(6) A moderate amount of clearance allowed for contingencies

At assembly, the bearing inner race with the least radial runout should be located at the bearing position nearest the greatest shaft overhang portion. Furthermore, the high points of race eccentricities should be aligned on the shaft (ref. 177).

3.1.4.3 RETAINING BOLTS AND LOCKING DEVICES

3.1.4.3.1 Bolt Mechanical Strength

The material properties, shape, and overall mechanical design of a retaining bolt shall be such that the bolt does not fail.

The bolt material should have the best combination of high strength, high coefficient of thermal expansion, and low modulus of elasticity. The junction of the shank and head should be designed with a generous radius or transition. The bolt threads should be of the fine pitch series. The bolt diameter may be increased from the cold to the hot turbine end to obtain a retaining bolt with uniform strength distribution along the length of the bolt (ref. 178) even when thermal gradients are large.

3.1.4.3.2 Bolt Preload

The retaining bolt preload shall prevent joint loosening and maintain the rigidity of the coupling under expected service conditions.

The preload should be adequate as to prevent yielding or unloading of the coupling due to (1) thermal change in the bolt and clamped parts (ref. 179), (2) load reduction as a result of axial thinning of the rotating parts caused by centrifugal force, (3) acceleration forces or resonance (refs. 180 and 181), and (4) plastic deformation. When evaluating the thermal change in the bolt and its effect on preload, account for variation in temperature along the length of the bolt; this variation should be measured or carefully calculated.

The preload should be such as to prevent motion between the clamped parts or the threads of the fastener components. The minimum preload for curvic couplings should be about 1.5 to 2 times the separating force. During development tests, it is advisable to measure bolt strain with a strain gage and slip-ring arrangement or some equally appropriate means.

3.1.4.3.2.1 Preload Measurement and Control

The method for measuring critical bolt preload shall provide reliable and repeatable results.

Torque is considered to be an unreliable method for preloading critical fasteners. When bolt load is critical (e.g., for the curvic-coupling retaining bolt), the preload should be controlled and specified in terms of overall bolt elongation. An alternative is to compress the rotor stack a measured amount and then assemble the bolt finger-tight. Avoid preloading the bolt to the extent that permanent deformation occurs and thereby results in a loose assembly.

If torque values are used for fasteners when preload is not critical, the torque should be specified with a tolerance on the applicable assembly drawing as well as on shop planning documents; a tolerance of ± 5 percent is recommended. Then the actual torque value during assembly should be recorded and verified. During development and demonstration, torque values in the tightening direction at teardown also should be recorded and compared with those taken at assembly. It may be necessary to specify drag and net torques separately. Differences between assembly and teardown torques greater than about 25 percent are indications that the bolt, the preload, or the locking device is inadequate to withstand the environmental loads, temperature, or vibration.

3.1.4.3.3 Vibration

The transverse and axial natural frequencies of long bolts shall not be excited by the shaft rotational frequency.

The transverse and axial natural frequencies of a long tie bolt should be determined by computation or by experiment, and these frequencies should not coincide with the shaft rotational frequency or multiples of 2 or 3 thereof.

3.1.4.3.4 Bolt Arrangement and Fit

The arrangement and fit of the bolt to the coupling shall not result in significant increase in bolt stress or interfere with the piloting of the coupling.

In multiple-bolt couplings, a close fit between the retaining bolt and the shaft or attached part may be required to minimize bolt stresses and deflections caused by centrifugal force. This close fit should not interfere with the piloting. A central bolt may be used for small curvic or parallel-sided face couplings where space does not permit multiple bolting, but multiple bolting is preferred for large couplings. The fits of parallel-sided face couplings with a central bolt arrangement should be tight enough to prevent a large lateral load on the bolt due to power torque.

3.1.4.3.5 Galling, Seizing, and Fretting

Fasteners and coupling parts in rotating assemblies shall not gall, seize, or fret.

Threads and other mating parts should be coated with a lubricant (refs. 52 and 53) compatible with the propellant and the environment, or plated with silver to prevent galling and seizing. Fretting usually is the result of a loose joint and can be eliminated by keeping joints tight.

3.1.4.3.6 Locking Device Action

Locking devices for fasteners and attachments on rotating parts shall provide positive locking action under all conditions of use.

Positive locking devices such as tab or crimp-type washers should be used on rotating assemblies. The crimp type with a wall thickness of 0.030 to 0.035 in. (0.762 to 0.889 mm) is recommended. Careful control of crimping is necessary to prevent cracking. Provision should be made for trapping failed fasteners or locking devices to prevent them from entering close clearances, holes, or passages. Fasteners with severable parts (e.g., safety wire) should not be used, because the severed part could lodge in a seal or bearing and thereby cause damage. Snap-rings are not recommended for rotating parts; however, if they are used, careful evaluation of groove detail, installation procedure, material selection, and loading is necessary.

3.1.4.4 ASSEMBLY AIDS

The location and size of slots, pins, offset holes, wrench flats, and other assembly aids shall not compromise shaft strength or balance.

Slots may be used to permit bearing race, gear, or sleeve removal; the slot design should follow the recommendations in section 3.1.1.4. Offset holes, pins, or similar devices should be used to ensure the correct assembly of look-alike parts. Wrench flats on shafts or couplings should be located where they have relatively little effect on shaft strength. Slots, holes, and wrench flats should be located symmetrically to minimize the effect on balance.

3.1.5 Quality Control

3.1.5.1 INSPECTION METHOD

The inspection method shall be appropriate for the portion of the shaft or coupling to be inspected and for the size and type of flaw that is cause for rejection of the part.

Magnetic particle inspection should be used for surface inspection of ferromagnetic materials, and penetrant inspection should be used for surface inspection of other materials. Ultrasonic inspection should be used to find plane-type, subsurface discontinuities such as

cracks. The ultrasonic inspection of raw materials before machining will minimize the scrapping of finished parts. The ultrasonic inspection of forgings should be accomplished after the last forging operating is completed. Radiographic inspection should be used to find volume-type, subsurface discontinuities such as holes (ref. 36). The maximum acceptable flaw size should be consistent with the static-strength and fatigue-life requirements of the design. The fracture-mechanics principles and analysis techniques of references 49 and 160 should be used in establishing inspection limits.

3.1.5.2 COMPONENT CONTAMINATION

The quality control procedure shall not result in chemical contamination of a component.

The chemicals used for inspection of the part should be removed during the cleaning procedure. Dye penetrant must be thoroughly baked out of parts that will be used in liquid fluorine service.

3.1.5.3 SPLINE INSPECTION

The degree of inspection of involute splines shall be consistent with the degree of loading or stress.

Lightly loaded splines require a minimum of inspection; highly loaded splines require close dimensional inspection of tooth thickness, form, and spacing so that there will be no interference and so that interchangeability is ensured. The recommended inspection specification is set forth in reference 182.

3.1.5.4 CURVIC COUPLING INSPECTION

Inspection of a curvic coupling shall verify sufficient tooth contact.

Use master couplings to inspect curvic couplings. The tooth contact surface between the masters should be 90 percent of the minimum theoretical surface at each 90° position (ref. 143). Axial and radial runouts between parts of the set apply at each of the 90° positions of orientation. For normal requirements, the bearing contact of the master with the part should be centrally located with 75 percent of the tooth width as the minimum contact. The depth of the contact area should be equal to the tooth contact depth. The stack height of the set should be marked on each piece of the master.

3.2 Shaft Dynamics

3.2.1 Dynamic Behavior

3.2.1.1 WHIRL MOTIONS

Shaft dynamic analyses shall be appropriate to the type of whirl motion.

For all designs, forward synchronous circular whirl motion should be assumed for calculations of critical speeds and shaft response. If the casing or bearing mount is asymmetrical about the shaft axis in either mass or stiffness, the forward synchronous elliptical and lateral vibration motion also should be analyzed for critical speeds and shaft response.

3.2.1.2 FORCED WHIRLS AND CRITICAL SPEEDS

3.2.1.2.1 Steady-State Operating Speed Limitations

There shall be no steady-state shaft operation near a major critical speed if bearing failure, rotor-tip rubbing, or other undesirable associated phenomenon can occur.

The lowest major critical speed whose mode shows a preponderance of the system potential energy to be due to rotor bending as compared with stator or bearing deformations should be no lower than 125 percent of the normal operating speed or 115 percent of the maximum overspeed, whichever is greater. The maximum bearing reactions at any steady-state speed should be compared with the bearing capacities, due regard being given to the required life, reliability, and applied bearing loads from sources other than shaft dynamics. Likewise, it is recommended that rotor whirl orbit amplitudes be computed and compared with available operating clearances (ref. 183).

Major critical speeds that involve appreciable stator or bearing deformation and that are lower than the operating speed are permissible when they comply with the following restrictions:

(1) The speed is no higher than 85 percent of the lowest steady-state operating speed.

(2) The speed is the lowest possible speed consistent with other design requirements (e.g., rotor running positions and displacements under worst loading should not exceed tip clearances).

(3) The rate of change in shaft speed while passing through the criticals is sufficient to preclude excessive response. Calculations (refs. 184 through 190) of possible response magnitudes should be made during the design phase.

(4) Self-excited whirls do not develop into untenable response levels.

If calculated critical speeds of the type discussed above are closer to the operating speed range than allowed by the restrictions given, and if the speeds cannot be moved appreciably without compromise of other design requirements, approval of the design regarding critical speeds should be based on comprehensive vibration tests of the complete rotor/stator assembly and on the comparison of experimentally determined operating clearances and bearing loads with the design allowables.

Tracking shaft motion with proximity probes (sec. 3.4.2) is especially recommended for initial testing of machines that operate above the first system major critical speed. This procedure allows evaluation of the potential of the rotor for self-excited whirling.

3.2.1.2.2 Assessing Importance of Critical Speeds

Analyses during the design phase shall define the major critical speeds.

To facilitate assessing the importance of various critical speeds, conduct analyses as described in section 2.2.1.2 so that the following information is obtained:

(1) Location of critical speeds relative to the operating speeds

(2) Mode shapes and kinetic energy distribution

(3) Response predictions: bearing reactions, whirl orbits, and sensitivity to imbalance

(4) Closeness of the critical to other identified resonant speeds

(5) Type of motion: synchronous or nonsynchronous, forward or backward, forced or self-excited, circular or noncircular

(6) Effort required to change critical speed or modify response level by design changes

Secondary critical speeds should be computed and listed for future reference as possible diagnostic aids in the event of failure preceded by peculiar shaft dynamic characteristics such as nonsynchronous vibrations, beats in response level, or other behavior described in references 58 through 61.

3.2.1.3 SELF-EXCITED WHIRLS AND INSTABILITIES

Shafts designed to operate above the first system critical speed shall not experience damaging effects of self-excited nonsynchronous whirls.

Rotors supported in rolling-contact bearings should be analyzed for self-excited whirl potentials by the methods presented in reference 83. This reference covers aerodynamic-induced instabilities and provides practical solutions to such problems.

Built-up shafts and rotors using press- or shrink-fitted items (e.g., sleeves and collars) should not be run above the system major critical speed whose mode has significant shaft bending, and damping is insufficient to preclude shaft rubbing, bearing overload, or shaft, coupling, or stator overstress. Reference 86 provides a detailed summary of additional causes and ways of eliminating harmful whirls induced by internal friction.

Operating a shaft with a dry-clearance bearing or a shaft rubbing on an unlubricated guard should be avoided throughout the entire speed range. If dry rubbing occurs, reverse whirl can become a near-resonant whirl over a large range of shaft speeds including speeds below the first system critical speed. To obtain the broadest band of whip-free rubbing, the rotor and stator natural frequencies should be kept dissimilar, and the rotor and stator dampings made close to one another (ref. 191). Other ways of mitigating whirls induced by dry friction, if they occur, are to (1) change the design by increasing operating clearances, (2) raise the rotor/stator system natural frequencies, (3) improve the rotor balance, or (4) coat the rubbing area with a low-friction-surface material.

Asymmetry in the stiffness of rotor casing or foundation should also be considered as a means of increasing the threshold speed of nonsynchronous self-excited whirls (ref. 192). Rotors using fluid-film bearings can be evaluated for stability by the methods described in references 54, 65, 68, and 83.

3.2.1.4 TORSIONAL CRITICAL SPEEDS

Shaft systems that have flexible couplings or that are part of a gearbox shall be free of harmful torsional critical speeds.

The torsional natural frequencies should be computed by appropriate methods such as those in references 88 through 90. To identify the shaft speeds that may be critical, the natural frequencies and the potential excitation frequencies should be cross plotted against shaft speed as shown in figure 4. Intersections determine critical speeds. Consult section 2.2.3 and references 63, 89, and 90 for sources of excitation. Steady-state shaft operating speeds should not coincide with the first system natural frequency or one-half or one-third of it. If the product of the number of gear teeth, or the number of impeller vanes, or the number of stator vanes multiplied by the rotational speed matches a natural frequency, operation at that speed is not recommended unless it can be shown by response computations or by test that adverse vibrations do not occur.

3.2.1.5 THIN-WALL HOLLOW-SHAFT VIBRATIONS

A thin-wall hollow shaft shall be free of harmful nodal-circle and nodal-diameter vibration critical speeds.

The methods and considerations of reference 193 should be used for analysis of potential nodal-circle and nodal-diameter vibration critical speed of hollow-drum-type shafts. If harmful vibration is predicted by analysis or develops in testing, the design thickness or excitation characteristics should be changed to detune the resonance.

3.2.2 Analysis of Shaft Dynamic Behavior

3.2.2.1 MODELING FOR THEORETICAL ANALYSES

3.2.2.1.1 Mass and Stiffness Distributions

The model shall simulate accurately variations of mass and stiffness throughout the entire rotor/bearing/casing system, include both flexural and shear deformation elements, and account for gyroscopic and inertia moments.

For the analysis of rotor/bearing/casing systems with rolling-contact bearings, multilevel lumped- or continuous-mass models are recommended; a typical model is shown in figure 30. For a lumped-mass model, the number of mass stations per level should exceed by a factor of four or five the number of that critical speed that follows after the upper limit of the operating speed. For all levels, a total of approximately 20 to 40 stations should be used.

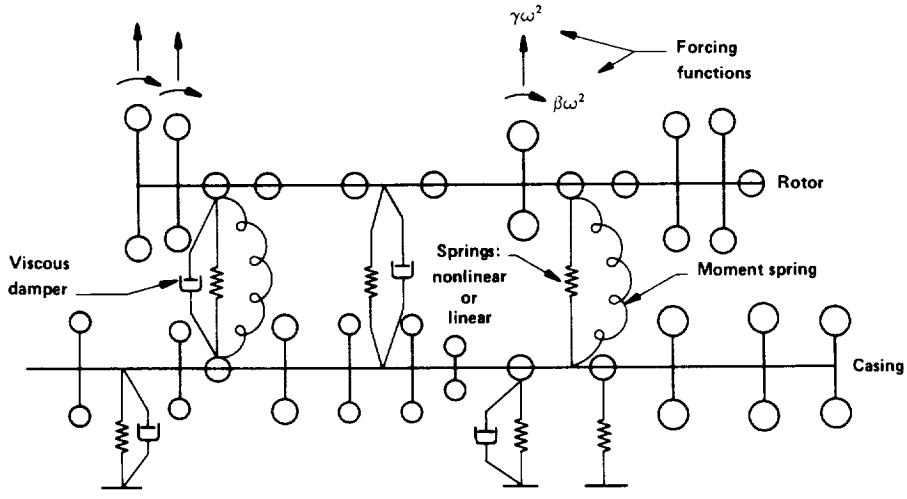

Figure 30. – Typical lumped-mass rotor/casing model

For systems with fluid-film bearings that are relatively soft as compared with the rotor stiffness or systems with flexibly mounted bearings, the single-level lumped- or continuous-mass models can be used.

Model basic elements of the Myklestad lumped-mass type (refs. 6, 92, 97, and 98) or the continuous-mass type (refs. 79 and 88) are recommended.

Gyroscopic-moment treatments for circular whirl and lateral vibration (refs. 98 and 183) are recommended for shafts supported by rolling-contact bearings. The treatment accounting for elliptical whirl motions (ref. 65) is recommended for shafts supported by fluid-film bearings.

When the accuracy of calculated model properties, (e.g., stiffness of a bearing support housing and bearing stiffness) is questionable and the parametric analyses show that these properties significantly influence the critical-speed characteristics, tests should be conducted to allow experimental determination of the proper model properties. See section 3.4 for recommended tests.

3.2.2.1.2 Mechanical Joints, Shaft-Riding Elements, and Abrupt Changes in Shaft or Casing Cross Section

The model shall simulate the actual stiffness influences associated with mechanical joints, shaft-riding elements, and abrupt changes in shaft or casing cross section.

"Equivalent-beam" sections or influence coefficients are recommended for representing the actual stiffnesses associated with the curvic coupling or similar joints, shaft-riding elements, and abrupt changes in shaft or casing cross section. Axial and moment load-deflection data obtained from tests of the actual joints or of similar previous designs are best for determining the equivalent system properties. For preliminary design, when applicable test data or good experience does not exist, it is recommended that curvic-coupling equivalent-beam sections be assumed to have a wall thickness of 1 to 3 percent of the tooth face width (i.e., $t_o/F = 0.01$ to 0.03) for a length equal to the whole depth of the teeth (fig. 31).

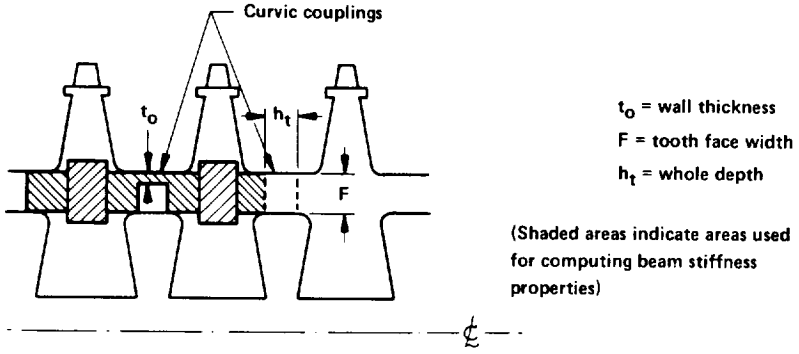

Figure 31. – Curvic coupling equivalent beam sections

The experimental data presented in figure 8.5 of reference 132 should be consulted for determining the stiffening effects of such items as shrunk-on hubs and shrunk-on shaft sleeves. Flexibility effects of conical transition sections or abrupt changes of diameter in the casing or in hollow shafts should be evaluated analytically using a digital computer program for a shell of revolution subjected to non-axisymmetrical loads (refs. 194 through 196).

3.2.2.1.3 Casing and Machine Mount Effects

The model shall accurately simulate the influences of the bearing mounts and casing.

The bearing mounts and casing should be represented by distributed-mass and variable-stiffness models similar to those used for the rotor unless the bearing mount is purposely designed to be flexible, or unless relatively soft fluid-film bearings are used. For these cases, only the bearing-mount stiffness need be modeled, and the casing can be considered as ground.

3.2.2.1.4 Bearing Spring and Damping Forces

The model shall include bearing spring and damping forces as appropriate.

Effects of preload, high-speed centrifugal and gyroscopic loads, and nonlinear load-deflection characteristics should be included in the analyses of angular-contact-bearing stiffness. Analyses of roller-bearing stiffness should include the effects of bearing internal play, shaft misalignment, and the load-deflection nonlinearities. It is recommended that spring rates of rolling-contact bearings be determined by the methods presented in reference 112. Models for rolling-contact bearings need not include damping forces unless special damping mechanisms are part of the design.

Fluid-film bearings must be represented by spring and damping forces that are defined as a function of shaft speed. As labyrinth seals and wear rings also can act like fluid-film bearings to produce stiffness and damping and affect the rotor stability, they should be given proper consideration in the shaft dynamics model. Fluid-film bearings may be characterized and evaluated by techniques given in the references cited in section 2.2.2.1.4.

3.2.2.1.5 Rotor Imbalance Forcing Functions

The model shall include imbalance forcing functions that will enable response evaluation.

Imbalance forcing functions should account for the residual imbalance after balancing, possible imbalance upon reassembly caused by such factors as pilot fits and runouts, possible balance change during operation resulting from load and thermal distortions, and conical or cylindrical whirl forces allowed by roller-bearing internal clearances.

Rotor imbalances that induce circular whirl motion may be represented by the expressions

$$F_s = (Ch_s \pm eW/g)\,\Omega^2 = \gamma\Omega^2$$

$$= (h_s \pm eM)\,\Omega^2 = \gamma\Omega^2 \qquad \text{(SI units)}$$

$$F_d = (Ch_d \pm \theta\, I_d/g)\,\Omega^2 = \beta\Omega^2$$

$$= (h_d \pm \theta\, I_d{}^1)\,\Omega^2 = \beta\Omega^2 \qquad \text{(SI units)}$$

where

F_s = static imbalance, lb (kg)

C = 1.62×10^{-4} lb-sec^2/in. = (lb/16 oz) x (1/g)

h_s = static balance error attained on balance machine, in.-oz (m-kg)

W = component weight, lb

g = acceleration due to gravity, 386 in./sec^2

e = radial eccentricity caused by fit changes, bearing internal play, runouts, etc. that are not corrected for by balancing, in. (m)

Ω = rotational speed, radians/sec

γ = static imbalance forcing function, lb/(rad/sec)^2 (kg/(rad/sec)^2)

M = component weight, kg

F_d = dynamic imbalance, in.-lb (m-kg)

h_d = dynamic balance error, in.^{2}-oz (m^2-kg)

I_d = component diametral moment of inertia, lb-in.^{2}

θ = angular eccentricity, rad.

β = dynamic imbalance forcing function, in.-lb/(rad/sec)^2 (m-kg/(rad/sec)^2)

I_d^1 = component diametral moment of inertia, (kg-m^2)

The ± sign in the equations are used to imply that, strictly speaking, the two quantities in the parentheses do not combine algebraically, but vectorially. However, as the actual vector orientation is unknown, these quantities usually are assumed to be algebraically additive.

For elliptical whirl motion, the forcing functions in reference 57 should be used.

3.2.2.1.6 Virtual Mass and Damping

When necessary, the model shall include the virtual mass and damping associated with shaft operation in a dense fluid or a geared system.

Virtual mass and damping effects of dense fluids (i.e., density of water or greater) can significantly affect critical speeds and shaft response. However, as adequate quantitative theoretical treatments are not available, experimental determinations of the proper model properties should be made. The gear restraint imposed on a pinioned shaft should be accounted for in the model by the technique given in reference 126.

3.2.2.2 MATHEMATICAL METHODS AND COMPUTER SOLUTIONS

Mathematical formulations and resulting computer programs shall be capable of accounting for all the applicable characteristics of the analytical model.

The types of computer programs recommended for the analysis of rotors supported on fluid-film bearings are those presented in references 65, 79, and 91. The types of computer programs recommended for the analysis of rotors supported by rolling-contact bearings are those presented in references 6, 88, 92, and 183. As noted earlier, the computer programs in references 65, 88, and 92 are generally available.

In utilizing any of the available computer programs, the following factors, which are not included in the programs, should be considered:

(1) Fluid-film bearings are not always soft enough relative to the casing to decouple the casing effectively from the rotor/bearing dynamics. The program in reference 65 is limited to a simple lumped mass at each bearing to represent the casing. However, this computer program for rotor/bearing dynamics could, if necessary, be expanded to include a continuous-mass beam model to represent the casing as well as the rotor.

(2) Angular-contact ball bearings can have highly nonlinear spring characteristics that are dependent on axial as well as radial and moment loads on the bearings. To account more accurately for the ball-bearing characteristics, the equations of reference 112 or 113 are incorporated into the rotor/bearing computer programs. This step allows inclusion of the effects of the bearing nonlinear spring characteristics, as influenced by thrust and imbalance, on the critical speeds.

3.2.2.3 PREDICTION ACCURACY

The expected accuracy of the theoretical predictions of critical speeds and response magnitudes shall be known.

Prediction accuracy determined experimentally on previous machines of similar configuration is the best basis for assessing expected accuracy for new machines. In addition, those factors that affect prediction accuracy (sec. 2.2.2.3) should be included in the assessment. Moreover, calculated critical speeds should never be considered more accurate than the predicted value ± 5 percent. The response magnitudes (shaft deflections, bearing loads, etc.) should be considered to be fairly unpredictable; they may be two or three times the calculated values.

3.2.3 Adjustment of Critical Speeds and Response Levels

A design change to adjust critical speeds and response levels shall be based on theoretical or experimental analyses that predict the magnitude of adjustment that can be expected and the impact of the design change on other design considerations such as strength, fabrication complexity, and cost.

Analytical evaluation of the influence of the various parameters affecting critical-speed locations and responses should be the basis for design selection or modification. Experimental confirmation using the techniques recommended in section 3.4 should be accomplished. Short of major shaft redesign, the following techniques should be considered for adjusting critical-speed locations:

(1) Change bearing stiffness by increasing the axial preload of angular-contact bearings, by replacing angular-contact with roller bearings, or by replacing each angular-contact bearing with duplex-bearing sets mounted back-to-back.

(2) Change bearing mount or casing stiffness.

(3) Change fits and axial preloading of shaft-mounted elements such as shrunk-on impellers, bearing races, and sleeves.

(4) Change axial preload of joint-retaining bolts.

Recommended techniques that should be considered for adjusting response levels are the following:

(1) Improve rotor balance by reducing the amount of residual imbalance, by increasing the quality of the balance with multiplane corrections and high-speed techniques, and by minimizing the potential for imbalance developing on reassembly in the turbopump.

(2) Change operating speed or critical speeds to detune shaft.

(3) Reduce internal clearance of roller bearings, and add or increase damping.

(4) Increase the rate of passing through the critical speed directly before the region of resonance, and reduce the acceleration just above the critical speed (ref. 67).

3.2.4 Balancing

The method of balancing and required balance accuracy shall be consistent with (1) mass and shape of the rotor, (2) shaft operating speeds and their relations to the critical speeds, and (3) required turbopump life.

Static balance may be used for rotors of large mass, large mass-moment-of-inertia, and small axial thickness. Dynamic low-speed balancing may be used for rotors operating below the first bending critical. Dynamic high-speed balancing is required when rotors operate above the first bending critical. If n is the number of shaft bending criticals through which the shaft is operated, then the rotor should be balanced in a minimum of n+2 planes (ref. 137).

As a general guide, the rotor should be balanced to an eccentricity of about 50 to 100μ in. (1.27 to 2.54μm). Separate balance of rotor components is advisable when the component is of large mass, large mass-moment-of-inertia, and appreciable axial length. The shaft or component should be supported at the same surfaces that determine the axis of rotation during turbopump operation.

The material for balancing should be added or removed where the diameter is large, so that the relative amount of material change is small. For components that will be used with liquid oxygen, grind material away rather than drill holes, because contaminants may collect in the holes.

Tie bolts should be piloted to maintain concentricity. To minimize required balance corrections, locate fasteners, slots, wrench flats, etc. symmetrically on the shaft.

3.3 Coupling Design

The coupling type shall satisfy applied loads, required alignment, and envelope limits.

Splines are recommended as the coupling to be used where there is torque load but no axial or thrust load and where there is sufficient space for separate piloting. Curvic couplings are recommended for use in highly loaded applications where there is both axial and torque loading and where precision piloting is needed. Parallel-sided face couplings are recommended for lightly loaded applications (both axial and torque) and for applications where space permits separate piloting.

3.3.1 Splines

3.3.1.1 SIZE AND CONFIGURATION

The spline design shall conform to the ASA standard ANSI B 92.1[1] *except when modifications will improve the performance.*

A circular-arc space width equal to one-half the circular pitch should be used for the internal member with tolerance in the plus direction. The clearance then establishes the maximum tooth width of the external member with tolerance on the minus side. If a side bearing fit is desired, the clearance should be in the order of 0.0001 in.(2.54 μ m).If a corrective helix angle is used, the hand of the helix angle should be that which tends to unwind the helix of the externally toothed member under torque load.

Inducers and impellers of oxidizer or monopropellant pumps should be driven by splines that are straddled by centering pilots. For these applications, the splines should have the relatively loose Class 1 side-fit dimensions, while the pilots should be tight at operating temperature. The fits to be used at the pilots will vary with rotor design and materials. It should be an interference fit at operating temperatures. For example, a recommended maximum interference for an aluminum pumping element mounted on an Inconel X750

[1]Reference 182

shaft is approximately 0.001-in. (25.4μm) interference for each inch (2.54 cm) of pilot diameter in the size range from 1 to 3 in. (2.54 to 7.62 cm); the minimum interference should be about 0.0009 in. (23μm) less than the maximum. Tests should be performed to ensure that the fit is tight enough to prevent any clearly defined fretting in the spline or other mating surfaces.

The use of side-fit splines with straddling pilot diameters is recommended for other main drives; however, a major-diameter-fit spline without pilots is an acceptable alternate for splines operating at moderate temperatures. The major-diameter-fit spline is to be preferred for appropriate applications where it allows the rotor length to be decreased as a result of eliminating the pilots.

When involute splines are used in a hot-turbine environment, the Class 1 side-fit spline with straddling pilot diameters is recommended. In this case, because of the temperature transients, the pilots should be tight at all temperatures if the centering of the turbine wheel is fixed by the pilots.

Main-drive splines should be 14½°, 30-percent stub tooth. An even number of teeth should be used. The full-fillet radii should be used whenever possible, and the dimensions on the drawing should control the upper and lower limit of the diametral pitch. When space does not permit both members to have fillet root, it should be on the external teeth because they are generally weaker in root tensile strength.

A crowned spline is suitable for misalignments in the range of 0.25° to 3°.

Accessory drive splines should be 30°, 50-percent stub tooth.

3.3.1.2 TEETH IN CONTACT

The number of teeth assumed to be in contact shall be based on the tolerances required and the degree of final inspection.

For lightly loaded splines, 25 percent of the teeth should be assumed to be in contact. A spline length of two-thirds to one shaft diameter is recommended. For highly loaded splines, 50 percent of the teeth may be assumed in contact provided that the tolerances are tightly controlled and finished parts are closely inspected. This inspection should include tooth thickness, form, spacing, and interference as well as inspection by gages to ensure interchangeability.

3.3.2 Curvic Couplings

3.3.2.1 PROPORTIONS FOR JOINT STIFFNESS

The ratio of the rotor disk diameter to the coupling outer diameter shall be as small as possible.

The ratio of the disk diameter to the curvic outer diameter (fig. 22) should not exceed 4 for maximum joint rigidity and stability.

3.3.2.2 SIZE AND CONFIGURATION

The coupling size and configuration shall satisfy the requirements imposed by critical loading conditions, necessary safety factors, and specified reliability.

For initial sizing, approximate analysis may be used. A useful formula (ref. 143), based on a face length of 12.5 percent of the coupling diameter and an ultimate strength of 150,000 psi (1.03 GN/m^2), gives the required curvic coupling outside diameter in inches as equal to the cube root of T/1310,where T is the shaft torque in in.-lbf. (In meters, the OD is equal to the cube root of $T/(9.03 \times 10^6)$, where T is the shaft torque in N-m).

For final sizing, detailed stress analysis should be used. The stress analysis should include tooth shear, contact surface stress, transverse shear, and tension across the tooth at the root. Effects of fretting on tooth cracking also should be considered (ref. 197). The axial force used for the analysis in conjunction with the power torque load should account for the retaining bolt preload of 1.5 to 2 times the separating force and its tolerance plus other operational applied loads (sec. 3.1.3). The coupling may be subjected to a higher-than-normal load at initial assembly in order to increase the contact area.

When standard tooth proportions are used, the contact surface area and shear area remain constant for a given coupling diameter regardless of the number of teeth. The tooth proportions, diametral pitch, and stress limits of reference 143 should be used for long-life, high-reliability applications. However, the reference 143 values are conservative for short-life applications (1 hour or less); hence, stress limits twice those of the reference may be used in short-life designs. Higher stress limits may be tolerated if joint strength is verified experimentally. A tooth contact angle of 30° is recommended. For highly loaded couplings, the surface contact area should be controlled by using close tolerances and rigid inspection.

The detail design should always be directed to eliminating stress raisers or reducing their effect. Typical means of accomplishing this are to avoid bolt holes in curvic coupling teeth and to follow the recommendations in section 3.1.1.4.

For multiple-reuse and long-life applications, an analysis of both high- and low-cycle fatigue should be made (sec. 3.1.3.3).

3.3.3 Parallel-Sided Face Couplings

Parallel-sided face couplings shall not be subject to heavy loads or critical piloting.

Structural analysis of the teeth, retaining bolt, and pilot should be accomplished to ensure that the coupling design has adequate strength to withstand the loads and intended environmental use. Particular attention should be given to tooth tolerances, clearances, and plastic deformation that may be necessary to develop significant tooth-to-tooth load sharing. With one tooth in contact, the pilot is subjected to a transverse load that may result in shaft misalignment due to pilot deflection.

3.4 Design Confirmation Tests

Tests shall provide confirmation of the rotor design adequacy.

Tests should be made to confirm all questionable assumptions used in the design analyses when it is expected that deviations from the assumptions seriously affect design adequacy. These tests should include shake and rotating system tests as well as special stiffness and strength tests as appropriate. The tests should evaluate

(1) Critical speeds, whirl deflection shapes and orbit magnitudes, and bearing reactions.

(2) Any unknown significant shaft dynamic characteristics such as self-excited whirls at supercritical speeds.

(3) The effects on shaft performance of tie-bolt preload, bearing clearances, amounts and locations of imbalance, and static forces applied to the shaft.

(4) The effects of acceleration rate and flexible-mount stiffness on the ease of passing through critical speeds.

(5) Curvic-coupling stiffness under axial and moment loads.

(6) Bolt preload as a function of bolt stretch and pretorque.

(7) Bearing-mount stiffness.

(8) Shaft and coupling ultimate static and fatigue strengths.

3.4.1 Nonrotating Tests

Nonrotating (shake) tests shall provide data suitable for evaluating the dynamic characteristics of the rotor/bearing subsystem.

The test data should be used primarily for built-up shafts to confirm the accuracy of the analytical model used for the rotor and bearings (sec. 3.2.2.1).

The first shake tests of the rotor system should be with the rotor supported by flexible wire to simulate a free-free bearing support condition. These tests should be used to give data regarding tie-bolt preload requirements, effective stiffness of joints and shaft-riding elements, and rotor-only free-free bending natural frequencies and mode shapes. These data provide an excellent check on the accuracy of the model used for the rotor in the analysis of rotor/bearing/casing system dynamics.

A second series of shake tests is recommended mainly if the rotor bearing system supports are purposely designed as flexible mounts. Then, a number of different flexible-mount configurations should be used to provide data for selecting the appropriate mount configuration that will "tune" the rotor to the desired dynamic characteristics. These tests also provide additional data on tie-bolt preload and rotor stiffness effects.

The instrumentation used in this series of tests may be any of the standard vibration-laboratory instrumentation that will yield the type of data desired.

3.4.1.1 DATA CORRELATION

The evaluation of findings from shake tests shall be consistent with the differences that exist between the shake test and the actual rotating test hardware and environment.

The following should be evaluated for differences:

(1) Levels of excitation.– A very low, constant-level excitation usually is used in shake tests, whereas excitation from a rotating imbalance force increases in proportion to the square of the rotational frequency.

(2) Gyroscopic and rotary inertia effects.– Natural frequencies during shake tests are lowered because of rotary inertia of the disks, whereas in forward circular whirl rotation the disks produce gyroscopic stiffening that raises the natural frequencies.

(3) Bearing clearances and effective stiffness.

(4) Damping.

(5) Rotor stiffness developed by shaft-riding elements, and rotor stiffness at the joints and couplings.

(6) The housing, casing, or support-mount dynamic stiffness characteristics.– Shake tests usually involve something other than the actual machine casing.

3.4.2 Rotating System Tests

During design or initial development stages, turbopump rotating tests shall provide system-dynamics data suitable for evaluating system characteristics.

Critical-Speed spin-rig tests.– This test series should consist of many spin tests with selected different bearing-mount configurations. The spin-rig rotor and bearing hardware should be sufficiently close to actual detail design configuration to simulate fully the actual mass and stiffness magnitudes and distribution. The casing need only be crudely simulated if the mount dynamically decouples the rotor/bearing-mount system from the turbopump casing.

This series of tests should be the main tool for achieving the overall test objectives for the rotor-dynamics design program. However, as the rig will not simulate all fluid dynamic properties or the clearances between rotor and stator parts of the prototype, the assurance that self-excited subsynchronous whirls will not occur or will not be damaging must await the full-scale prototype tests.

Full-Scale prototype rotating system tests.– These tests should consist of the normal development tests planned for the turbopumps. Rotor dynamic data should be obtained by using appropriate instrumentation to monitor shaft motion and general turbopump vibration level. Accelerometers, velocity probes, and distance detectors should be placed at locations known from the prior system-dynamics analyses and tests to be sensitive indicators of vibration levels. Data from this series of tests should confirm findings from the earlier test series and identify any new characteristics associated with the prototype hardware that was not evidenced at the lower level of simulation of the spin-rig test series. These spin tests should be accomplished early enough to allow a redesign cycle if necessary.

3.4.2.1 INSTRUMENTATION

3.4.2.1.1 Type of Instrumentation

The test instrumentation shall be appropriate for the dynamics data desired and for the test conditions.

As applicable, the following should be considered:

(1) Distance detectors to monitor shaft motion; because of their sensitivity to temperature, the distance detectors should be calibrated.

(2) Velocity probes for frequencies up to 1000 Hz; accelerometers for frequencies above 1000 Hz.

(3) Output signal filtered to isolate the frequency of interest.

(4) An oscilloscope to monitor visually the wave form and amplitude.

(5) Instrumentation system frequency response substantially higher than the maximum frequency of interest.

(6) Instrumentation capabilities compatible with the environment.

(7) A tracking filter for variable speed tests.

(8) Rokide or plasma spray to bond strain gages to high-temperature (>1500° F (1089 K)) rotating parts.

(9) Readings clearly representative of shaft motion and not unduly influenced by the mount response.

(10) Instrumentation that does not alter the response of the shaft by mass loading or aerodynamic interference.

3.4.2.1.2 Instrumentation Location

Instrumentation locations shall be adequate to monitor general vibration levels.

Instrumentation should be placed at locations known from prior system dynamic tests to be the best locations for indicating overall vibration levels. Usually, accelerometers and velocity probes placed near bearing locations serve well. Place the distance detectors in 90°-displaced pairs at various locations along the shaft, preferably where nodes are not expected; both lateral and axial shaft motion should be measured. Distance detectors measure relative motion between the shaft and the distance detector mount only; therefore, it may be necessary to place accelerometers or velocity probes on these mounts to measure the mount absolute motions.

3.4.2.2 INTERPRETATION OF DATA

The interpretation of vibration data shall be adequate to determine normal levels of vibrations and to identify abnormal conditions.

The following techniques should be considered, as applicable, to aid in data interpretation:

- View unfiltered vibration wave form.
- Plot first-order vibration amplitudes versus shaft speed.
- View the Lissajous pattern at the various speeds of interest.
- Analyze data using narrow-bandwidth filters to produce a plot of vibration intensity versus frequency (i.e., power spectral density analyses) for a constant shaft speed.

Vibrations with frequency equal to shaft speed are called first-order vibrations. Typical causes of various-order vibrations are as follows:

(1) Half order: Self-excited whirl, cage rotational frequency.

(2) First order: Rotor imbalance.

(3) Second order: Bearing misalignment, assembly looseness, and impending coupling failure.

(4) Higher order: Blade passing, gear mesh, bearing noise, torque pulsations, and background vibrations.

3.4.3 Special Tests

Special tests shall evaluate critical design factors that cannot be determined accurately by other means.

When rotor or stator component or assembly characteristics are difficult to calculate accurately, and when the characteristics can cause a significant influence on the proper functioning of the shaft, experimental analysis using models or the actual component should be employed. As applicable, bearing and bearing-support-housing static and dynamic load deflection tests should be used for stiffness evaluations. Retaining bolts holding turbine or pump parts to the shaft should be calibration tested for preload. With this information, the required assembly technique to ensure that the desired preload is achieved during assembly can be established.

REFERENCES

1. Anon.: Liquid Rocket Engine Turbopump Bearings. NASA Space Vehicle Design Criteria Monograph, NASA SP-8048, March 1971.

2. Anon.: Liquid Rocket Engine Turbines. NASA Space Vehicle Design Criteria Monograph (to be published).

3. Anon.: Liquid Rocket Engine Axial Flow Turbopumps. NASA Space Vehicle Design Criteria Monograph (to be published).

4. Anon.: Liquid Rocket Engine Centrifugal Flow Turbopumps. NASA Space Vehicle Design Criteria Monograph (to be published).

5. Anon.: Liquid Rocket Engine Turbopump Rotating Shaft Seals. NASA Space Vehicle Design Criteria Monograph (to be published).

6. Bohm, R. T.: Tame Menace of Turbine Vibration. SAE J., vol. 74, no. 2, Feb. 1966, pp. 44-48.

7. Linn, F. C.; and Prohl, M. A.: The Effect of Flexibility of Support Upon the Critical Speeds of High Speed Rotors. Trans. Soc. Nav. Arch. and Marine Engrs., vol. 59, 1951.

8. Jekat, W. K.: Bearings, Seals, and Rotor Dynamics of Turboexpanders and Silar Hi-Speed Machinery. Paper 65-WA/PID-7, ASME Winter Annual Meeting (Chicago, IL), Nov. 7-11, 1965 (Abstract, Mech. Eng., vol. 88, Feb. 1966, p. 75).

9. Bohm, R. T.: Optimum Bearing Locations for Maximum Critical Speed. Mach. Des., vol. 31, no. 26, Dec. 24, 1959, pp. 117-119.

10. Spotts, M. F.: Design of Machine Elements. Prentice-Hall, Inc., 1961.

11. Sadowy, M.: Shafts, Couplings, Keys, etc. Sec. 27, Mechanical Design and System Handbook, H. A. Rothbart, ed., McGraw-Hill Book Co., 1964.

12. Shigley, J. E.: Mechanical Engineering Design. Ch. 5. McGraw-Hill Book Co., 1963.

13. Peterson, R. E.: Stress Concentration Design Factors. John Wiley & Sons, Inc., 1953.

14. Roark, R. J.: Formulas for Stress and Strain. Third ed., McGraw-Hill Book Co., 1954.

15. Lipson, C.; and Juvinall, R. C.: Handbook of Stress and Strength (Design and Material Applications). The Macmillan Co., 1963.

16. Frocht, M. W.; and Landsberg, D.: Factors of Stress Construction Due to Elliptical Fillets. J. Appl. Mech., Trans. ASME, Series E, vol. 81, 1959, pp. 448-450.

17. Fessler, H.; and Roberts, E. A.: Bending Stresses in a Shaft With a Transverse Hole. Univ. of Nottingham, England, 1967.

18. Heywood, R. B.: Designing Against Fatigue of Metals. Reinhold Publishing Corp., 1962.

19. Peterson, R. E.: Grooves, Fillets, Oil Holes, and Keyways. ASME Handbook, Metals Engineering Design, second ed., Pt. 2, sec. 7-6, Oscar J. Horger, ed., McGraw-Hill Book Co., 1965.

20. Thum, A.; and Bautz, W.: The Relief Transition. RSIC-212, Redstone Scientific Information Center (Redstone Arsenal, AL), July 1964. (translated from Forschung auf dem Gebiete des Ingenieurwesens, 6, no. 6, pp. 269-273, 1935.)

21. Spotts, M. F.: A Direct Method for Calculating Stress-Raising Effects in Press-Fitted Shafts. Mach. Des., vol. 33, no. 13, June 22, 1961, pp. 151-152.

22. Horger, O. J.: Press- and Shrink-Fitted Assembly. ASME Handbook, Metals Engineering Design, second ed., Pt. 2, sec. 8-13, Oscar J. Horger, ed., McGraw-Hill Book Co., 1965.

23. Hanley, B. C.; and Dolan, T. J.: Surface Finish. ASME Handbook, Metals Engineering Design, second ed., Pt. 2, sec. 7-5, Oscar J. Horger, ed., McGraw-Hill Book Co., 1965.

24. Hartman, M. A.: Advances in Aerospace Power Gearing. Power Transmission Design, Nov. 1967, pp. 40-47.

25. Heyn, W. O.: Shaft Surface Finish Is An Important Part of the Sealing System. J. Lub. Tech., Trans. ASME, series F, vol. 90, 1968, pp. 375-381.

26. Campbell, J. E.: Effects of Hydrogen Gas on Metals at Ambient Temperature. DMIC Report S-31, Defense Metals Information Center, Battelle Memorial Institute (Columbus, OH), Apr. 1970.

27. Anon.: Effects of High Pressure Hydrogen on Metals. NASA Tech Brief 70-10162, 1970.

28. Cataldo, E. E.: Stress Corrosion. Res. Achievements Review, vol. 2, no. 4, NASA TMX-53610, Marshall Space Flight Center (Huntsville, AL), 1966, pp. 7-14.

29. Anon.: Investigation of Aluminum Components Susceptible to Stress Corrosion. AGC TL 4U6256, Aerojet-General Corp., 1964.

30. O'Connor, J. J.: Development and Demonstration of Manufacturing Techniques for Joining Bimetal Shafts. Rep. PWA-3079 (AD 813119), Pratt & Whitney Aircraft (East Hartford, CT), Apr. 1967.

31. Jaffe, J. E.; and Rittenhouse, J. B.: Behavior of Materials in Space Environments. ARS J., vol. 32, May 1962, pp. 321-346.

32. Courtney, W.; Lavelle, J.; Britton, R.; and Denholm, A. S.: Sealing Techniques for Rotation in Vacuum. Astronaut. Aeron., vol. 2, no. 2, Feb. 1964, pp. 40-44.

33. Cornwall, E. P.: Welded Joints for Hard-Vacuum Systems. Mach. Des., vol. 35, Aug. 15, 1963, pp. 135-138.

34. Janser, G. R.: Summary of Materials Technology of M-1 Engine. NASA CR-54961, 1966.

35. Schwartzberg, F.R.; Osgood, S. H.; and Herzog, R. G.: Cryogenic Materials Data Handbook. AFML-TDR-64-280, 2 vols., Air Force Materials Laboratory (WPAFB, OH), July 1968.

36. Anon.: Development of a 1,500,000 lb Thrust (Nominal Vacuum) Liquid Hydrogen/Liquid Oxygen Engine. Rep. 2555-M-1-F, Aerojet-General Corp., Aug. 30, 1967, p. 289.

37. Spinelli, F.: Development and Demonstration of Manufacturing Techniques for Joining Bimetal Shafts. Rep. PWA 2946 (AD 803255), Pratt & Whitney Aircraft (East Hartford, CT),Oct. 1966.

38. Manjoine, J. J.: Flow and Fracture in Metals. Mech. Eng., vol. 89, no. 9, Sept. 1967, pp. 54-59.

39. Montgomery, J. D.: Fatigue Testing of T56 Aircraft Jet Engine Propeller Tests. Final Report for Nov. 1, 1963 to Mar. 1, 1964 (AD 603142), Oklahoma Univ. Res. Inst. (Norman, OK).

40. Haugen, E. B.: Probabilistic Approaches to Design. John Wiley & Sons, Inc., 1968.

41. Kececioglu, D.; and Cormier, D.: Designing a Specified Reliability into a Component. Proc. Third Annual Aerospace and Maintainability Conference (Washington, DC), June 1964, pp. 546-565.

42. Mischke, C.: A Method of Relating Factor of Safety and Reliability. Paper 69-WA/DE-6, ASME Winter Annual Meeting (Los Angeles, CA), Nov. 16-20, 1969.

43. Gabriel, D. S.; and Helms, I. L.: Nuclear Rocket Engine Program Status - 1970. Paper 70-711, AIAA 6th Propulsion Joint Specialist Conference (San Diego, CA), June 15-19, 1970.

44. Mittenbergs, A. A.: The Materials Problem in Structural Reliability. Annals of Reliability and Maintainability, vol. 5 - Achieving System Effectiveness, AIAA, 1966, pp. 148-158.

45. Bouton, I.; Trent, D. J.; and Chenoweth, H. B.: Design Factors for Structural Reliability. Annals of Reliability and Maintainability, vol. 5 - Achieving System Effectiveness, AIAA, 1966, pp. 229-235.

46. Marin, J.: Mechanical Behavior of Engineering Materials. Ch. 4. Prentice-Hall, Inc., 1962

47. Marin, J.: Theories of Failure. ASME Handbook, Metals Engineering Design, second ed., Pt. 5, sec. 2-2, Oscar J. Horger, ed., McGraw-Hill Book Co., 1965, pp. 525-526.

48. Manson, S. S.: Thermal Stress and Low Cycle Fatigue. McGraw-Hill Book Co., 1966.

49. Yukawa, S.; Timo, D. P.; and Rubio, A.: Fracture Design Practices for Rotating Equipment. Ch. 2, Fracture, vol. 5, Fracture Design of Structures, Harold Liebowitz, ed., Academic Press, 1969.

50. Anon.: Bearing Catalog AR-159. Rollway Bearing Co., Inc. (Syracuse, NY),1959.

51. Anon.: Engineering Support Documentation for SNAP-8 Turbine Alternator Assembly. Rep. 2954 (6 vols.), Aerojet-General Corp., Nov. 1965.

52. Campbell, M.; Thompson, M. B.; and Hopkins, V.: Liquid Lubricant Handbook for Use in the Space Industry. Contract NAS8-1540, Control No. TP85-137, Midwest Research Institute (Kansas City, MO), 1966.

53. Campbell, M.; Thompson, M. B.; and Hopkins, V.: Solid Lubricant Handbook for Use in Space Industry. Contract NAS8-1540, Control No. TP85-137, Midwest Research Institute (Kansas City, MO), 1968.

54. Sternlicht, B.; and Lewis, P.: Vibration Problems With High Speed Turbomachinery. J. Eng. Ind., Trans. ASME, Series B, vol. 90, 1968, pp. 174-186.

55. Dimentberg, F. M.: Flexural Vibrations of Rotating Shafts. Butterworth & Co. (London), 1961.

56. Lewis, P.; and Malanoski, S. B.: Rotor-Bearing Dynamics Design Technology. Pt. IV: Ball Bearing Design Data. AFAPL-TR-65-45, Air Force Aero Prop. Lab. (WPAFB, OH), May 1965.

57. Lund, J. W.; et al.: Rotor-Bearing Dynamics Design Technology. Pt. III: Design Handbook for Fluid Film Type Bearings. AFAPL-TR-65-45, Air Force Aero Prop. Lab. (WPAFB, OH), May 1965.

58. Yamamoto, T.: On the Critical Speeds of a Shaft. Memoirs of the Faculty of Engineering, Nagoya Univ. (Nagoya, Japan),vol. 6, no. 2, Nov. 1954.

59. Yamamoto, T.: On the Vibrations of a Rotating Shaft. Memoirs of the Faculty of Engineering, Nagoya Univ., (Nagoya, Japan),vol. 9, no. 1, May 1957.

60. Yamamoto, T.: On Critical Speeds of a Shaft Supported by a Ball Bearing. J. Appl. Mech., Trans. ASME, Series E, vol. 81, June 1959, pp. 199-204.

61. Wirt, L. W.: An Introduction to the Works of Toshio Yamamoto Which Treat the Vibration Problems Encountered in High-Speed Rotating Machinery. Strain Gage Readings, vol. 5, no. 1, April-May 1962, pp. 7-20.

62. Cavicchi, R.H.: Critical-Speed Analysis of Flexibly Mounted Rigid Rotors. NASA TN D-4607, 1968.

63. Rieger, N. F.: Rotor-Bearing Dynamics Design Technology, Pt. I: State of the Art. AFAPL-TR-65-45, Air Force Aero Prop. Lab. (WPAFB, OH), May 1965.

64. Poritsky, H.: Rotor-Bearing Dynamics Design Technology. Pt. II: Rotor Stability Theory. AFAPL-TR-65-45, Air Force Aero Prop. Lab. (WPAFB, OH), May 1965.

65. Lund, J. W.: Rotor-Bearing Dynamics Design Technology. Pt. V: Computer Program Manual for Rotor Response and Stability. AFAPL-TR-65-45, Air Force Aero Prop. Lab. (WPAFB, OH), May 1965.

66. Morris, J.: The Impact of Bearing Clearances on Shaft Stability. Aircraft Eng., vol. 29, no. 346, Dec. 1957, pp. 382-383.

67. Tondl, A.: Some Problems of Rotor Dynamics. Chapman and Hall (London), 1965.

68. Gunter, E. J., Jr.: Dynamic Stability of Rotor-Bearing Systems. NASA SP-113, 1966.

69. Hersey, M. D.: Theory and Research in Lubrication. Ch. XII, Vibrations and Whirl. John Wiley & Sons, Inc., 1966.

70. Grassam, N. S.; and Powell, J. W.: Gas Lubricated Bearings. Butterworth & Co. (London), 1964.

71. Benko, G. B.: Notes on the Measurements of Vibrations on Rotating Systems. Paper 6, Symposium on Vibrations in Hydraulic Pumps and Turbines (Manchester, England),Sept. 14-16, 1966. Publ. Inst. Mech. Engrs. (London).

72. Ehrich, F. F.; and Connor, J. J.: Stator Whirl With Rotors in Bearing Clearance. J. Eng. Ind., Trans. ASME, Series B, vol. 89, 1967, pp. 381-390.

73. Ehrich, F. F.: The Influence of Trapped Fluids on High Speed Rotor Vibration. J. Eng. Ind., Trans. ASME, Series B, vol. 89, 1967, pp. 806-812.

74. Ehrich, F. F.: Subharmonic Vibration of Rotors in Bearing Clearance. ASME paper 66-MD-1, Design Engineering Conference and Show (Chicago, IL), May 9-12, 1966. (Abstract:Mech. Eng., vol. 88, Aug. 1966).

75. Black, H. F.: Synchronous Whirling of a Shaft Within a Radially Flexible Annulus Having Small Radial Clearance. Paper 4, Symposium on Vibrations in Hydraulic Pumps and Turbines (Manchester, England), Sept. 14-16, 1966. Publ. Inst. Mech. Engrs. (London).

76. Ruffini, A. J.: Bearing Noise. Pt. I - Analysis of Rolling-Element Bearings. Mach. Des., vol. 35, no. 11, May 9, 1963, pp. 232-235.

77. Horlock, J. H.: Axial Flow Compressors. Butterworth & Co. (London), 1958.

78. Yeh, L.: Critical Speed Investigations of Turbomachines. Proc. Inst. Mech. Engrs. (London), vol. 180, Pt. 31, 1965-1966, pp. 23-37.

79. Lund, J. W.; and Orcutt, F. K.: Calculations and Experiments on the Unbalance Response of a Flexible Rotor. J. Eng. Ind., Trans. ASME, Series B, vol. 89, 1967, pp. 785-796.

80. Gunter, E. J., Jr.: Analysis of Rocketdyne Nuclear Feed System Turbopump Failure. W-12-229, Research Laboratories for the Engineering Sciences, Univ. of Virginia (Charlottesville, VA), June 1966.

81. Gunn, S. V.; and Dunn, C.: Dual Turbopump Liquid Hydrogen Feed System Experience. Paper presented at Ninth Liquid Propulsion System Symposium (St. Louis, MO), Oct. 25-27, 1967.

82. Williams, F. B.: Design, Fabricate, and Test Breadboard Liquid Hydrogen Pump (U). Rep. PWA FR-2884, Pratt & Whitney Aircraft (W. Palm Beach, FL), Aug. 1967, pp. V-8, V-9. (Confidential).

83. Alford, J. S.: Protecting Turbomachinery From Self-Excited Rotor Whirl. J. Eng. Power, Trans. ASME, Series A, vol. 87, 1965, pp. 333-344.

84. Den Hartog, J. P.: Mechanical Vibrations. Fourth ed., McGraw-Hill Book Co., 1956, pp. 320-321.

85. Van De Verg, N.: Bearing-Shaft Dynamics for Operation in Space. Rep. 2348,Aerojet-General Corp. (Azusa, CA),June 1962.

86. Gunter, E. J., Jr.: The Influence of Internal Friction on the Stability of High Speed Rotors. J. Eng. Ind., Trans. ASME, Series B, vol. 89, 1967, pp. 683-688.

87. Billett, R. A.: Shaft Whirl Induced by Dry Friction. Engineer, vol. 220, no. 5727, Oct. 29, 1965, pp. 713-714.

88. Eshleman, R. L.: Procedure for Calculating Natural Frequencies of Shafting Systems. Rep. K6086 (AD 811785),IIT Research Center (Chicago, IL), Feb. 11, 1967.

89. Ker Wilson, W.: Practical Solution of Torsional Vibration Problems. John Wiley & Sons, Inc., vol. 1, 1941; vol. 2, 1962.

90. Nestorides, E. J., ed.: A Handbook on Torsional Vibration. Brit. Int. Comb. Engine Res. Assoc., Research Laboratory, Cambridge Univ. Press (London), 1958.

91. Tang, R. M.; and Trumpler, P. R.: Dynamics of Synchronous-Processing Turborotors With Particular Reference to Balancing. Pt. 1, Theoretical Foundations. J. Appl. Mech., Trans. ASME, Series E, vol. 86, 1964, pp. 115-122.

92. Severud, L. K.; and Reeser, H. G.: Analysis of the M-1 Liquid Hydrogen Turbopump Shaft Critical Whirling Speed and Bearing Loads. NASA CR-54825, Dec. 20, 1965.

93. Ludwig, G. A.: Vibration Analysis of Large High-Speed Rotating Equipment. J. Eng. Ind., Trans. ASME, Series B, vol. 88, 1966, pp. 201-210.

94. Myklestad, N. O.: New Method of Calculating Natural Modes of Coupled Bending-Torsion Vibration of Beams. J. Appl. Mech., Trans. ASME, Series E,vol. 67, 1945, pp. 61-67.

95. Myklestad, N. O.: A Simple Tabular Method of Calculating Deflections and Influence Coefficients of Beams. J. Aeron. Sci., vol. 13, no. 1, Jan. 1946, pp. 23-28.

96. Prohl, M. A.: A General Method of Calculating Critical Speed of Flexible Rotors. J. Appl. Mech., Trans. ASME, Series E, vol. 67, 1945, pp. A-142 through A-148.

97. Pestel, E. C.; and Leckie, F. A.: Matrix Methods in Elastomechanics, McGraw-Hill Book Co., 1963.

98. Finkelstein, R. R.: Myklestad's Method for Predicting Whirl Velocity as a Function of Rotational Velocity for Flexible Multimass Rotor Systems. J. Appl. Mech., Trans. ASME, Series E, vol. 87, 1965, pp. 589-591.

99. Stodola, A.: Steam and Gas Turbines. McGraw-Hill Book Co., 1927.

100. Caruso, W. J.: Prediction of Critical Speeds of Steam Turbines by Dynamic Stiffness Method. ASME Colloquium on Mechanical Impedance Methods for Mechanical Vibrations (New York, NY), Robt. Plunkett, ed., ASME, 1959, p. 137.

101. Koenig, E. C.: Analysis for Calculating Lateral Vibration Characteristics of Rotating Systems With Any Number of Flexible Supports. Pt. 1 - Method of Analysis. Paper 61-APMW-16A, West Coast Conference, Appl. Mech. Div., ASME (Seattle, WA), Aug. 28-30, 1961.

102. Gunther, T. G.; and Lovejoy, D. C.: Analysis for Calculating Lateral Vibration Characteristics of Rotating Systems With Any Number of Flexible Supports. Pt. 2 - Application of the Method of Analysis. Paper 61-APMW-16B, West Coast Conference, Appl. Mech. Div., ASME (Seattle, WA), Aug. 28-30, 1961.

103. Gurov, A. F.: Joint Oscillations in Gas Turbine Engines. Tech. Transl. TT65-60123 (AD 608455), Foreign Technology Div.,Air Force Systems Command (WPAFB, OH), Nov. 5, 1964.

104. Severud, L. K.; Smithers, O. L.; and Mironenko, G.: Titan IIIM-87 Turbopump Structural Analysis. Vol. III High Speed Shaft Redesign Analysis of Whirl and Torsional Critical Speeds and Associated Characteristics. Aerojet-General Corp., June 24, 1968.

105. Hollister, G. S.; and Zienkiewicz, O.: Stress Analysis. John Wiley & Sons, Inc., 1965.

106. Hull, E. H.: Shaft Whirling As Influenced by Stiffness Asymmetry. J. Eng. Ind., Trans. ASME, Series B, vol. 83, 1961, pp. 219-226.

107. Bisson, E.; and Anderson, W. J.: Advanced Bearing Technology. NASA SP-38, 1965.

108. Palmgren, A.: Ball and Roller Bearing Engineering. Third ed., SKF Industries, Inc. (Philadelphia, PA), 1959.

109. Kumbarger, J. H.: How Clearance Affects Life of Rolling Bearings. Mach. Des., vol. 33, no. 12, June 8, 1961, pp. 145-149.

110. Harris, T. A.: How To Compute the Effects of Preloaded Bearings. Prod. Eng., vol. 36, no. 15, July 19, 1965, pp. 84-93.

111. Harris, T. A.: Rolling Bearing Analysis. John Wiley & Sons, Inc., 1966.

112. Jones, A. B.: The Mathematical Theory of Rolling-Element Bearings. Sec. 13, Mechanical Design and Systems Handbook, Harold A. Rothbart, ed., McGraw-Hill Book Co., 1964.

113. Jones, A. B.: Analysis of Stresses and Deflections. Vols. I and II. New Departure Div., General Motors Corp. (Bristol, CT), 1946.

*114. Severud, L. K.; and Bartholf, L. W.: SNAP-8 Alternator Whirl Critical Speed and Response Analysis. Memorandum 3252:747, Aerojet-General Corp., unpublished, Mar. 13, 1968.

115. Means, H.: Brayton-Cycle Turbomachinery Rolling Element Bearing System. NASA CR-54815, Feb. 1966.

*116. Barrish, T.: Theoretical Analysis for Equivalent Center of Angular-Contact Bearings. Report to Aerojet-General Corp., LRP, M-1 Pumps Project, Nov. 2, 1963.

117. Lund, J. W.; and Sternlicht, B.: Rotor-Bearing Dynamics With Emphasis on Attenuation. J. Basic Eng., Trans. ASME, Series D, vol. 84, 1962, pp. 491-502.

118. Muster, D.; and Sternlicht, B., eds.: Proc. Intl. Symposium on Lubrication and Wear. Ch. 3. McCutchan Publishing Corp. (Berkeley, CA), 1965.

119. Lund, J. W.: Spring and Damping Coefficients for the Tilting-Pad Journal Bearing. Trans. ASLE, vol. 7, no. 4, Oct. 1964, pp. 342-352.

* Dossier for design criteria monograph "Liquid Rocket Engine Turbopump Shafts and Couplings." Unpublished, 1969. Collected source material available for inspection at NASA Lewis Research Center, Cleveland, Ohio.

120. Sternlicht, B.: Hydrodynamic Lubrication. Sec. 12, Mechanical Design and Systems Handbook, Harold A. Rothbart, ed., McGraw-Hill Book Co., 1964.

121. Satchwell, D. L.: More Accurate Balancing for High Speed Rotors. Mach. Des., vol. 37, no. 22, Sept. 1965, pp. 183-184.

122. Hill, H. C.: Slipper Bearings and Vibration Control in Small Gas Turbines. Trans. ASME, vol. 80, no. 8, Nov. 1958, pp. 1756-1764.

*123. Schlappi, H. C.: 87-5 Turbopump Lower High Speed Bearing Problem. Final Rep. RMR 0112, Aerojet-General Corp., Aug. 29, 1963.

*124. Mironenko, G.: Titan III M-87 High Speed Shaft Critical Speed and Bearing Load Analysis. Rep. SA-MOL-TPA-223, Aerojet-General Corp., July 15, 1966.

*125. Goudreau, G.: Preliminary Vibration Analysis of the NERVA Mark IV Turbopump Assembly. Rep. SA-N-86, Aerojet-General Corp., Jan. 31, 1966.

126. Siereg, A.: Whirling of Shafts in Geared Systems. J. Eng. Ind., Trans. ASME, Series B, vol. 89, 1967, pp. 278-283.

127. Myklestad, N. O.: Numerical Analysis of Forced Vibrations of Beams. J. Appl. Mech., Trans. ASME, Series E, vol. 75, 1953, pp. 53-56.

128. Thomson, W. T.: Matrix Solution for the Vibration of Non-Uniform Beams. J. Appl. Mech., Trans. ASME, Series E, vol. 72, 1950, pp. 337-339.

129. Hurty, W. C.; and Rubinstein, M. F.: Dynamics of Structures. Prentice-Hall, Inc. 1964.

130. Hamburg, G.; and Parkinson, J.: Flexible Bearing Supports Help Stop Vibration in Gas Turbine Shafts. SAE J., vol. 69, no. 9, Sept. 1961, pp. 75-77.

131. Anon.: New Bearing Mount Puts On the Squeeze. Prod. Eng., vol. 37, no. 7, Mar. 28, 1966, p. 96.

132. Van Nimwegen, R. R.: Critical Speed Problems Encountered in the Design of High-Speed Turbomachinery. Paper 928C, SAE Natl. Transportation, Powerplant, and Fuels and Lubricants Meeting (Baltimore, MD), Oct. 1964.

133. Duncan, A. B.: Vibrations in Boiler Feed Pumps: A Critical Review of Experimental and Service Experience. Paper 8, Symposium on Vibration in Hydraulic Pumps and Turbines (Manchester, England), Sept. 14-16, 1966. Publ. Inst. Mech. Eng. (London).

134. Snow, E. W.: Discussion of "Protecting Turbomachinery from Self-Excited Rotor Whirl," by J. S. Alford. J. Eng. Power, Trans. ASME, Series A, vol. 87, 1965, p. 344.

*135. Severud, L. K.: Shaft and Coupling Design Practices at Airesearch Mfg. Div., The Garrett Corp. (Phoenix, AZ). Memorandum 3252:787, Aerojet-General Corp., unpublished, May 1968.

* Dossier for design criteria monograph "Liquid Rocket Engine Turbopump Shafts and Couplings." Unpublished, 1969. Collected source material available for inspection at NASA Lewis Research Center, Cleveland, Ohio.

136. Kulina, M.; Mullon, J.; Matesh, M.; and Saltzman, H.: A New Concept for Critical Speed Control. Paper 67-0347, SAE Natl. Aeronautic Meeting (New York, NY), Apr. 24-27, 1967.

137. Federn, K.: Fundamentals of a Systematic Suppression of Flexible Shaft Rotor Vibration. Verein Deutsches Ingenieure Berichte (Dusseldorf, W. Germany), vol. 24, 1957.

138. Prause, R. H.; Meacham, H. C.; and Voorhees, J. E.: The Design and Evaluation of a Supercritical-Speed Helicopter Power-Transmission Shaft. J. Eng. Ind., Trans. ASME, Series B, vol. 89, 1967, pp. 719-728.

139. Fanella, R. J.; and Schaefer, R. W.: Study and Development of Design Criteria for High Speed Power Transmission Shafts. WADC-TR-59-714 (AD 277279), WADC (WPAFB, OH), 1959, p. 39.

140. Parkinson, A. G.; Jackson, R. L.; and Bishop, R. E. D.: Some Experiments on the Balancing of Small Flexible Rotors. Part I - Theory; Part II - Experiments. J. Mech. Eng. Sci., vol. 5, nos. 1 and 2, 1963, pp. 114-128 and pp. 133-145.

141. Bishop, R. E. D.; and Gladwill, G. M. L.: The Vibration and Balancing of an Unbalanced Flexible Rotor. J. Mech. Eng. Sci., vol. 1, no. 1 ,1959 , pp. 66-77.

142. Hahn, E. E.; et al.: Development of Methods and Equipment for Balancing Flexible Rotors. Rep. ARF 78753-FR-62-5 (AD 276476), Armour Res. Foundation, Illinois Inst. of Tech. (Chicago, IL), May 1962.

143. Anon.: Curvic Coupling Design. Gleason Manual, Form SD 3116 B, The Gleason Works, 1000 University Ave., Rochester, NY, Mar. 1966.

144. Kuzmenko, V. S.: New Devices for Measuring Torque and Shaft Horsepower Transmitted by Marine Engine Shafts. (AD 478952), Naval Scientific and Technical Information Center (London, England). (Translated from Trudy Leningrad Inst. Vodnogo Transports, no. 12, 1961, pp. 29-40.)

145. Plumpe, D. J.: A Ship Propeller Shaft Strain Measuring and Telemetering System. R&D Rep. DTMB-1714 (AD 649879), U. S. Navy David Taylor Model Basin (Washington, DC), Jan. 1963.

146. Stein, P. K.: Measuring Bearing Strain. Instruments and Control Systems, vol. 37, Nov. 1964, pp. 132-139.

147. Benko, G. B.; and Holman, E. K.: Parametric Resonances in Umbrella-Type Generating Units. Paper 3, Symposium on Vibrations in Hydraulic Pumps and Turbines (Manchester, England), Sept. 14-16, 1966. Publ. Inst. Mech. Engrs. (London).

148. Motsinger, R. N.: Discussion and Review of Slipring Instrumentation Design. Strain Gage Readings, vol. III, no. 1, Apr. - May, 1960, pp. 3-36.

149. Stein, P. K.: Strain-Gage-Based Shaft-Whirl Instrumentation in Gas Turbines. Strain Gage Readings, vol. IV, no. 3, Aug.-Sept. 1961, pp. 3-13.

150. Ness, H.: Analyzing Vibration in Rotating Machinery. Quality Assurance, Nov. 1964.

151. Foster, G. B.: Recent Developments in Machine Vibration Monitoring. IEEE Trans. of Ind. and Gen. Applications, vol. IGA-3, no. 2, Mar. - Apr. 1967, pp. 149-158.

*152. Severud, L. K.: Shaft and Coupling Design Practices at Avco, Lycoming Division (Stratford, CT). Memo 3252:819, Aerojet-General Corp., unpublished, July 1, 1968.

153. Sonder, G.: Abusive Testing of Turboshaft Engines. Proc. Ann. Natl. Forum, Am. Helicopter Soc. (Washington, DC), May 12-14, 1965.

154. Gerard, G.; and Becker, H.: Handbook of Structural Stability. Pt. III-Buckling of Curved Plates and Shells. NACA TN 3783, Aug. 1957.

155. Harris, T. A.: Optimizing the Fatigue Life of Flexibly-Mounted Rolling Bearings. Paper presented at 20th ASLE Annual Meeting (Detroit, MI), May 4-7, 1965.

*156. Severud, L. K.: Shaft and Coupling Design Practices at Rocketdyne (Canoga Park, CA). Memorandum 3252:787, Aerojet-General Corp., unpublished, May 15, 1968.

157. Cataldo, C. E.: Compatibility of Metals With Hydrogen. NASA TMX-53807, 1968.

158. Logan, H. L.: The Stress Corrosion of Metals. John Wiley & Sons, Inc., 1966.

159. Anon.: Design Guidelines for Controlling Stress Corrosion Cracking. NASA-MSFC Drawing 10M33107, 1970.

160. Anon.: Fracture Control of Metallic Pressure Vessels. NASA Space Vehicle Design Criteria Monograph, NASA SP-8040, May 1970.

161. Anon.: Metallic Materials and Elements for Aerospace Vehicle Structures. MIL-HDBK-5A, Dept. of Defense, Feb. 8, 1966.

162. Manson, S. S.; and Halford, G.: A Method of Estimating High-Temperature, Low-Cycle Fatigue Behavior of Metals. NASA TMX-52270, 1967.

163. Clauss, F. J.: Engineer's Guide to High-Temperature Materials. Addison-Wesley Publishing Co., Inc., 1969.

164. Lipson, C.: Wear Considerations in Design. Prentice-Hall, Inc., 1967.

165. Hardrath, H. F.: Fatigue and Fracture Mechanics. Paper presented at AIAA/ASME 11th Structures and Materials Conference (Denver, CO), Apr. 22, 1970.

166. Anon.: Fracture Toughness Testing and Its Applications. ASTM STP 381, Am. Soc. for Testing and Materials (Philadelphia, PA), 1965.

167. Juvinall, R. C.: Engineering Considerations of Stress, Strain and Strength. McGraw-Hill Book Co., 1967.

168. Modayag, A. F.: Metal Fatigue: Theory and Design. John Wiley & Sons, Inc., 1969.

* Dossier for design criteria monograph "Liquid Rocket Engine Turbopump Shafts and Couplings." Unpublished, 1969. Collected source material available for inspection at NASA Lewis Research Center, Cleveland, Ohio.

169. Miner, M. A.: Cumulative Damage in Fatigue, J. Appl. Mech., Trans. ASME, Series E, vol. 67, 1945, p. A-159.

170. Parkes, E. W.: Structural Effects of Repeated Thermal Loading. Chap. 11, Thermal Stress, P. P. Benham and R. Hoyle, eds., Sir Isaac Pitman and Sons, Ltd. (London), 1964.

171. Burgreen, D.: Structural Growth Induced by Thermal Cycling. Paper 68-WA/Met-14, ASME Winter Annual Meeting, Dec. 1-5, 1968.

172. Burgreen, D.: The Thermal Ratchet Mechanism. Paper 68-WA/Met-13, ASME Winter Annual Meeting, Dec. 1-5, 1968.

173. Anon.: Fatigue at High Temperatures. ASTM STP 459, L. F. Coffin, ed., Am. Soc. for Testing and Materials (Philadelphia, PA), 1969.

174. Manson, S. S.; Freche, J. C.; and Ensign, C. R.: Application of a Double Linear Damage Rule to Cumulative Fatigue. ASTM STP 415, Fatigue Crack Propagation, Am. Soc. for Testing and Materials (Philadelphia, PA), 1967.

175. Spera, D. A.: The Calculation of Thermal-Fatigue Life Based on Accumulated Creep Damage. NASA TM X-52558, 1969.

176. Wilhem, D. P.: Fracture Mechanics Guidelines for Aircraft Structural Applications. Tech. Rep. AFFDL-TR-69-111, Air Force Flight Dynamics Laboratory (WPAFB, OH), Feb. 1970.

177. Schalla, C. A.: Design Control of Cantilever Shaft Critical Speeds. Paper 63-AHGT-27, ASME Aviation and Space Hydraulic and Gas Turbine Conference and Products Show (Los Angeles, CA), Mar. 3-7, 1963.

178. Nichols, H. E.; and Fink, R. W.: Two Stage Potassium Test Turbine. Vol. II: Mechanical Design and Development. NASA CR-923, 1968.

179. Baumgartner, T. C.: Fastener Performance at Elevated Temperatures. Paper 67-DE-18, ASME Design Engineering Conference and Show (New York, NY), May 15-18, 1967.

180. Zamparo, O. J.: Design Recommendations for Keeping Bolted Joints Tight Under Severe Vibration Conditions. Mach. Des., vol. 33, no. 22, Oct. 26, 1961, pp. 163-166.

181. Junker, G. H.: New Criteria for Self-Loosening of Fasteners Under Vibration. Paper 69-0055, SAE Intl. Automotive Engineering Congress (Detroit, MI), Jan. 13-17, 1969.

182. Anon.: Involute Splines and Inspection (Revision and Redesignation of ASA B5.15-1960). ANSI B92.1-1970, ANSI (New York, NY), 1970.

183. Sevcik, J. K.: System Vibration and Static Analysis. Paper 63-AHGT-57, ASME Aviation and Space Hydraulic and Gas Turbine Conference and Products Show (Los Angeles, CA), Mar. 3-7, 1963.

184. Lewis, F. M.: Vibration During Acceleration Through A Critical Speed. J. Appl. Mech., Trans. ASME, Series E, vol. 54, 1932, pp. 253-261.

185. Macchia, D.: Acceleration of an Unbalanced Rotor Through the Critical Speed. Paper 63-WA-9, ASME Winter Annual Meeting (Philadelphia, PA) Nov. 17-22, 1963 (Abstract: Mech. Eng., vol. 86, Jan. 1964, p. 69).

186. Baker, J. G.: Mathematical-Machine Determination of Vibration of Accelerated Unbalanced Rotor. J. Appl. Mech., Trans. ASME , Series E, vol. 61, 1939, pp. A145-A150.

187. McCann, G. D., Jr.; and Bennett, R. R.: Vibrations of Multifrequency Systems During Acceleration Through Critical Speeds. J. Appl. Mech., Trans. ASME, Series E, vol. 71, 1949, pp. 375-382.

188. Howitt, F.: Accelerating A Rotor Through A Critical Speed. Engineer, vol. 212, no. 5518, Oct. 27, 1961, pp. 691-692.

189. Gluse, M. R.: Acceleration of an Unbalanced Rotor Through Its Critical Speeds. Naval Eng. J., vol. 79, no. 1, Feb. 1967, pp. 135-144.

190. Tuplin, W. A.: Notes on the Whirling of Shafts. Engineer, vol. 216, no. 5618, Sept. 27, 1963, pp. 506-510.

191. Ehrich, F. F.: The Dynamic Stability of Rotor/Stator Radial Rubs in Rotating Machinery. J. Eng. Ind., Trans.ASME, Series B, vol. 91, 1969, pp. 1025-1028.

192. Gunter, E. J., Jr.; and Trumpler, P. R.: The Influence of Internal Friction on the Stability of High Speed Rotors With Anisotropic Supports. J. Eng. Ind., Trans. ASME, Series B, vol. 91, 1969, pp. 1105-13.

193. Armstrong, E. K.; Cristie, P. I.; and Hunt, T. M.: Vibration in Cylindrical Shafts. Proc. Inst. Mech. Engrs. (London), vol. 180, part 31, 1965-1966, pp. 38-48.

194. Zienkiewicz, O. C.: The Finite Element Method in Structural and Continum Mechanics. McGraw-Hill Publishing Co., Ltd., 1967.

195. Shaeffer, H. G.: Computer Program for Finite-Difference Solutions of Shells of Revolution Under Asymmetric Loads. NASA TN D-3926, 1967.

196. Percy, J. H.; Navaratna, D. R.; and Klein, S.: Sabor III: A Fortran Program for the Linear Elastic Analysis of Thin Shells of Revolution Under Axisymmetric Loading by Using the Matrix Displacement Method. Rep. ASRL-TR-121-6 (AD 617308), Aeroelastic and Structures Res. Lab., Mass. Inst. of Tech. (Cambridge, MA), May 1965.

197. James, J. B.: Development of the Liquid-Hydrogen Turbopump for the J-2 Rocket Engine (U). AIAA Propulsion Specialists Conf., Air Force Academy (Colorado Springs, CO), June 14-18, 1965. (Confidential)

GLOSSARY

Term or Symbol	Definition
built-up shaft	shaft with a multiplicity of components such as collars, sleeves, and couplings
case hardening	infiltration of a metallic surface with carbon to provide selective increase in hardenability
CH 900	temper designation by Armco Steel Co. to indicate coldworking followed by furnace heating to 900°F (756 K)
Charpy V-notch	notched specimen used to determine material impact properties
critical speed	shaft rotational speed at which a rotor/stator system natural frequency coincides with a possible forcing frequency
crowned spline	spline modified along the face width or profile to anticipate misalignment
curvic coupling	trade name of the Gleason Works for a face-gear type of coupling generated in manner similar to that used for bevel gears
DN	bearing speed-capability index, the product of bearing bore size (D) in mm and rotation speed (N) in rpm
datum	reference surface for locating bearings on the shaft; normally the shaft longitudinal axis or the shaft shoulder
double pilot	registry between mating components wherein two surfaces establish relative location or where location is transferred from one surface to another
dynamic imbalance	distribution of rotor mass such that the principal inertia axis of the rotor is rotationally misaligned with the bearing axis. Moments are generated when the rotor rotates about the bearing axis. Dynamic imbalance, also referred to as moment imbalance, requires measurement and correction in two or more planes perpendicular to the rotor axis.
endurance limit	level of stress at which the material can endure an unlimited number of cycles

Term or Symbol	Definition
FORTRAN	acronym for formula translation: the special system of communication by which information and instructions are provided to a computer
fluid-film bearing	type of bearing wherein separation of the bearing and journal depends on the shearing of a lubricating film
free free	term used to designate a complete lack of restraint applied to the first lateral bending mode of shaft resonance
fretting	mechanism of wear that acts on mating metallic materials to produce surface damage when one surface moves relative to another
g	acceleration due to gravity
galling	progressive surface damage of mating surfaces resulting in increased friction and possible seizure
gyroscopic moment	moment induced on rotating components by the angular displacement of the rotating axis, as in a gyroscope
Hz	cycles per second
HCF	high-cycle fatigue
hydrostatic bearing	fluid-film bearing wherein the pressure required to maintain separation of the surfaces is externally supplied
K	spring rate
Lamé's equation	equation for stresses in thick cylinders
LCF	low-cycle fatigue
Lissajous pattern	pattern displayed on the oscilloscope screen when shaft whirl motions at a given station on the shaft sensed by pickups spaced 90° apart (and lying in the same plane) are fed separately to the horizontal and vertical inputs of the oscilloscope
lumped mass	an analytical concept wherein a mass is treated as if it were concentrated at a point
M	mass

Term or Symbol	Definition
mode	any of the various stationary-vibration patterns of which an elastic body is capable
N	turbopump shaft rotational speed
N_{CR}	critical speed
N_T	turbine shaft speed
NDT	nondestructive test
nitriding steel	steel alloyed with nitride-forming elements; exposure of the alloy to active nitrogen results in a thin hard case that is especially wear resistant
nodal circle	pattern of vibration nodes that forms a circle
nodal diameter	pattern of vibration nodes that forms a diametral line
P_d	gear or spline pitch diameter
pilot	mechanical element acting on another mechanical element to provide correct alignment or proper relative position
PV	index of seal or bearing operation, the product of unit loading (P) and rubbing velocity (V)
R	radial load
Rockwell "C"	hardness scale
rms	root mean square
rolling-contact bearing	"antifriction" bearing of the ball or roller type
rpm	revolutions per minute
rps	revolutions per second
SCT900	temper process consisting of subcooling treatment followed by furnace heating to 900°F (756 K)

Term or Symbol	Definition
shaft-riding elements	term used to designate components such as collars and sleeves
sigma	term in statistics; the standard deviation from the mean
spring constant or spring rate	change of mechanical spring force per unit of deflection in a flexure element
squeeze-film damping	friction damping produced by pressure and flow forces in a thin film of lubricant (oil) subjected to high load and shear
stack height	term applied to bevel gears to indicate the measured distance from the cone center to a locating surface
static imbalance	distribution of the rotor mass such that the rotor center-of-gravity axis is translationally eccentric to the bearing axis. This mass eccentricity generates centrifugal forces that are reacted by the bearings when the rotor rotates about the bearing axis. Static imbalance, also referred to as force imbalance, can be corrected by adding or subtracting mass in a single plane perpendicular to rotor axis.
stiffness	resistance to deflection
subcritical	coined word denoting operation below a critical speed
supercritical	coined word denoting operation above a critical speed
tangled-yarn	term used to describe a nonrepetitive whirl orbit
T.I.R.	total indicator reading or runout
torr	unit of pressure equivalent to 1 mm of mercury (133.32 N/m^2)
β	dynamic imbalance forcing function
γ	static imbalance forcing function
δ	bearing clearance; also, amount of deflection
λ	nondimensional natural frequency of a two-degree-of-freedom system
Ω	shaft rotational speed
ω	shaft whirl speed

MATERIALS

Designation	Specification or Description
A-286	commercial designation for an austenitic iron-base alloy
AM-350, -355	commercial designations for semi-austenitic precipitation-hardening steels
AMS 4775	Aerospace Material Specification (SAE) for nickel-chromium braze alloy
ARMCO 21-6-9 ARMCO 22-13-5	Armco Steel Co. designation for nickel-chromium-molybdenum stainless steels
Aerozine 50 or A-50	50/50 blend of hydrazine and unsymmetrical dimethylhydrazine
CRES	corrosion resistant steel
H-11	AISI designation for chromium-molybdenum-vandadium tool steel
Inconel 718 Inconel X-750	International Nickel Co. designations for austenitic nickel-base alloys
Invar	International Nickel Co. designation for a nickel alloy with very low coefficient of thermal expansion
K-monel	International Nickel Co. designation for a nickel-copper-aluminum-titanium alloy; age-hardenable; nonmagnetic down to -150°F (172 K)
Linde LW-5	Union Carbide Corp. designation for flame-sprayed tungsten carbide
LO_2 or LOX	liquid oxygen, propellant grade per MIL-P-25508D
LH_2	liquid hydrogen, propellant grade per MIL-P-27201A
M-50	AISI designation for a high-molybdenum-alloy tool steel
N_2O_4	nitrogen tetroxide, propellant grade per MIL-P-26539
Rene 41	General Electric Co. designation for an austenitic nickel-base alloy
Rokide	proprietary refractory manufactured by The Carborundum Co.
RP-1	high-energy kerosene, propellant grade per MIL-P-25576

Designation	Specification or Description
Vascojet 1000	trade name of the Vanadium Corp. of America for a vanadium-alloy tool steel
Waspaloy	Pratt & Whitney Aircraft designation for a precipitation-hardening nickel-base superalloy
17-4 PH, 17-7 PH	commercial designations for semi-austenitic precipitation-hardening stainless steels
300, 310, 316	commercial designations for austenitic nickel-chromium steels
440 C	commercial designation for martensitic chromium steel
4340, 4620 9310, 52100	AISI designations for alloy steels
6061-T6, 2219-T6, 7075-T73	commercial designations for heat-treated aluminum alloys

PUMPS, ENGINES, AND VEHICLES

Designation	Identification
ARES	100,000-lb (445 kN) thrust high-pressure, staged-combustion rocket engine designed by Aerojet-General Corporation; uses N_2O_4/A-50
J-2	200,000-lb (890 kN) thrust rocket engine for S-II and S-IVB; produced by the Rocketdyne Division of North American Rockwell Corp; uses LOX/LH_2
H-1	200,000-lb (890 kN) thrust rocket engine for Saturn S-IB vehicle; produced by Rocketdyne Div., North American Rockwell Corp; uses LOX/RP-1
M-1	1.2 million-lb (5.34 MN) thrust rocket engine designed by the Aerojet-General Corporation; uses LOX/LH_2
Mark 4, Mark 9, Mark 25	liquid-hydrogen turbopumps developed by Rocketdyne Division of North American Rockwell Corp.
NERVA	nuclear fueled rocket engine under development by Aerojet-General Corp.
RL-129	250,000-pound (1.11 MN) thrust rocket engine developed by Pratt & Whitney Aircraft Division of United Aircraft Corp.; uses LOX/LH_2

Designation	Identification
RL 10	15,000-lb (66.7 kN) thrust rocket engine developed by Pratt & Whitney Aircraft Division of United Aircraft Corp.; uses LOX/LH_2
SNAP 8	nuclear auxiliary power system developed by Aerojet-General Corporation
Titan I, II, III, IIIM	a family of launch vehicles using the XLR-87-AJ and XLR-91-AJ series of rocket engines developed by Aerojet General Corporation
T53	jet engine manufactured by AiResearch Division of the Garrett Corp.
XLR-87-AJ-3, -5, -7, -9	Aerojet-General engines for the first stage of the Titan vehicles • the -3 uses LOX/RP-1 and develops 150,000 lb. (667 kN) thrust • the -5, -7, -9 use N_2O_4/A-50, and develop 215,000 lb (956 kN) thrust
XLR-91-AJ-3, -5, -7, -9	Aerojet-General engines for the second stage of the Titan vehicles • the -3 uses LOX/RP-1, and develops 90,000 lb. (400 kN) thrust • the -5, -7, -9 use N_2O_4/A-50, and develop 100,000 lb. (445 kN) thrust

Abbreviations	Identification
AIAA	American Institute of Aeronautics and Astronautics
AISI	American Iron and Steel Institute
AFAPL	Air Force Aero Propulsion Laboratory
AMS	Aerospace Material Specification
ANSI	American National Standards Institute
ASME	American Society of Mechanical Engineers
ASA	American Standards Association
ASTM	American Society for Testing and Materials
COSMIC	Computer Software Management and Information Center (Univ. of Georgia, Athens, GA)
IIT	Illinois Institute of Technology
SAE	Society of Automotive Engineers

NASA SPACE VEHICLE DESIGN CRITERIA MONOGRAPHS ISSUED TO DATE

ENVIRONMENT

SP-8005	Solar Electromagnetic Radiation, Revised May 1971
SP-8010	Models of Mars Atmosphere (1967), May 1968
SP-8011	Models of Venus Atmosphere (1968), December 1968
SP-8013	Meteoroid Environment Model–1969 (Near Earth to Lunar Surface), March 1969
SP-8017	Magnetic Fields–Earth and Extraterrestrial, March 1969
SP-8020	Mars Surface Models (1968), May 1969
SP-8021	Models of Earth's Atmosphere (120 to 1000 km), May 1969
SP-8023	Lunar Surface Models, May 1969
SP-8037	Assessment and Control of Spacecraft Magnetic Fields, September 1970
SP-8038	Meteoroid Environment Model–1970 (Interplanetary and Planetary), October 1970
SP-8049	The Earth's Ionosphere, March 1971
SP-8067	Earth Albedo and Emitted Radiation, July 1971
SP-8069	The Planet Jupiter (1970), December 1971
SP-8084	Surface Atmospheric Extremes (Launch and Transportation Areas), May 1972
SP-8085	The Planet Mercury (1971), March 1972
SP-8091	The Planet Saturn (1970), June 1972
SP-8092	Assessment and Control of Spacecraft Electromagnetic Interference, June 1972

STRUCTURES

SP-8001	Buffeting During Atmospheric Ascent, Revised November 1970
SP-8002	Flight-Loads Measurements During Launch and Exit, December 1964
SP-8003	Flutter, Buzz, and Divergence, July 1964
SP-8004	Panel Flutter, Revised June 1972
SP-8006	Local Steady Aerodynamic Loads During Launch and Exit, May 1965
SP-8007	Buckling of Thin-Walled Circular Cylinders, Revised August 1968
SP-8008	Prelaunch Ground Wind Loads, November 1965
SP-8009	Propellant Slosh Loads, August 1968
SP-8012	Natural Vibration Modal Analysis, September 1968
SP-8014	Entry Thermal Protection, August 1968
SP-8019	Buckling of Thin-Walled Truncated Cones, September 1968
SP-8022	Staging Loads, February 1969
SP-8029	Aerodynamic and Rocket-Exhaust Heating During Launch and Ascent, May 1969
SP-8030	Transient Loads From Thrust Excitation, February 1969
SP-8031	Slosh Suppression, May 1969
SP-8032	Buckling of Thin-Walled Doubly Curved Shells, August 1969
SP-8035	Wind Loads During Ascent, June 1970
SP-8040	Fracture Control of Metallic Pressure Vessels, May 1970
SP-8042	Meteoroid Damage Assessment, May 1970
SP-8043	Design-Development Testing, May 1970
SP-8044	Qualification Testing, May 1970
SP-8045	Acceptance Testing, April 1970
SP-8046	Landing Impact Attenuation for Non-Surface-Planing Landers, April 1970

SP-8050	Structural Vibration Prediction, June 1970
SP-8053	Nuclear and Space Radiation Effects on Materials, June 1970
SP-8054	Space Radiation Protection, June 1970
SP-8055	Prevention of Coupled Structure-Propulsion Instability (Pogo), October 1970
SP-8056	Flight Separation Mechanisms, October 1970
SP-8057	Structural Design Criteria Applicable to a Space Shuttle, January 1971
SP-8060	Compartment Venting, November 1970
SP-8061	Interaction with Umbilicals and Launch Stand, August 1970
SP-8062	Entry Gasdynamic Heating, January 1971
SP-8063	Lubrication, Friction, and Wear, June 1971
SP-8066	Deployable Aerodynamic Deceleration Systems, June 1971
SP-8068	Buckling Strength of Structural Plates, June 1971
SP-8072	Acoustic Loads Generated by the Propulsion System, June 1971
SP-8077	Transportation and Handling Loads, September 1971
SP-8079	Structural Interaction with Control Systems, November 1971
SP-8082	Stress-Corrosion Cracking in Metals, August 1971
SP-8083	Discontinuity Stresses in Metallic Pressure Vessels, November 1971
SP-8095	Preliminary Criteria for the Fracture Control of Space Shuttle Structures, June 1971
SP-8099	Combining Ascent Loads, May 1972

GUIDANCE AND CONTROL

SP-8015	Guidance and Navigation for Entry Vehicles, November 1968
SP-8016	Effects of Structural Flexibility on Spacecraft Control Systems, April 1969

SP-8018	Spacecraft Magnetic Torques, March 1969
SP-8024	Spacecraft Gravitational Torques, May 1969
SP-8026	Spacecraft Star Trackers, July 1970
SP-8027	Spacecraft Radiation Torques, October 1969
SP-8028	Entry Vehicle Control, November 1969
SP-8033	Spacecraft Earth Horizon Sensors, December 1969
SP-8034	Spacecraft Mass Expulsion Torques, December 1969
SP-8036	Effects of Structural Flexibility on Launch Vehicle Control Systems, February 1970
SP-8047	Spacecraft Sun Sensors, June 1970
SP-8058	Spacecraft Aerodynamic Torques, January 1971
SP-8059	Spacecraft Attitude Control During Thrusting Maneuvers, February 1971
SP-8065	Tubular Spacecraft Booms (Extendible, Reel Stored), February 1971
SP-8070	Spaceborne Digital Computer Systems, March 1971
SP-8071	Passive Gravity-Gradient Libration Dampers, February 1971
SP-8074	Spacecraft Solar Cell Arrays, May 1971
SP-8078	Spaceborne Electronic Imaging Systems, June 1971
SP-8086	Space Vehicle Displays Design Criteria, March 1972
SP-8098	Effects of Structural Flexibility on Entry Vehicle Control Systems, June 1972

CHEMICAL PROPULSION

SP-8087	Liquid Rocket Engine Fluid-Cooled Combustion Chambers, April 1972
SP-8081	Liquid Propellant Gas Generators, March 1972
SP-8052	Liquid Rocket Engine Turbopump Inducers, May 1971

SP-8048	Liquid Rocket Engine Turbopump Bearings, March 1971
SP-8064	Solid Propellant Selection and Characterization, June 1971
SP-8075	Solid Propellant Processing Factors in Rocket Motor Design, October 1971
SP-8076	Solid Propellant Grain Design and Internal Ballistics, March 1972
SP-8039	Solid Rocket Motor Performance Analysis and Prediction, May 1971
SP-8051	Solid Rocket Motor Igniters, March 1971
SP-8025	Solid Rocket Motor Metal Cases, April 1970
SP-8041	Captive-Fired Testing of Solid Rocket Motors, March 1971